Doctoral Dissertation

# Studies on the Improvement of the Interfacial Compatibility of Polyhydroxyalkanoate-based Composites

ポリヒドロキシアルカン酸複合材料の

界面親和性改善に関する研究

田宮　俊樹

January 2021

Graduate School of Engineering

Osaka University

# Contents

**Page**


General Introduction ..... - 1 -
1.1. Background ..... - 1 -
1.2. Bio-based plastics ..... - 2 -
1.3. Poly(hydroxyalkanoate)s (PHAs) ..... - 6 -
1.4. Polymer blend with PHAs and PHAs-based composite materials ..... - 9 -
1.6. This study ..... - 11 -
Contents of this thesis ..... - 12 -
References ..... - 14 -
Chapter 1 ..... - 19 -
1.1. Introduction ..... - 19 -
1.2. Experimental section ..... - 21 -
1.2.1. Materials ..... - 21 -
1.2.2. Synthesis of *p*-azidemethylstyrene (AMS) ..... - 22 -
1.2.3. Synthesis of Vinyl-PHBH from Propargyl-PHBH ..... - 23 -
1.2.4. Radical polymerization of MMA and Vinyl-PHBH ..... - 23 -
1.2.5. Characterization of the synthesized polymers ..... - 24 -
1.2.6. The physical properties of PHBH/PMMA doped with PMMA-*g*-PHBH ..... - 25 -
1.3. Results and discussion ..... - 25 -
1.3.1. Characterization of Vinyl-PHBH and MMA ..... - 25 -
1.3.2. Morphology observation of PHBH/PMMA blends with PMMA-*g*-PHBH ..... - 27 -
1.3.3. Thermal analysis of PHBH/PMMA/PMMA-*g*-PHBH blends ..... - 29 -
1.3.4. Mechanical properties of PHBH/PMMA/PMMA-*g*-PHBH blends ..... - 33 -
1.4. Conclusions ..... - 35 -
1.5. References ..... - 36 -
Chapter 2 ..... - 39 -
2.1 Introduction ..... - 39 -
2.2 Experimental section ..... - 41 -
2.2.1. Materials ..... - 41 -
2.2.2. Synthesis of poly(*p*-azidemethylstyrene-*co*-styrene) [P(AMS-*co*-St)] ..... - 41 -
2.2.3. Preparation of PSt-*g*-PHBH by click chemistry ..... - 42 -
2.2.3. Preparation of PSt-*g*-PHBH by click chemistry ..... - 43 -

2.2.4. Fabrication of PSt-*g*-PHBH film ..... - 44 -
2.2.5. Characterization ..... - 44 -
2.3 Results and discussion ..... - 46 -
2.3.1. Synthesis of PSt-*g*-PHBH ..... - 46 -
2.3.2. Homogeneity and transparency of PSt-*g*-PHBH film ..... - 49 -
2.3.3. Glass transition behavior of PSt-*g*-PHBH ..... - 53 -
2.3.4. Mechanical properties of PSt-*g*-PHBH ..... - 55 -
2.4 Conclusions ..... - 58 -
2.5 References ..... - 60 -
Chapter 3 ..... - 62 -
3.1. Introduction ..... - 62 -
3.2 Experimental section ..... - 63 -
3.2.1. Materials ..... - 63 -
3.2.2. Preparation of $SiO_2$-PHBH ..... - 64 -
3.2.3. Fabrication of PHBH/$SiO_2$-PHBH composite films ..... - 65 -
3.2.4. Measurement ..... - 66 -
3.3 Results and Discussion ..... - 67 -
3.3.1. Characterization of $SiO_2$-PHBH ..... - 67 -
3.3.2. Thermal analysis of PHBH/$SiO_2$ and PHBH/$SiO_2$-PHBH composite films ..... - 70 -
3.3.3. Mechanical properties of PHBH/$SiO_2$ and PHBH/$SiO_2$-PHBH ..... - 72 -
3.4 Conclusion ..... - 77 -
3.5 References ..... - 78 -
Concluding Remarks ..... - 80 -
List of Publications ..... - 82 -
Acknowledgments ..... - 83 -

# General Introduction

## 1.1. Background

In modern society, thermoplastic is one of the most useful materials thanks to its easy processing, light-weight, and low-cost. Especially, polyethylene (PE), polypropylene (PP), and poly(vinyl chloride) (PVC) are well-known as commodity plastics, which are employed for daily necessaries including food packaging,[1] medical items,[2] building materials,[3] and so on. Nowadays, metals, glass-based products, and ceramics are gradually replaced with organic thermoplastics to make industrial products such as automobiles, airplanes, and ships more lightweight and inexpensive, leading to saving energy consumption. For example, automotive bodies are usually fabricated with PP,[4,5] and airplane parts are also made from polycarbonate (PC).[6,7] In terms of electronic parts, recently, the replacement of semiconductive materials to organic plastics has been developed because of the good flexibility and moldability. For example, polyimide (PI) and poly(ethylene terephthalate) (PET) are used for the substrate,[8,9] and poly(3-hexylthiophene-2,5-diyl), a kind of π-conjugated polymers, is expected to be applied for organic semiconductive equipment and organic light-emitting devices[10,11]. Thus, plastic-based materials have become essential materials in our daily life.

However, most plastic resins are derived from petroleum, which is concerned about its depletion on the earth, leading to decrease energy resources in the future. Currently, 4–8% of petroleum is annually used to produce raw plastic[12] and the consumption of petroleum resins is significantly increasing the amount of $CO_2$ and other kinds of toxic gas inducing air pollution. For the past few years, solving these environmental issues corresponds to one of the Sustainable Development Goals SDGs, adopted at the United Nations Summit in 2015.[13] Therefore, renewable materials instead of fossil-based resins should be developed to realize a sustainable and green society.

## 1.2. Bio-based plastics

To overcome the environmental issues concerning oil-based thermoplastics, bio-based plastics have attracted as an alternative material to fossil-derived thermoplastics for the last few decades.[14] As one of the most popular bio-based plastics, poly(lactic acid) (PLA) is synthesized by chemical polymerization of lactic acid (LA) derived from starch through enzymatic hydrolysis and fermentation (**Scheme 1**).[15] To obtain PLA with high molecular weight, a multistep process is needed mentioned below (**Scheme 1**): (1$^{st}$ step) formation of low molecular weight PLA, (2$^{nd}$ step) depolymerization of low molecular weight PLA to produce the lactide, (3$^{rd}$ step) polymerization of lactide.[15] PLA has not only biodegradability and biocompatibility but also high elastic modulus and tensile strength because of its high crystallinity[16]; besides, PLA has good thermal stability because of its crystalized temperature ($T_c$ = 60 °C) and melting point ($T_m$ = 170 °C corresponding to $\alpha$ phase crystalline).[17] On the contrary, high crystallinity induces low ductility and mechanical toughness.[16] Except for PLA, some bio-based polyesters with characteristic functions have been studied; for instance, poly(ethylene 2,5-furandicarboxylate) (PEF) is synthesized by polymerization of ethylene glycol and 2,5-furandicarboxylic acid (**Scheme 2a**).[18] For PEF, the 2,5-fuandicaroboxylic acid monomer is derived from polysaccharides including cellulose and starch through bio- and chemical processes.[18,19] In terms of the physical properties, PEF has a high glass transition temperature ($T_g$ ~ 87 °C), attractive thermal stability, and strong mechanical stiffness, which can be substituted PET ($T_g$ ~ 80 °C).[20] In the last ten years, bio-based PI was synthesized from 4-aminocinnamic acid photo-dimer (**Scheme 2b**).[21] Remarkably, 4-aminocinnamic acid is obtained from polysaccharides through a fermentation process. Although this polymer is an amorphous polymer to form a transparent film, its mechanical strength is relatively higher because cyclobutane moieties in the backbone work as a spring. In addition, polyamide-based on 4-aminocinnamic acid photo-dimer was also successfully synthesized, which exhibited high mechanical properties with good transparency.[22] Thus, recently, the attractive functional bio-based polymer prepared from the

monomer derived from renewable resources have been extremely studied to replace the traditional petroleum-based thermoplastics.

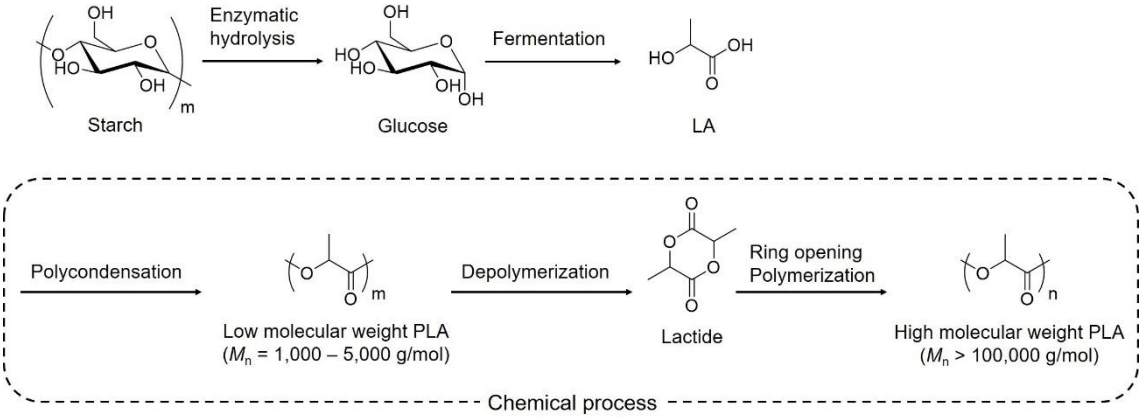


**Scheme 1.** Production of PLA with LA synthesized by the fermentation process of starch.

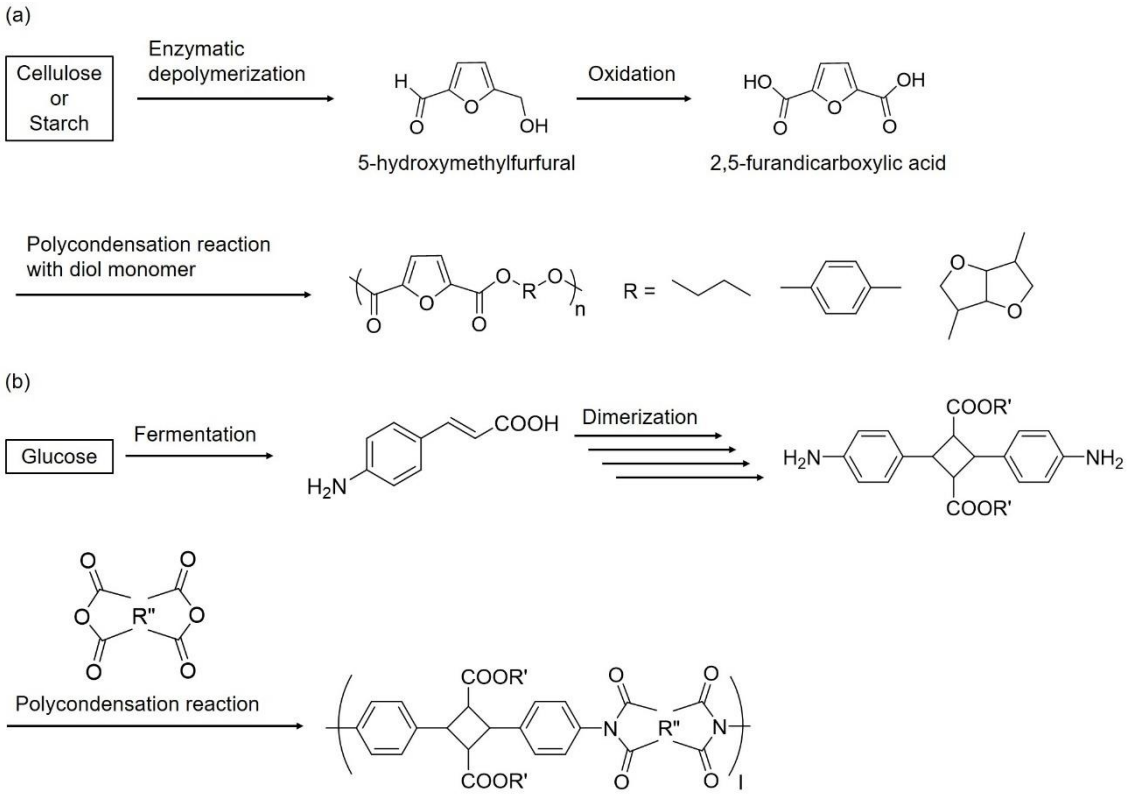


**Scheme 2.** Synthesis process of bio-based (a) polyester and (b) polyimide.

Currently, it is studied that nylon,[18,23] PE,[24] and a vinyl polymer such as polyolefins, polystyrenes, and poly(meth)acrylate[25] are synthesized from natural resources instead of petroleum. Regarding nylon, some kinds of nylon plastics are practically obtained from plant

oils. For example, sebacic acid was derived from castor oil as a starting material to quantitatively produce nylon610 (**Scheme 3b**).[26] Recently, green synthesis routes of hexamethylene diamine from 5-hydroxymethylfurfural have been studied (**Scheme 3a**).[27] As shown in **Scheme 2**, 5-hydroxymethylfurfural is derived from glucose with an enzymatic process. In the latest study, nylon-6 may be obtained from levulinic acid natural resources.[28] Bio-based PE (Bio-PE) is produced from bio-based ethylene derived from natural resources like sugar cane, sugar beet, and starch crops (**Scheme 4**).[24] Of course, by changing the polymerization method of ethylene, different types of Bio-PE like high-density polyethylene, linear low-density polyethylene, and low-density polyethylene can be obtained to tune the crystallinity and mechanical strength. Polymerization of vinyl monomer based on natural products has been also studied along with the development of polymerization technique.[25] The obtained polymers are alternative plastics for petroleum-based plastics such as polyolefin,[29] polystyrene,[29–31] and acrylate polymer,[31,32] shown in **Figure 1**. To produce these polymers quantitatively, the appropriate polymerization reaction must be selected in response to monomer species because the reactivity of vinyl monomer is strongly dependent on the adjacent group for polymerization (**Table 1**).

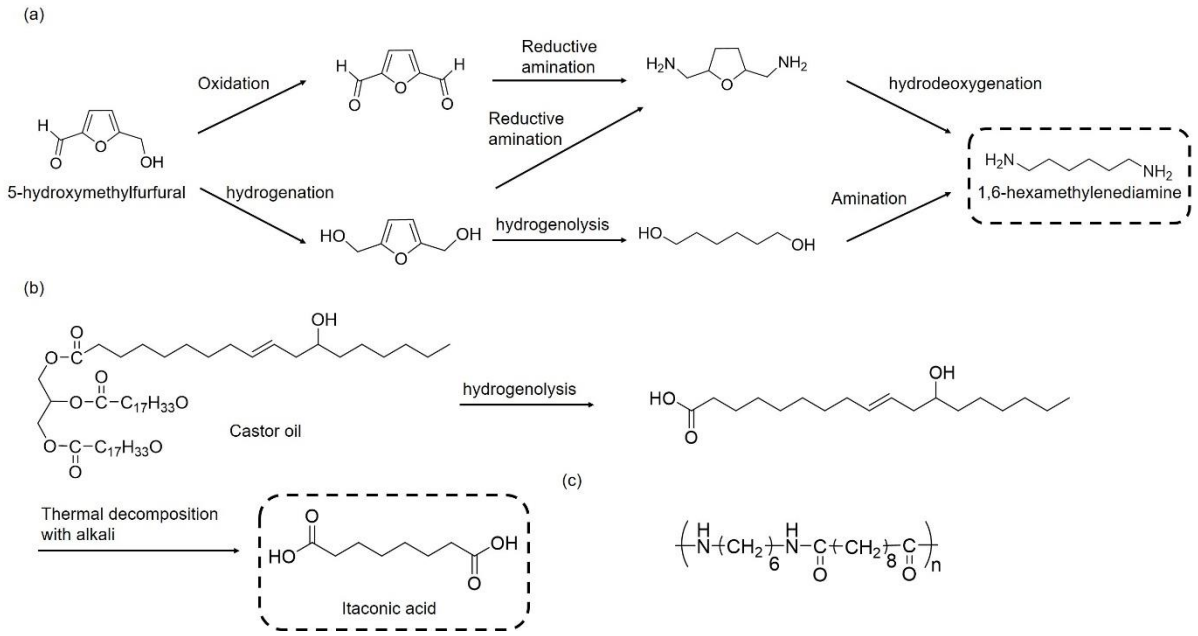


**Scheme 3.** Example of bio-based nylon610 production *via* synthesis of (a) diamine monomer and (b) dicarboxylate monomer derived from natural resources and (c) chemical structure of nylon 610.

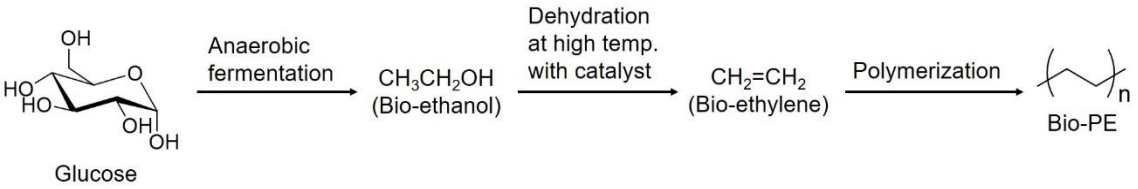


**Scheme 4.** Production process of bio-based PE.

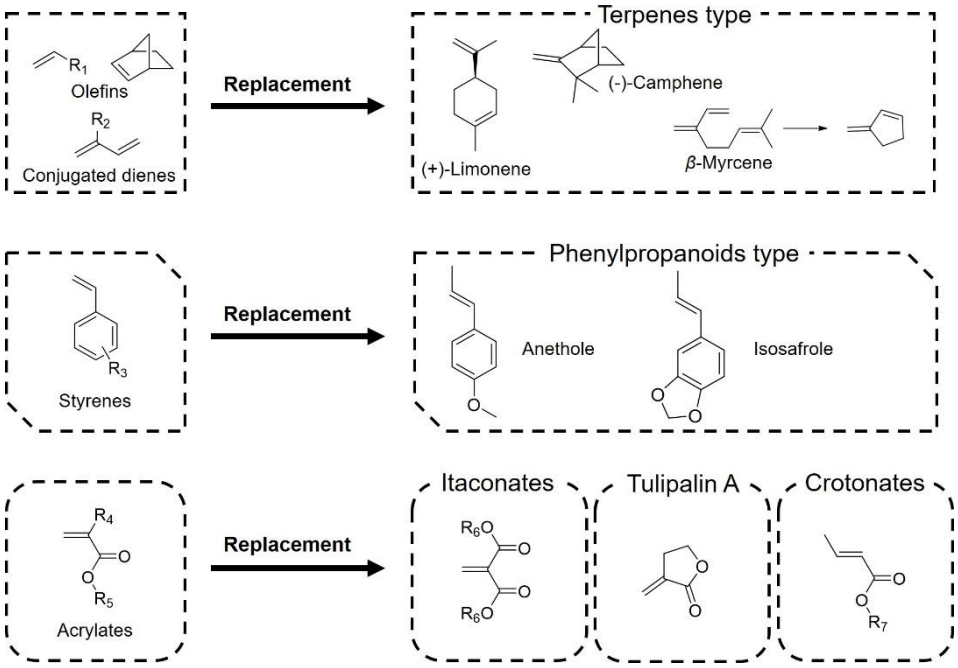


**Figure 1.** Alternative polyolefins, polystyrene, and poly(meth)acrylate polymerized vinyl monomer derived from natural products.

**Table 1.** Appropriate polymerization technique for bio-based vinyl monomers.

| Monomer species | Radical polymerization | Anionic polymerization | Cationic polymerization |
|---|---|---|---|
| Terpenes | ○ | × | ○ |
| Phenylpropanoids | ○ | ○ | ○ |
| Itaconic acid derivatives | ○ | ○ | × |
| α-methylene butyrolactones | ○ | ○ | × |
| Crotonates | ○ | ○ | × |

Note: '○' means 'polymerized', '×' means 'not polymerized'.

As shown in **Figure 2**, bio-based plastics can be broadly classified into the following two categories in terms of synthesis methods: (1) chemical polymerization, (2) polymerization *via* biosynthesis. Although bio-based plastics mentioned above have been developed currently with the response to solve the environmental problems, specific polymerization techniques, catalysts, multi-step chemical reactions are needed to obtain these polymers. These drawbacks may lead to some environmental issues when producing bio-based plastics. In recent studies, PLA was successfully produced through bio-process without chemical treatment; however, this method cannot achieve the quantitative synthesis and the obtained polymer is a random copolymer.[33,34] Therefore, it is hopeful that the bio-based monomers are polymerized through the fermentation process without a specific catalyst and toxic by-products.

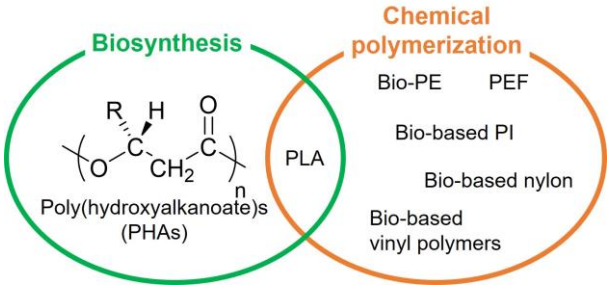


**Figure 2.** Classification of bio-based plastics into the kinds of polymerization .

## 1.3. Poly(hydroxyalkanoate)s (PHAs)

PHAs are synthesized by a fermentation process from natural resources such as plant oils and saccharides to storage an intercellular-carbon and energy (**Figure 2**), which conception illustrated is displayed in **Figure 3**.[35] After PHAs consumption, the PHAs-based products are degraded by bacteria digestion to generate $H_2O$ and $CO_2$; subsequently, plants produce the oils or polysaccharides as starting compounds for PHAs from $H_2O$ and $CO_2$. This cycle is called 'Carbon neutral', indicating that the amount of

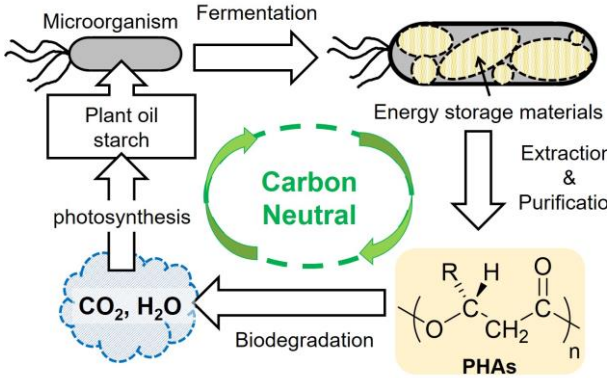


**Figure 3.** Concept of carbon neutral society using PHAs materials.

$CO_2$ emitted and absorbed in the same when something is produced, or a series of anthropogenic activities are carried out. Here, the history of PHAs development research is described as below. In 1925, poly(3-hydroxybutyrate) (PHB), a kind of PHAs, was produced by Lemoigne through the fermentation process, which is the polymer with 3-hydroxybutyric acid with 100% R-configuration regularity in the optical linearly linked.[36] PHB is a highly crystalline polymer, resulting in a high elastic modulus comparable to PP; however, PHB is brittle and low flexibility because of its high crystallinity, leading to limit its industrial applications.[37,38] To overcome the lack of PHB mechanical properties, PHA-based random copolymers have been developed over the last few decades.[39,40] Unlike bio-based polymers mentioned above such as PLA, the chemical structures of PHA monomers and copolymerization ratio of PHA copolymers can be freely changed by selecting the species of microorganisms and the kind of plant oils and saccharides as starting materials. These chemical structure changes can control the physical properties of PHAs including crystallinity, mechanical strength, and biodegradability. **Figure 4** shows the examples of the PHA copolymers produced by fermentation under various conditions.[41] As for the alkyl chain length of PHA side groups, PHAs are mainly categorized into two groups: (1) short-chain length PHAs (scl-PHAs) and medium-chain length PHAs (mcl-PHAs). In detail, scl-PHAs have C1, C2 alkyl chains on their side chains; conversely, mcl-PHAs have more than C3 alkyl chains.[42,43] The change in the length of PHA side alkyl chains can tune the crystallinity, mechanical properties; concretely, increasing the alkyl chain length decrease the crystallinity of PHAs, leading to improve the mechanical flexibility and decline the stiffness such as Young's modulus and tensile strength because the bulky side moieties prevent the crystallization of PHA backbones.[44,45] Aromatic groups can be also introduced to PHAs side chains by bacteria fermentation.[46] Furthermore, the backbone length of the PHA unit is also extended by changing the fermentation condition and starting materials.[47,48] This structure change can also control the crystallinity of PHAs, changing the mechanical properties. On the contrary, reactive chains can be introduced to PHAs side chains in the same ways.[49] It is reported that PHAs with the C=C end group is successfully prepared and endowed with the

fluorescence property by further chemical modifications.[50] Also, the photo-crosslinked gel is prepared by PHAs with C=C moieties with thiol-ene reaction, applied for tissue engineering.[51,52] Thus, the modifications of PHAs structure *via* fermentation are surprisingly useful to control its physical properties and add new functionalities.

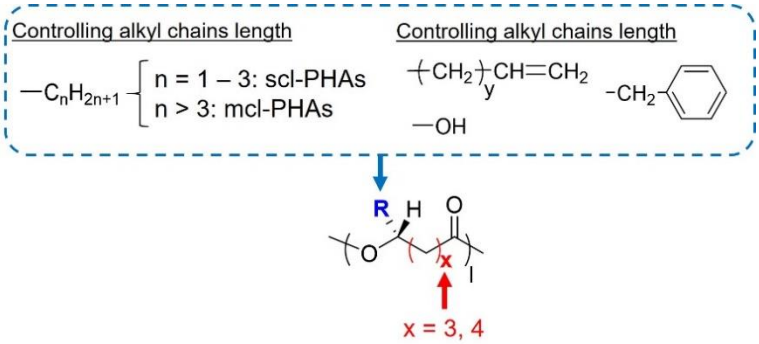


**Figure 4.** PHAs with various chemical structures by microbial polymerization.

A typical mcl-PHAs consisting of 3-hydroxybutyrate (3HB) and 3-hydroxyhexanoate (3HHx) units, poly(3-hydroxybutyrate-*co*-3-hydroxyhexanoate) (PHBH), have been developed,[39,53] which synthesis scheme is described in **Scheme 5**. In Japan, KANEKA Co., Ltd. industrially produces PHBH at a scale of more than 5,000 t/year.[42] It has been reported that the mechanical properties of PHBH strongly depend on the content of the 3HHx unit in PHBH; especially, toughness and ductility of PHBH is increased with the content of 3HHx units increased.[53] Although the synthesis of PHBH achieved the improvement in the flexibility of PHB, Young's modulus and mechanical strength of PHBH decreased because the crystallinity of PHBH became low with bulky 3HHx units increased.[54] Therefore, to employ PHBH as an industrial material, it is important to improve the mechanical strength by maintaining the unique ductility of PHBH.

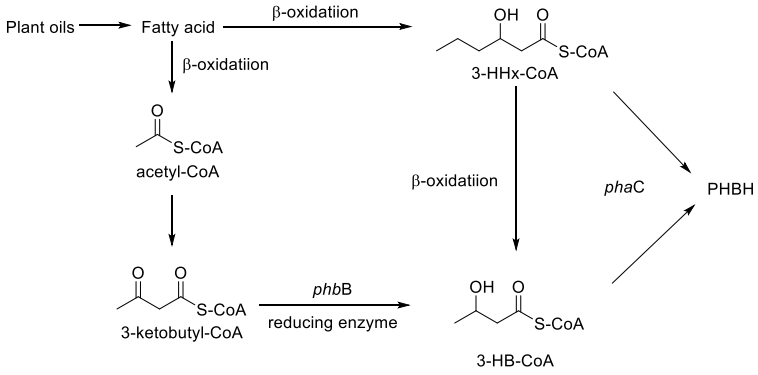


**Scheme 5**. Synthesis of PHBH by micrbial fermentation.

## 1.4. Polymer blend with PHAs and PHAs-based composite materials

Generally, a binary polymer blend is one of the most common strategies to improve the physical properties of plastics. As for PHBH, many researchers have reported various PHBH-based blends to adjust its physical properties. For example, PHBH/PC had high thermal stability.[55] When blending PHBH with poly(vinyl alcohol), the biodegradability and the hydrophilicity of blends were controlled by the change in PHBH/PVA weight ratio.[56] Also, the biodegradability and mechanical characteristics of PHBH were tuned by poly(ε-caprolactone) (PCL) to use for tissue engineering.[57,58] Furthermore, bio-based PHBH/PLA blends were good mechanical strength and ductility for biomaterial applications.[59,60] Hence, polymer blend strategies are expected to the expansion of the PHAs applications in various fields including industrial uses, biomedical tools, and commodity items. These contributions will also promote its consumption, realizing a green sustainable society.

However, it is generally said that for binary polymer blend, a polymer is immiscible for another polymer (**Figure 5**). Because of the low miscibility of the polymer blend, the phase separation is generated in the bulk film, leading to a deterioration of its mechanical properties.[61,62] This decrease is related that the stress ununiformly propagated in the film; therefore, the compatibility of the binary blend should be improved. Indeed, the PHBH-base polymer blends mentioned above are immiscible. To enhance the miscibility of PHBH-based blends, melt kneading is one of the effective strategies; this method is that more than two kinds of polymers are mixed under a liquid state to get homogeneous blends (**Figure 6**).[63–65] Moreover, reactive processing has also been employed to obtain homogeneous polymer blends. This method means that during the kneading, the graft copolymer or crosslinking is generated in polymer blends using polymers with reactive groups or mixing with a radical initiator such as a peroxide compound, and the generated copolymers by reactive processing

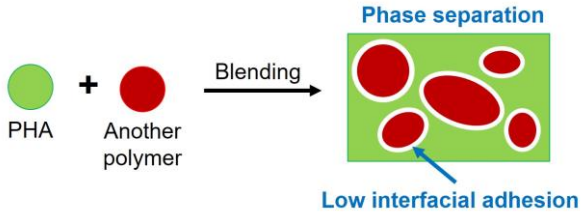


**Figure 5.** Typical issues for polymer blends.

play an important role as a compatibilizer.[61,66–69] Regarding PHAs, the interfacial compatibility between PHAs and other polymers was improved with peroxide reagent, epoxy group, and maleic anhydride moiety.[69–71] However, it may be concerned that PHAs are thermally decomposed by the kneading and reactive processing, leading to reduce its characteristic physical properties.[72] Therefore, it is important to enhance the compatibility of PHAs-based blends without deterioration of PHAs.

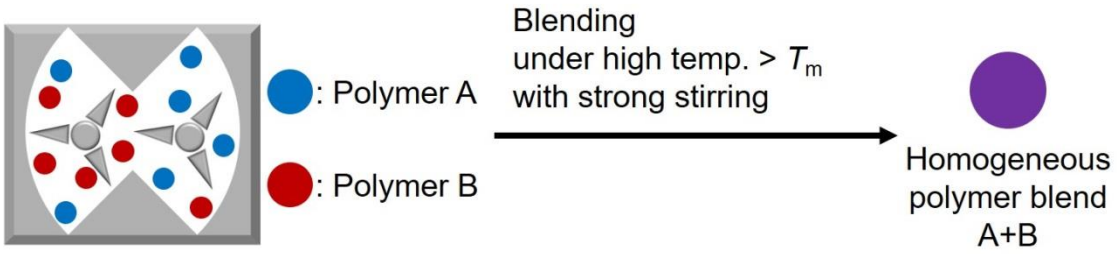


**Figure 6**. Schematic images of uniform polymer blend preparation by melt kneading.

On the other hand, the fabrication of composite materials consisting of PHAs is also one of the most reasonable methods to improve mechanical stiffness. Indeed, to improve Young's modulus and tensile strength of PHAs, some researchers prepared and evaluated PHAs with inorganic fillers, such as silica particles ($SiO_2$),[54,73] clay,[74–76] ceramics,[77] sea sand,[78] and glass fiber[79,80]. However, because of the low interfacial adhesion between hydrophilic filler surface and the hydrophobic PHA matrix, elastic modulus and mechanical strength of PHA/filler composite materials remain low[54]; moreover, the low interfacial adhesion between filler and matrix causes the agglomeration of fillers and generates crack and void on the PHA/filler interface; these phenomena induce the decrease in the yield stress and toughness of PHAs[74,78] (**Figure 7**). Therefore, to prepare an effective filler for PHAs, the interfacial compatibility between PHAs and the inorganic filler must be improved, leading to expanded usage of PHAs. Hence, for improving the mechanical properties of PHAs/fillers composites, their interfacial adhesion must be enhanced with maintaining the uniform dispersity of filler.

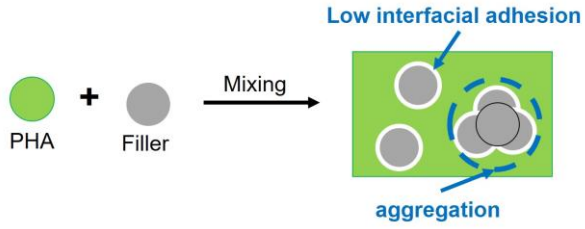


**Figure 7.** Problems for PHAs/filler composites.

## 1.6. This study

In this doctoral thesis, the author proposes the use of end-reactive PHBH as a new strategy to enhance the interfacial compatibility between PHA and different materials in the polymer blends and composite materials. In this study, propargyl-terminated PHBH (Propargyl-PHBH) is employed as an end-reactive PHBH (**Figure 8**). Propargyl-PHBH was found to be quantitatively introduced at the terminal moiety of PHAs by the addition of propargyl alcohol through the chemical treatment[81] or the fermentation process[82,83]. Propargyl group is a functional group that is used for copper-catalyzed azide-alkyne cycloaddition (CuAAC) reaction, a kind of click chemistry (**Scheme 6**). Click chemistry is a powerful tool because of its high reactivity under mild conditions.[84,85] Then, it has been investigated that synthesis of the graft copolymers,[86] block copolymers,[87] and branched polymers,[88] and surface modification of the fillers[89] are succeeded through click chemistry. The obtained copolymer can also play a role as a compatibilizer. As well, a surface-modified filler can improve the mechanical properties of PHBH more efficiently than the non-modified filler and conventional methods.

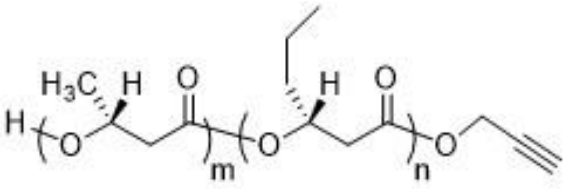


**Figure 8.** Chemical structure of Propargyl-PHBH.

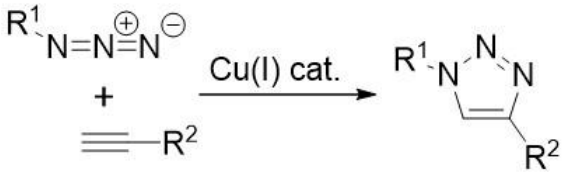


**Scheme 6.** CuAAC reaction with ethynyl group and azide group.

# Contents of this thesis

This doctoral thesis consists of the introduction, three parts, and the conclusion mentioned below.

**Chapter 1**

In this chapter, for improving the mechanical characteristics of PHBH to eventually broaden its industrial applications, it was blended with poly(methyl methacrylate) (PMMA), a rigid polymer. Moreover, blending PHBH was also expected to increase the toughness of PMMA. Nevertheless, PHBH/PMMA blends lack interfacial adhesion due to low miscibility, thus restricting potential applications. This work focuses on enhancing the compatibility of the PHBH/PMMA blend by developing a compatibilizer. The synthesis of PMMA-*g*-PHBH, a graft copolymer, was carried out using methyl methacrylate and vinyl-terminated PHBH derived from propargyl-terminated PHBH. The findings obtained from scanning electron microscopy and thermal analysis showed improvement in the miscibility of PHBH and PMMA upon the inclusion of PMMA-*g*-PHBH in the blend structure. The mechanical properties of the blends can also be tuned by controlling the weight fraction of PHBH/PMMA/PMMA-*g*-PHBH. This chapter proves that PMMA-*g*-PHBH acts as an effective compatibilizer for PHBH/PMMA blends.

**Chapter 2**

This chapter reported the preparation of the graft copolymer consisting of PHBH and polystyrene (PSt) which is a rigid, transparent, and low-cost polymer, to expand the application of PHBH. PSt-*g*-PHBH was synthesized from propargyl-terminated PHBH (Propargyl-PHBH) and azide-modified PSt *via* copper-catalyzed azide-alkyne cycloaddition reaction. PHBH/PSt blend films showed heterogeneous, opaque, and brittle. In contrast, PSt-*g*-PHBH films exhibited surprisingly good homogeneity, transparency, and high mechanical properties (Young's modulus ~ 1.24 GPa and tensile strength ~ 30 MPa). Furthermore,

thermal analysis and theoretical discussion based on the Pukánszky model explained that the compatibility and stress transfer capacity of PHBH/PSt blend films were enhanced by grafting to PSt backbones with Propargyl-PHBH. Hence, the physical properties of PHBH such as optical and mechanical properties are improved by grafting to PSt. The present study can contribute to expanding the application of PHBH to various fields such as engineering materials, commodity plastics, and food packaging.

**Chapter 3**

In this chapter, for the purpose of enhancing the interfacial adhesion of $SiO_2$ and PHBH, the PHBH-grafted $SiO_2$ ($SiO_2$-PHBH) fillers were prepared from propargyl-terminated PHBH and azide-modified $SiO_2$ by click chemistry. Scanning electron microscopy (SEM) revealed that $SiO_2$-PHBH fillers dispersed uniformly in PHBH. In contrast, the $SiO_2$ fillers were aggregated in PHBH. Thermal analysis of the PHBH/$SiO_2$-PHBH composite films revealed that the glass transition temperature shifted to a high temperature. Young's modulus and yield stress of the PHBH/$SiO_2$-PHBH composite films were increased with increasing concentration of $SiO_2$-PHBH. In contrast, PHBH/$SiO_2$ composite films showed only a small increase in the elastic modulus and a decrease in the yield stress. These results revealed that $SiO_2$-PHBH improves the mechanical properties of PHBH, and it is expected to expand the industrial applications of PHBH.

# References


[1] A. Sangroniz, J. B. Zhu, X. Tang, A. Etxeberria, E. Y. X. Chen, H. Sardon, *Nat. Commun.* **2019**, *10*, 1.

[2] Y. Wang, E. J. Jeon, J. Lee, H. Hwang, S. W. Cho, H. Lee, *Adv. Mater.* **2020**, *32*, 1.

[3] J. Thorneycroft, J. Orr, P. Savoikar, R. J. Ball, *Constr. Build. Mater.* **2018**, *161*, 63.

[4] M. Ajorloo, M. Ghodrat, W. H. Kang, *J. Polym. Environ.* **2020**, DOI 10.1007/s10924-020-01961-y.

[5] Y. Tao, S. Hinduja, R. Heinemann, A. Gomes, P. J. Bártolo, *Polymers* **2020**, *12*, 1.

[6] Z. Gong, J. Gong, X. Yan, S. Gao, B. Wang, *J. Phys. Chem. C* **2011**, *115*, 18468.

[7] U. A. Dar, Y. J. Xu, S. M. Zakir, M. U. Saeed, *J. Appl. Polym. Sci.* **2017**, *134*, 1.

[8] M. Z. Pakhuruddin, K. Ibrahim, A. A. Aziz, *Optoelectron. Adv. Mater. Rapid Commun.* **2013**, *7*, 377.

[9] M. G. Faraj, K. Ibrahim, M. K. M. Ali, *Optoelectron. Adv. Mater. Rapid Commun.* **2011**, *5*, 879.

[10] J. Qian, X. Li, D. J. Lunn, J. Gwyther, Z. M. Hudson, E. Kynaston, P. A. Rupar, M. A. Winnik, I. Manners, *J. Am. Chem. Soc.* **2014**, *136*, 4121.

[11] P. A. Finn, I. E. Jacobs, J. Armitage, R. Wu, B. D. Paulsen, M. Freeley, M. Palma, J. Rivnay, H. Sirringhaus, C. B. Nielsen, *J. Mater. Chem. C* **2020**, *8*, 16216.

[12] S. B. Borrelle, C. M. Rochman, M. Liboiron, A. L. Bond, A. Lusher, H. Bradshaw, J. F. Provencher, *Proc. Natl. Acad. Sci. U. S. A.* **2017**, *114*, 9994.

[13] M. Haward, *Nat. Commun.* **2018**, *9*, 9.

[14] G. Q. Chen, M. K. Patel, *Chem. Rev.* **2012**, *112*, 2082.

[15] J. B. Zeng, K. A. Li, A. K. Du, *RSC Adv.* **2015**, *5*, 32546.

[16] B. A. Calderón, M. S. McCaughey, C. W. Thompson, V. L. Barinelli, M. J. Sobkowicz, *ACS Appl. Polym. Mater.* **2019**, *1*, 1410.

[17] T. Kanno, H. Uyama, *RSC Adv.* **2017**, *7*, 33726.

[18] M. A. Ali, T. Kaneko, *Ind. Eng. Chem. Res.* **2019**, *58*, 15958.

[19] A. F. Sousa, C. Vilela, A. C. Fonseca, M. Matos, C. S. R. Freire, G. J. M. Gruter, J. F. J. Coelho, A. J. D. Silvestre, *Polym. Chem.* **2015**, *6*, 5961.

[20] G. Z. Papageorgiou, V. Tsanaktsis, D. G. Papageorgiou, K. Chrissafis, S. Exarhopoulos, D. N. Bikiaris, *Eur. Polym. J.* **2015**, *67*, 383.

[21] P. Suvannasara, S. Tateyama, A. Miyasato, K. Matsumura, T. Shimoda, T. Ito, Y. Yamagata, T. Fujita, N. Takaya, T. Kaneko, *Macromolecules* **2014**, *47*, 1586.

[22] S. Tateyama, S. Masuo, P. Suvannasara, Y. Oka, A. Miyazato, K. Yasaki, T. Teerawatananond, N. Muangsin, S. Zhou, Y. Kawasaki, L. Zhu, Z. Zhou, N. Takaya, T. Kaneko, *Macromolecules* **2016**, *49*, 3336.

[23] V. Froidevaux, C. Negrell, S. Caillol, J. P. Pascault, B. Boutevin, *Chem. Rev.* **2016**, *116*, 14181.

[24] V. Siracusa, I. Blanco, *Polymers* **2020**, *12*, DOI 10.3390/APP10155029.

[25] K. Satoh, *Polym. J.* **2015**, *47*, 527.

[26] W. Y. Jeon, M. J. Jang, G. Y. Park, H. J. Lee, S. H. Seo, H. S. Lee, C. Han, H. Kwon, H. C. Lee, J. H. Lee, Y. T. Hwang, M. O. Lee, J. G. Lee, H. W. Lee, J. O. Ahn, *Green Chem.* **2019**, *21*, 6491.

[27] A. B. Dros, O. Larue, A. Reimond, F. De Campo, M. Pera-Titus, *Green Chem.* **2015**, *17*, 4760.

[28] A. Marckwordt, F. El Ouahabi, H. Amani, S. Tin, N. V. Kalevaru, P. C. J. Kamer, S. Wohlrab, J. G. de Vries, *Angew. Chem. Int. Ed.* **2019**, *58*, 3486.

[29] T. Nishida, K. Satoh, S. Nagano, T. Seki, M. Tamura, Y. Li, K. Tomishige, M. Kamigaito, *ACS Macro Lett.* **2020**, *9*, 1178.

[30] H. Takeshima, K. Satoh, M. Kamigaito, *Polym. Chem.* **2019**, *10*, 1192.

[31] Y. Terao, K. Satoh, M. Kamigaito, *Biomacromolecules* **2019**, *20*, 192.

[32] K. Satoh, D. H. Lee, K. Nagai, M. Kamigaito, *Macromol. Rapid Commun.* **2014**, *35*, 161.

[33] S. Taguchi, M. Yamada, K. Matsumoto, K. Tajima, Y. Satoh, M. Munekata, K. Ohno, K. Kohda, T. Shimamura, H. Kambe, S. Obata, *Proc. Natl. Acad. Sci. U. S. A.* **2008**, *105*, 17323.

[34] F. Shozui, K. Matsumoto, R. Motohashi, J. Sun, T. Satoh, T. Kakuchi, S. Taguchi, *Polym. Degrad. Stab.* **2011**, *96*, 499.

[35] G. Q. Chen, *Chem. Soc. Rev.* **2009**, *38*, 2434.

[36] R. W. Lenz, R. H. Marchessault, *Biomacromolecules* **2005**, *6*, 1.

[37] C. Mangeon, L. Michely, A. Rios De Anda, F. Thevenieau, E. Renard, V. Langlois, *ACS Sustain. Chem. Eng.* **2018**, *6*, 16160.

[38] D. Garcia-Garcia, O. Fenollar, V. Fombuena, J. Lopez-Martinez, R. Balart, *Macromol. Mater. Eng.* **2017**, *302*, 1600330.

[39] Y. Doi, S. Kitamura, H. Abe, *Macromolecules* **1995**, *28*, 4822.

[40] L. Urbina, P. Wongsirichot, M. Á. Corcuera, N. Gabilondo, A. Eceiza, J. Winterburn, A. Retegi, *Eur. Polym. J.* **2018**, *108*, 1.

[41] P. C. Sabapathy, S. Devaraj, K. Meixner, P. Anburajan, P. Kathirvel, Y. Ravikumar, H. M. Zabed, X. Qi, *Bioresour. Technol.* **2020**, *306*, 123132.

[42] S. Taguchi, K. Matsumoto, *Polym. J.* **2020**, DOI 10.1038/s41428-020-00420-8.

[43] Z. Li, J. Yang, X. J. Loh, *NPG Asia Mater.* **2016**, *8*, e265.

[44] J. S. F. Barrett, A. A. Abdala, F. Srienc, *Macromolecules* **2014**, *47*, 3926.

[45] A. Larrañaga, F. Pompanon, N. Gruffat, T. Palomares, A. Alonso-Varona, A. Larrañaga Varga, M. A. Fernandez-Yague, M. J. P. Biggs, J. R. Sarasua, *Eur. Polym. J.* **2016**, *85*, 401.

[46] S. Mizuno, A. Hiroe, T. Fukui, H. Abe, T. Tsuge, *Polym. J.* **2017**, *49*, 557.

[47] T. H. Ying, D. Ishii, A. Mahara, S. Murakami, T. Yamaoka, K. Sudesh, R. Samian, M. Fujita, M. Maeda, T. Iwata, *Biomaterials* **2008**, *29*, 1307.

[48] S. S. Costa, A. L. Miranda, M. G. de Morais, J. A. V. Costa, J. I. Druzian, *Int. J. Biol. Macromol.* **2019**, *131*, 536.

[49] H. Dong, S. Liffland, M. A. Hillmyer, M. C. Y. Chang, *J. Am. Chem. Soc.* **2019**, *141*, 16877.

[50] L. P. Yu, X. Zhang, D. X. Wei, Q. Wu, X. R. Jiang, G. Q. Chen, *Biomacromolecules* **2019**, *20*, 3233.

[51] A. C. Levine, A. Sparano, F. F. Twigg, K. Numata, C. T. Nomura, *ACS Biomater. Sci. Eng.* **2015**, *1*, 567.

[52] X. Zhang, Z. Li, X. Che, L. Yu, W. Jia, R. Shen, J. Chen, Y. Ma, G. Q. Chen, *Biomacromolecules* **2019**, *20*, 3303.

[53] H. Alata, T. Aoyama, Y. Inoue, *Macromolecules* **2007**, *40*, 4546.

[54] Y. Xie, D. Kohls, I. Noda, D. W. Schaefer, Y. A. Akpalu, *Polymer* **2009**, *50*, 4656.

[55] Y. Xin, H. Uyama, *Chem. Lett.* **2012**, *41*, 1509.

[56] R. A. Rebia, S. Rozet, Y. Tamada, T. Tanaka, *Polym. Degrad. Stab.* **2018**, *154*, 124.

[57] J. Lim, M. S. K. Chong, E. Y. Teo, G. Q. Chen, J. K. Y. Chan, S. H. Teoh, *J. Biomed. Mater. Res. - Part B Appl. Biomater.* **2013**, *101 B*, 752.

[58] J. Ivorra-Martinez, I. Verdu, O. Fenollar, L. Sanchez-Nacher, R. Balart, L. Quiles-Carrillo, *Polymers* **2020**, *12*, DOI 10.3390/POLYM12051118.

[59] Y. Gao, L. Kong, L. Zhang, Y. Gong, G. Chen, N. Zhao, X. Zhang, *Eur. Polym. J.* **2006**, *42*, 764.

[60] Y. He, Z. Hu, M. Ren, C. Ding, P. Chen, Q. Gu, Q. Wu, *J. Mater. Sci. Mater. Med.* **2014**, *25*, 561.

[61] C. Koning, M. Van Duin, C. Pagnoulle, R. Jerome, *Prog. Polym. Sci.* **1998**, *23*, 707.

[62] N. Goonoo, A. Bhaw-Luximon, D. Jhurry, *Polym. Int.* **2015**, *64*, 1289.

[63] A. Ostafinska, I. Fortelny, M. Nevoralova, J. Hodan, J. Kredatusova, M. Slouf, *RSC Adv.* **2015**, *5*, 98971.

[64] S. Shi, P. Huang, M. Nie, Q. Wang, *Polymer* **2017**, *132*, 23.

[65] S. Saha, A. K. Bhowmick, A. Kumar, K. Patra, P. J. Cottinet, K. Thetpraphi, *Ind. Eng. Chem. Res.* **2020**, *59*, 3413.

[66] N. P. Levenhagen, M. D. Dadmun, *Macromolecules* **2019**, *52*, 6495.

[67] S. Luo, J. Cao, A. G. McDonald, *ACS Sustain. Chem. Eng.* **2016**, *4*, 3465.

[68] A. K. Pal, F. Wu, M. Misra, A. K. Mohanty, *Compos. Part B Eng.* **2020**, *198*, 108141.

[69] P. Xu, Q. Zeng, Y. Cao, P. Ma, W. Dong, M. Chen, *Carbohydr. Polym.* **2017**, *174*, 716.

[70] Y. Ke, X. Y. Zhang, S. Ramakrishna, L. M. He, G. Wu, *Mater. Sci. Eng. C* **2017**, *70*, 1107.

[71] L. Wei, A. G. McDonald, N. M. Stark, *Biomacromolecules* **2015**, *16*, 1040.

[72] X. Yang, J. Clénet, H. Xu, K. Odelius, M. Hakkarainen, *Macromolecules* **2015**, *48*, 2509.

[73] D. Li, J. Fu, X. Ma, *Polym. Compos.* **2019**, *41*, 381.

[74] Q. Zhang, Q. Liu, J. E. Mark, I. Noda, *Appl. Clay Sci.* **2009**, *46*, 51.

[75] J. Yang, Y. Li, G. Qin, *J. Macromol. Sci. Part B Phys.* **2017**, *56*, 373.

[76] A. W. Ajmal, F. Masood, T. Yasin, *Appl. Clay Sci.* **2018**, *156*, 11.

[77] S. Ke, Y. Yang, L. Ren, Y. Wang, Y. Li, H. Huang, *Compos. Sci. Technol.* **2012**, *72*, 370.

[78] M. Seggiani, P. Cinelli, N. Mallegni, E. Balestri, M. Puccini, S. Vitolo, C. Lardicci, A. Lazzeri, *Materials* **2017**, *10*, 326.

[79] A. Willson, K. Takashi, *Polym. Compos.* **2018**, *39*, 491.

[80] A. Willson, K. Takashi, *Polym. Compos.* **2018**, *39*, 1331.

[81] P. Lemechko, E. Renard, G. Volet, C. S. Colin, J. Guezennec, V. Langlois, *React. Funct. Polym.* **2012**, *72*, 160.

[82] M. Hyakutake, S. Tomizawa, I. Sugahara, E. Murata, K. Mizuno, H. Abe, T. Tsuge, *Polym. Degrad. Stab.* **2015**, *117*, 90.

[83] T. Tsuge, *Polym. J.* **2016**, *48*, 1051.

[84] V. V. Rostovtsev, L. G. Green, V. V. Fokin, K. B. Sharpless, *Angew. Chem. Int. Ed.* **2002**, *114*, 2708.

[85] B. T. Worrell, J. a. Malik, V. V. Fokin, *Science* **2013**, *340*, 457.

[86] A. C. Engler, H. Il Lee, P. T. Hammond, *Angew. Chem. Int. Ed.* **2009**, *48*, 9334.

[87] P. M. Reichstein, J. C. Brendel, M. Drechsler, M. Thelakkat, *ACS Appl. Nano Mater.* **2019**, *2*, 2133.

[88] H. Naguib, X. Cao, H. Gao, *Macromol. Chem. Phys.* **2019**, *220*, 1.

[89] M. Arslan, M. A. Tasdelen, *Polymers* **2017**, *9*, 499.

# Chapter 1

## Enhancing compatibility between immiscible biomass plastic and oil-based plastic by using a graft copolymer synthesized from propargyl-terminated poly(3-hydroxybutyrate-*co*-3-hydroxyhexanoate)

## 1.1. Introduction

As mentioned in the general introduction, PHBH, a series of PHAs, has gained significant attention as a bio-derived, non-toxic, and biodegradable plastic that is produced by the fermentation of sugars or plant oils. The physical properties of PHBH such as crystallinity, ductility, and mechanical strength can be easily tuned by the amount of bulky 3HHx units.[1,2] Although this advantage overcomes the brittleness of PHB, its Young's modulus and tensile strength are decreased because of lowering the crystallinity, and not enough for the industrial applications including packaging products, commodity, and engineering materials.

The author explains that in the general introduction, a polymer binary blend is one of the promising strategies, rendering physical properties to PHBH for expanding its applications in daily life.[3–6] In this part, PMMA was chosen for polymer blends with PHBH. PMMA is one of the widely employed polymers for the production of organic glass and commodity plastics due to its exceptionally high elastic modulus and rigidity, which could also serve as one of the potential polymers for blending with PHBH since blending rigid PMMA can improve the elastic modulus and maximum strength of PHBH.[7,8] Conversely, PMMA has low ductility and toughness, limiting its applications.[9] Therefore, it is hoped that the binary blending of PHBH and PMMA will overcome the mechanical weaknesses of individual components including the low elastic modulus and tensile strength of PHBH and

low toughness of PMMA. This proposal will also promote the usage of PHBH as a bio-based flexibilizer, thus improving the fragility of polymers.

However, mentioned above, PHBH-based blends generally cause phase separation in the film due to the low miscibility of PHBH with other polymers.[10] Such a phase separation phenomenon in the PHBH/PMMA blend decreases the mechanical toughness and ductility of the blends, thereby restricting their industrial applications.[11–13] Thus, it is necessary to augment the compatibility of the PHBH/PMMA blend which could be achieved by adding additives into the polymeric blend. In such a condition, the incorporation of a compatibilizer is argued to improve the interfacial adhesion between PHBH and PMMA. For instance, as a compatibilizer for the improvement of interfacial adhesion between the polymeric blends, the applications of graft copolymers,[14–16] block copolymers,[17,18] Janus particles,[19,20] and surface-modified carbon nanotubes[13,21,22] have been investigated. In this chapter, the author attempted the development of a compatibilizer based on PHBH graft copolymers, which was prepared by facile methods under mild conditions.[14–16] Moreover, the type of monomers and the reaction conditions are the two governing factors that determine the design of polymeric structures.[14,23] Mentioned in the general introduction, recently, end-functionalized PHAs have been used for the synthesis of block copolymers, graft copolymers, and branched copolymers through the various facile processes.[24–26] Propargyl-PHBH, one of the end-functionalized PHAs, is expected to synthesize a graft copolymer *via* CuAAC reaction.[27–31] In the latest research, Oyama and his coworkers reported that PHBH-*b*-PCL was prepared from Propargyl-PHBH, used as a compatibilizer for PHBH/PCL blends.[18]

In this chapter, the author proposed the development of a compatibilizer that is synthesized from vinyl-terminated PHBH (Vinyl-PHBH) and methyl methacrylate (MMA) *via* the '*grafting through*' method to improve the compatibility and enhance the mechanical properties of PHBH and PMMA blend. Vinyl-PHBH was derived from Propargyl-PHBH

through the CuAAC reaction. **Figure 1.1** shows the incorporation of a compatibilizer in PHBH and PMMA blend to render good miscibility thus improving the mechanical properties. The morphological, thermal, and mechanical characterizations of PHBH/PMMA blends with the obtained graft copolymer were investigated to elucidate the physicochemical and structural characteristics and further compared with neat PHBH/PMMA blends. This chapter presents the novel application of PHBH as an additive both in terms of a flexibilizer and a compatibilizer for polymer blends constituting rigid polymers such as PMMA by using end-reactive PHBH. Furthermore, the obtained results will promote the utilization of bioplastics, thus reducing the environmental burdens caused due to the reckless usage of non-biodegradable plastic materials in the field of material engineering.

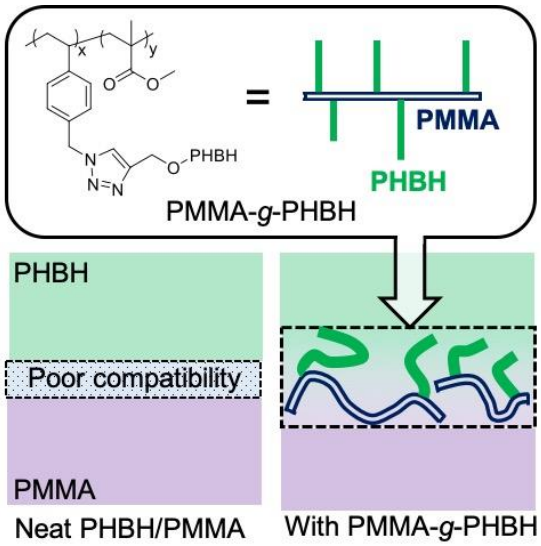


**Figure 1.1.** Illustration of immiscible PHBH/PMMA blends with low interfacial adhesion and improvement in the interfacial compatibility between PHBH and PMMA upon inclusion with PMMA-*g*-PHBH.

## 1.2. Experimental section

### 1.2.1. Materials

PHBH ($M_w$ = 660,000, 3HHx units = 11 mol% determined by $^1$H NMR measurement) and Propargyl-PHBH ($M_n$ = 25,000, 3HHx units = 11 mol%) were kindly offered by KANEKA Co. (Osaka, Japan). The synthesis method of Propargyl-PHBH was described in the previous report.[32] Propargyl-PHBH was dissolved in chloroform and reprecipitated in methanol before use. *p*-Chloromethylstyrene (CMS) was purchased from Tokyo Chem. Ind.

(TCI, Tokyo, Japan). MMA was purchased from Nacalai Tesque Inc. (Nacalai, Kyoto, Japan). These monomers were purified by using the alumina column to remove inhibitors. 2,2'-Azobis(isobutyronitrile) (AIBN) was obtained from FUJIFILM Wako Pure Chemical Corporation (Wako, Osaka, Japan) and used after recrystallization in methanol. *N*,*N*-dimethylformamide (DMF) was purchased from Nacalai and reserved with molecular sieves (4A) to remove residual water. *N,N,N',N'',N''*-pentamethyldiethylenetriamine (PMDETA, TCI), methanol (Wako), copper(I) bromide (Wako), diethyl ether (Wako), PMMA (Nacalai, degree of polymerization = 1,000), sodium azide (Nacalai), dichloromethane (Nacalai), chloroform (Nacalai), toluene (Nacalai), and sodium sulfate (Nacalai) were used as received.

### 1.2.2. Synthesis of *p*-azidemethylstyrene (AMS)

AMS was synthesized using CMS and sodium azide by following Hackethal's report.[33] CMS (4.4 g, 30 mmol) and sodium azide (3.9 g, 60 mmol) were mixed with dried DMF (30 mL) before being subjected to $N_2$ bubbling for 10 min. The mixture was then stirred for 12 h at 25 °C. The product was extracted from diethyl ether (200 mL) and washed with Milli-Q water/brine several times, followed by drying over sodium sulfate. To obtain AMS, the solvent was removed by evaporation (3.3 g, yield: 69%, Conv. > 99% observed by $^1$H NMR).

$^1$H NMR ($CDCl_3$, 400 MHz): 7.42 ppm (d, 2H, *J* = 7.9, Ar-H), 7.27 ppm (d, 2H, *J* = 7.9, Ar-H), 6.72 ppm (dd, 1H, *J* = 10.9, CH=C), 5.79 ppm (d, 1H, *J* = 17.0, C=C$H_2$), 5.27 ppm (d, 1H, *J* = 11.6, C=C$H_2$), 4.31 ppm (s, 2H, C$H_2N_3$).

### 1.2.3. Synthesis of Vinyl-PHBH from Propargyl-PHBH

**Scheme 1.1** shows the schematic of the coupling procedure of the propargyl group of PHBH with the azide group of AMS. At first, Propargyl-PHBH (25 g, propargyl group = 1 mmol) was dissolved in dichloromethane (100 mL) followed by the addition of AMS (3.2 g, 20 mmol), PMDETA (173 mg, 1 mmol), and copper(I) bromide (144 mg, 1 mmol) after $N_2$ bubbling for 30 min. The reaction mixture was stirred at 25 °C for 24 h under an $N_2$ atmosphere. The solution was concentrated under reduced pressure to decrease the amount of dichloromethane and the residue was poured into cold methanol (800 mL) to form precipitates. This procedure was repeated several times. After filtration and drying, the obtained product was dissolved in chloroform (100 mL) and subsequently stirred with aluminum oxide to remove residual Cu catalyst. After filtration, the obtained polymer solution was poured into cold methanol (1 L). The collected white powder was dried overnight under reduced pressure (22 g, yield: 86%).

### 1.2.4. Radical polymerization of MMA and Vinyl-PHBH

PMMA-*g*-PHBH was synthesized by radical copolymerization of MMA and Vinyl-PHBH as shown in **Scheme 1.1**. Initially, Vinyl-PHBH (1.0 g, vinyl groups = 42 μmol) was dissolved in toluene (8 mL) at 50 °C. After that, $N_2$ was sparged into the reaction mixture followed by the addition of MMA (1.3 g, 13 mmol) and AIBN (21 mg, 0.13 μmol) with continuous stirring. The reactant mixture was stirred to dissolve AIBN in the solution. Then, the mixture was stirred at 65 °C for 24 h under the argon atmosphere, and the product was collected by reprecipitation into methanol (150 mL). The obtained powder was dissolved in chloroform (conc. = 0.1 g/mL), and a sufficient amount of methanol was added until the

solution became opaque (methanol/chloroform = 8/1 v/v). Finally, the obtained materials were filtrated and dried overnight under vacuum conditions (1.7 g, yield: 74%).

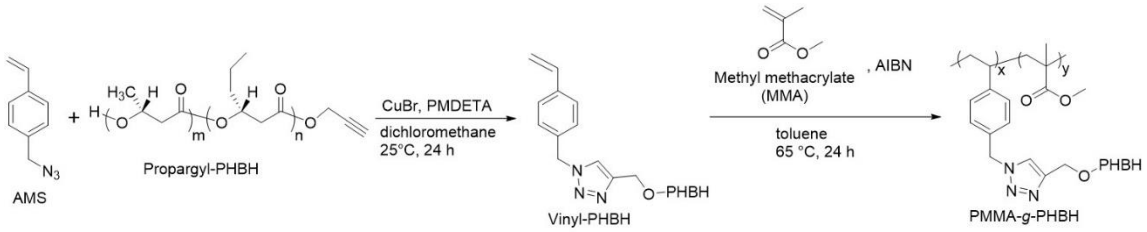


**Scheme 1.1.** Preparation of PMMA-*g*-PHBH by using Propargyl-PHBH as a starting material.

### 1.2.5. Characterization of the synthesized polymers

The molecular weight of the products was measured by size exclusion chromatography (SEC) with a refractive index detector (Tosoh Co., Yamaguchi, Japan) and TSK gel $GMH_{HR}$-M and $GMH_{HR}$-H columns (Tosoh Co., Yamaguchi, Japan). The SEC test was carried out with a flow rate of 1.0 mL/min and a temperature of 40 °C using chloroform as eluent under calibration of the polystyrene standards ($M_n = 5.89 \times 10^2 - 1.11 \times 10^6$). The structure of the prepared polymers was confirmed by $^1$H NMR spectroscopy with a JNM-ECS400 (400 MHz, JEOL Ltd., Tokyo, Japan) in scan times of 512 by using $CDCl_3$ (Cambridge Isotope Laboratories, Inc., Massachusetts, USA) as the solvent. The weight fraction of PMMA to the PMMA-*g*-PHBH was confirmed by thermal gravimetric analysis (TGA) with an SSC/7200+TG/DTA220 (Hitachi High-Tech Science Co., Tokyo, Japan) under $N_2$ atmosphere at a scanning rate of 10 °C/min from 40 °C to 550 °C. The determination of melting point ($T_m$) and glass transition temperature ($T_g$) of the polymers were conducted by differential scanning calorimetry (DSC) with a DSC6220 (Hitachi High-Tech Science Co., Tokyo, Japan). The samples (*ca.* 6 mg) were melted at 180 °C for 2 min and cooled to −50 ºC at a cooling rate of 10 °C/min. Then, the temperature was maintained at -50 °C for 2 min, and the sample was reheated at a rate of 10 °C/min to reach 180 °C. The above DSC measurement was carried out under $N_2$ gas at a flow rate of 50 mL/min.

### 1.2.6. The physical properties of PHBH/PMMA doped with PMMA-*g*-PHBH

For the characterization of the polymer blends with PMMA-*g*-PHBH, the polymeric films were prepared by the solvent casting method, and the procedure is as follows. Firstly, PHBH and PMMA (PHBH/PMMA = 90/10, 70/30, 50/50, and 30/70 wt%/wt%, total mass = 1 g) mixed with PMMA-*g*-PHBH (0, 1, 5, 10 wt% to PHBH/PMMA) were dissolved in chloroform (13 mL) with continuous stirring to prepare a 5 wt% polymeric solution. Subsequently, the solutions were degassed for 1 min and poured into a PFA petri dish ($\phi$ = 10 cm). After overnight drying at room temperature, the sample was pressed at 70 °C under 10 MPa for 10 min to remove the residual solvent. The surface morphologies of the blends were observed by scanning electron microscopy (SEM, SU3500 instrument, Hitachi High-Technologies Co., Tokyo, Japan). DSC measurements evaluated the thermal properties of the PHBH/PMMA/PMMA-*g*-PHBH mixture under the same condition mentioned above. The mechanical property of the prepared films was measured by a Shimadzu EZ Graph (Shimadzu Co., Kyoto, Japan) with a cross-head speed of 10 mm/min. For tensile tests, these films were cut into a dumbbell-shaped sheet (W 0.2 cm × D 2.0 cm) with a thickness of approximately 100 μm.

## 1.3. Results and discussion

### 1.3.1. Characterization of Vinyl-PHBH and MMA

The chemical structures of Vinyl-PHBH and PMMA-*g*-PHBH were identified by $^{1}$H NMR, which spectra were displayed in **Figure 1.2**. $^{1}$H NMR results demonstrate that Vinyl-PHBH and PMMA-*g*-PHBH were successfully synthesized from the following signature peaks. The signal of the propargyl group proton (a) at 4.7 ppm was erased, whereas the

signals related to the vinyl group (j and k) and aromatic (l) protons were newly detected at 5.7 – 5.8, 6.7, and 7.4 – 7.5 ppm, respectively. These results prove that Propargyl-PHBH was easily converted to Vinyl-PHBH with AMS by the CuAAC reaction. After the copolymerization, the signals corresponding to the vinyl group disappeared completely and the peak of the methoxide group of PMMA (2) appeared at 3.6 ppm. Additionally, the signals derived from the aromatic ring of the end-group of PHBH around 7.0 ppm (l') were broadened corresponding to the polymerization with vinyl end-group of PHBH and MMA. The molecular weight of the resultant polymers was determined by SEC measurement. $M_n$ of the graft copolymer was 56,000 which was higher than that of Vinyl-PHBH ($M_n$ = 25,000) and its polydispersity index was slightly increased from 1.8 to 2.0 compared with that of Vinyl-PHBH due to the grafting of PHBH chains to the PMMA backbone. TGA was conducted to measure the weight fraction of PMMA in PMMA-*g*-PHBH. TGA curve of PMMA-*g*-PHBH exhibited two-step weight loss around 250 °C and 300 °C, which was related to the decomposition of PHBH and PMMA leading chains, respectively.[34] As a result, the weight ratio of PMMA was approximately 27 wt%, which is relatively close to the value calculated from $^1$H NMR. $T_g$ of the samples was detected by DSC measurement. The DSC chart shows that $T_g$ of PMMA-*g*-PHBH appeared at −0.4 °C, which lies between that of PHBH (−4.4 °C) and PMMA (100 °C).[34] Since $T_g$ of a graft copolymer exists between the backbone polymer and the grafted polymer, the obtained results confirm the copolymer formation of MMA and Vinyl-PHBH.[35] The shifting of $T_g$ could be due to the PMMA chains' retainment of the glassy state at $T_g$ of PHBH, while the main chains of PHBH decreased in their mobilities. Hence, the characterization mentioned below indicates that Vinyl-PHBH and MMA were successfully copolymerized to synthesize PMMA-*g*-PHBH.

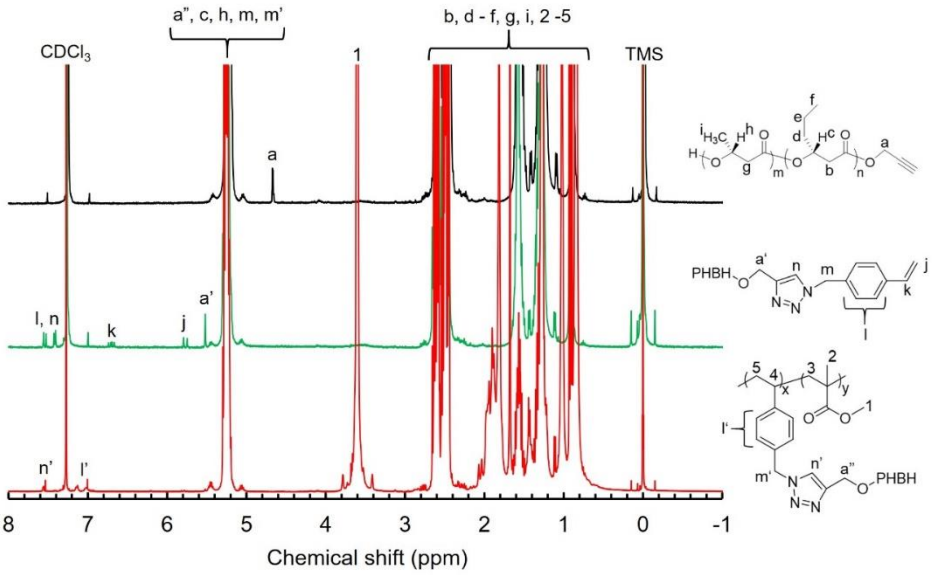


**Figure 1.2.** $^{1}$H NMR spectra of Propargyl-PHBH (black line), Vinyl-PHBH (green line), and PMMA-*g*-PHBH (red line).

### 1.3.2. Morphology observation of PHBH/PMMA blends with PMMA-*g*-PHBH

The surface morphology of the PHBH/PMMA blend films was observed under the SEM. From the SEM images, it was found that PHBH/PMMA blends with a weight ratio of 90/10, 70/30, 50/50, and 30/70 showed a clear phase-separated structure like a sea-island morphology (**Figure 1.3**). In PHBH/PMMA blends with a weight ratio of 90/10, 70/30, and 50/50, it was observed that the PMMA island-phase was dispersed in the PHBH sea-phase. Furthermore, the area of the PMMA island region to be decreasing with an increase in the PHBH weight ratio. In contrast, PHBH/PMMA blend at 30/70 (wt%/wt%) exhibited reverse morphology, meaning that PHBH islands were uniformly dispersed in the PMMA matrix. In terms of the blend films with PMMA-*g*-PHBH, the surface of all the films was found to be smoother and more uniform as compared to the pristine blends. For PHBH/PMMA blends with composition 90/10–30/70 wt%, the sea-island phase-separated morphology was observed to be gradually diminished with an increase in PMMA-*g*-PHBH concentration. On the contrary, the size and the number of sea regions were reduced after using only 1 wt% of

the prepared graft copolymer. Moreover, with a further increase in the concentration of PMMA-*g*-PHBH to 5 and 10 wt%, the area of sea parts was substantially decreased, and their surface was drastically changed to homogeneous morphology. Thus, it is evident from the obtained results that the PMMA-*g*-PHBH inhibited the phase separation of PHBH and PMMA and the formation of cracks in their blends thereby allowing PHBH/PMMA blend to improve their miscibility with each other.

From the SEM images, it could be said that the development of sea-island phase separation and generation of cracks in PHBH/PMMA blends is attributed to the immiscibility of PHBH with that of PMMA. Such a phase separation phenomenon of PHBH/PMMA blend has also been reported by similar immiscible combinations of PMMA and bio-based polyesters such as PLLA,[7] PHB,[36] and PHBV [37]. In the case of PMMA-*g*-PHBH additive, the obtained SEM micrographs of PHBH/PMMA/PMMA-*g*-PHBH clearly demonstrated a decrease in the size of phase separation structures due to improvement in the miscibility between PHBH and PMMA and enhancement in their interfacial adhesion [16–22]. This phenomenon might be due to the penetration of the graft copolymer into the interfaces between PHBH and PMMA.[18,19] Hence, SEM observations revealed that PMMA-*g*-PHBH worked as a compatibilizer for the PHBH/PMMA immiscible blends.

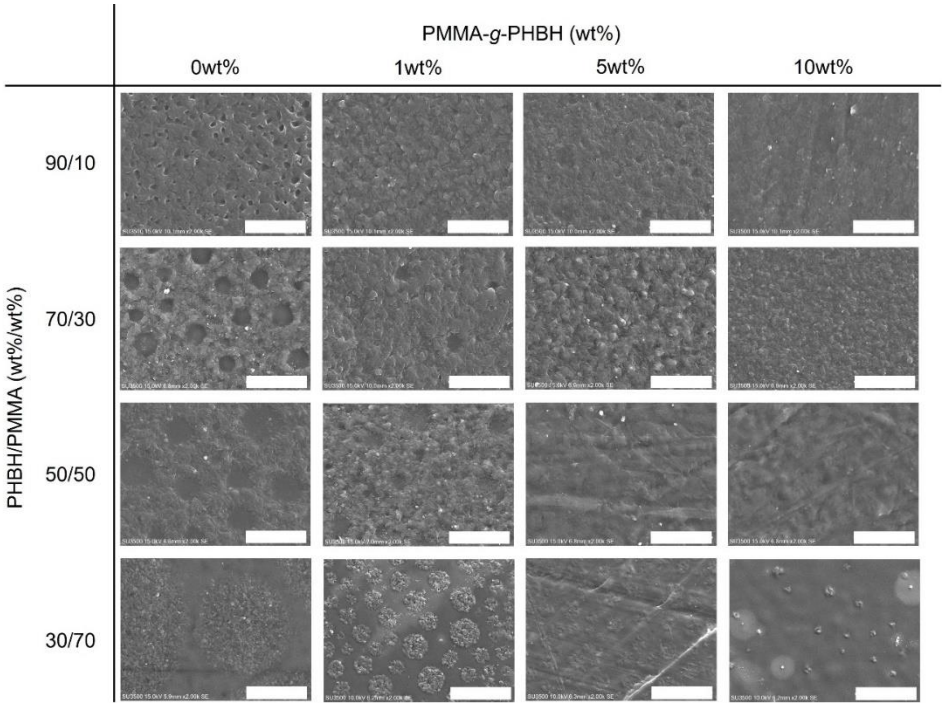


**Figure 1.3.** SEM micrographs showing the surface morphology of PHBH/PMMA blends (90/10, 70/30, 50/50, and 30/70 wt%/wt%) with PMMA-*g*-PHBH (0–10 wt%) prepared by solvent casting method [Scale bars: 20 μm].

### 1.3.3. Thermal analysis of PHBH/PMMA/PMMA-*g*-PHBH blends

The thermal properties of neat PHBH/PMMA were investigated using DSC, as shown in **Figures 1.4 and 1.5**. The first cooling run of PHBH/PMMA blends at a weight ratio of 90/10 and 70/30, showed peaks at 73 °C and 70 °C, respectively, corresponding to the cold crystallization temperature ($T_{cc}$) of PHBH. However, after the addition of PMMA-*g*-PHBH to the blends, it was observed that the peak top of $T_{cc}$ slightly shifted to a lower temperature and crystallization enthalpy ($\Delta H_{cc}$) significantly decreased as mentioned in **Table 1.1**. For the samples consisting of PHBH in 50 and 30 wt%, the peak corresponding to $T_{cc}$ of PHBH completely disappeared in the first cooling charts, whereas the second heating charts of these blends apparently exhibited the crystallization temperature ($T_c$) of PHBH around 50 °C as displayed in **Figure 1.5**. While after incorporation of PMMA-*g*-PHBH to PHBH/PMMA mixture with a blended ratio of 50/50 and 30/70, the $T_c$ peak gradually wiped out with

increasing weight fraction of PMMA-*g*-PHBH additive. While for $T_m$, the second heating charts of all the neat blends showed the two peaks corresponding to $T_m$ of PHBH at around 120 °C and 160 °C, respectively [5,26]. It was found that the addition of PMMA-*g*-PHBH also diminishes the peak corresponding to $T_m$ of PHBH in the blend of PHBH/PMMA with a mixed ratio of 50/50 and 30/70. Moreover, for all the blends, $T_m$ peak of PHBH was maintained at around 120 °C and 160 °C while the melting enthalpy ($\Delta H_m$) was significantly decreased by changing the amount of the resultant graft copolymer (**Table 1.1**). Based on the obtained data, it could be said that the addition of PMMA-*g*-PHBH leads to a decrease in the crystallinity of the PHBH/PMMA blends. The thermal analysis shows that PMMA-*g*-PHBH declines the crystallinity of PHBH in PHBH/PMMA blends.

The DSC results showed that the prepared blends without the compatibilizer caused a decrease in $T_{cc}$ and $\Delta H_{cc}$ and an increase in $T_c$ of PHBH. The changes in $T_{cc}$ (or $T_c$) and $\Delta H_{cc}$ suggest that the crystallinity of PHBH was decreased in the presence of PMMA. The decrease in the crystallinity of PHBH is related to the ability of amorphous PMMA chains to hinder the crystallization of PHBH backbones in their blend film due to the slight miscibility of PMMA with PHBH, as shown in **Figure 1.6**.[36] In the case of the addition of using PMMA-*g*-PHBH as a compatibilizer, the change in the $\Delta H_{cc}$ and $\Delta H_m$ of PHBH/PMMA blends indicates the decrease in the crystallization of PHBH. The decrease in the crystallinity of PHBH indicates that the PMMA interrupted the crystallization of PHBH backbones because of the increase in the miscibility of PHBH and PMMA by the developed graft copolymer.[36,38] The difference in the crystallization behavior of PHBH can be supported by the diminishing phase separation between PHBH and PMMA when the resultant graft copolymer was added (**Figure 1.3**). Therefore, it could be proposed that after mixing PMMA-*g*-PHBH to PHBH/PMMA blends the improvement in miscibility with PMMA can lower the crystallinity of PHBH.

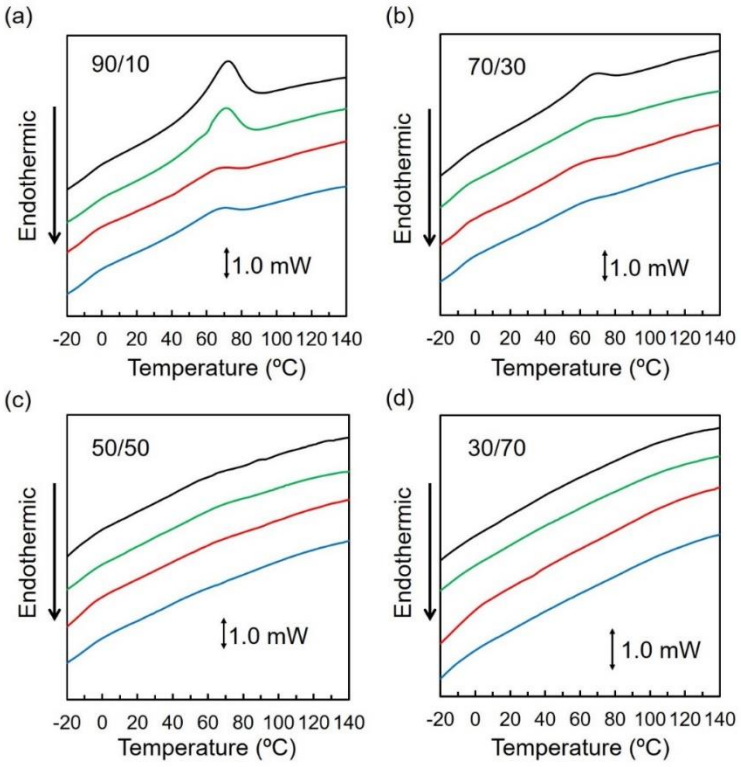


**Figure 1.4.** DSC traces of first cooling run of PHBH/PMMA blends with a mixed ratio of (a) 90/10, (b) 70/30, (c) 50/50, and (d) 30/70 (wt%/wt%) with the change in PMMA-*g*-PHBH weight ratio (black: 0 wt%, green: 1 wt%, red: 5 wt%, blue: 10 wt%).

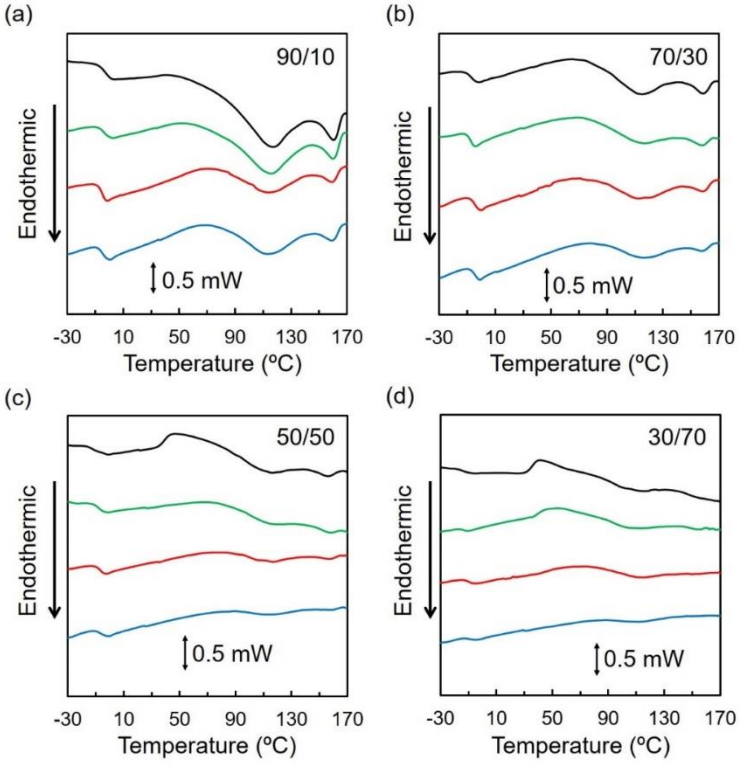


**Figure 1.5.** DSC traces of second heating run of PHBH/PMMA blends with a mixed ratio of (a) 90/10, (b) 70/30, (c) 50/50, and (d) 30/70 (wt%/wt%) with the change in PMMA-*g*-PHBH weight ratio (black: 0 wt%, green: 1 wt%, red: 5 wt%, blue: 10 wt%).

**Table 1.1.** Thermal properties of PHBH/PMMA/PMMA-*g*-PHBH blends.

| PHBH/PMMA (wt%) | PMMA-*g*-PHBH (wt%) | $T_m$ (°C) [(a)] | $T_c$ (°C) | $\Delta H_c$ (J/g) | $\Delta H_m$ (J/g) [(b)] |
|---|---|---|---|---|---|
| 90/10 | 0 | 116 / 161 | 73 [(a)] | 20.9 [(a)] | 39.4 |
| | 1 | 116 / 160 | 71 [(a)] | 16.8 [(a)] | 39.7 |
| | 5 | 114 / 159 | 69 [(a)] | 8.5 [(a)] | 22.4 |
| | 10 | 113 / 160 | 68 [(a)] | 8.3 [(a)] | 22.3 |
| 70/30 | 0 | 114 / 159 | 70 [(a)] | 10.1 [(a)] | 22.4 |
| | 1 | 115 / 158 | 68 [(a)] | 5.6 [(a)] | 16.4 |
| | 5 | 115 / 158 | 61 [(a)] | 3.3 [(a)] | 16.6 |
| | 10 | 116 / 159 | 60 [(a)] | 3.2 [(a)] | 12.5 |
| 50/50 | 0 | 117 / 156 | 48 [(b)] | 8.3 [(b)] | 23.8 |
| | 1 | 116 / 157 | 61 [(b)] | 4.3 [(b)] | 12.4 |
| | 5 | 117 / 157 | 61 [(b)] | 2.6 [(b)] | 9.3 |
| | 10 | - | - | - | 5.9 |
| 30/70 | 0 | 116 | 41 [(b)] | 3.6 [(b)] | 17.5 |
| | 1 | 113 | 54 [(b)] | 3.1 [(b)] | 9.8 |
| | 5 | - | - | - | - |
| | 10 | - | - | - | - |

Dash (-) means that the value of physical properties was not able to be determined from DSC charts. (a) Detected in DSC 1st cooling, (b) detected in DSC 2nd heating.

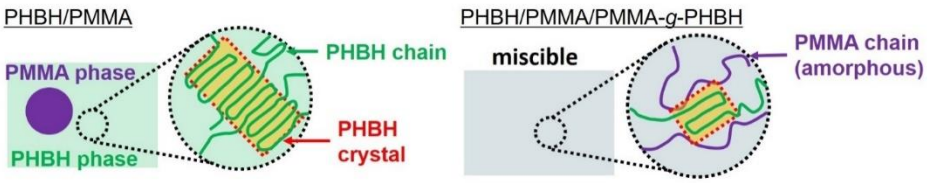


**Figure 1.6.** Mechanism of the decrease in the PHBH crystallinity by PHBH/PMMA compatibilization.

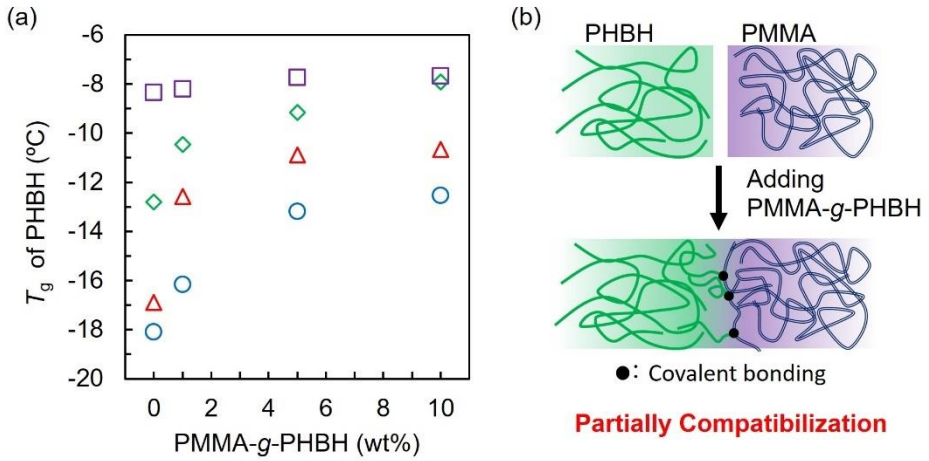


**Figure 1.7.** (a) $T_g$ of PHBH/PMMA blends with a mixed ratio of 90/10 (purple square), 70/30 (green diamond), 50/50 (red triangle), and 30/70 (blue circle) wt%/wt% as a function of the PMMA-*g*-PHBH content (wt%) (b) illustration of the proposed mechanism of Tg increment by the compatibilization of PHBH/PMMA blend with PMMA-*g*-PHBH.

### 1.3.4. Mechanical properties of PHBH/PMMA/PMMA-*g*-PHBH blends

Mechanical properties such as Young's modulus, elongation at break, and toughness of the prepared films were studied by the tensile test. The obtained data of the mechanical properties are summarized in **Figure 1.8** and **Tables 1.2** and **1.3**. PHBH exhibited an elastic modulus of 510 MPa; however, upon the addition of PMMA, Young's modulus of the PHBH/PMMA blends monotonically increased to 920 MPa. The yield strength of the blend was found to be higher (~ 16 MPa) than that of PHBH (~ 13 MPa), regardless of the PMMA weight ratio. However, the strain at break for the PHBH/PMMA blends showed a dramatic decrease from 460 % to 12 %. The PHBH/PMMA blends were found to be more rigid and ductile upon the combination of PHBH and PMMA. Conversely, the addition of PMMA-*g*-PHBH improved the ductility and toughness for all the blends, as observed during the mechanical characterization. In the case of 30/70 wt% of PHBH/PMMA with the 10 wt% of the graft copolymer, it is worth highlighting that the elongation at break reached 95 % in contrast to the virgin blend of PHBH/PMMA exhibiting a much lower elongation at a break of 10 %. On the other hand, for the samples with the PHBH content of 50 – 90 wt%, the addition of the graft copolymer significantly rendered high flexibility to the blends, leading to the slight decrease in Young's modulus and could be seen in **Table 1.2**. Hence, the analysis of the mechanical tests suggests that the mechanical properties of the polymer blends consisted of PHBH and PMMA could be adjusted by tuning the mixed ratio of PHBH, PMMA, and PMMA-*g*-PHBH.

The PHBH/PMMA/PMMA-*g*-PHBH blends exhibited higher elongation at break and toughness in comparison with those of the PHBH/PMMA blends without the graft copolymer. The improved toughness of the blend is attributed to increased interfacial adhesion between PHBH and PMMA by mixing the resultant graft copolymer, which has also been observed in the form of homogeneous morphology from sea-island phase separation of the PHBH/PMMA

blend (**Figure 1.3**). The improvement in interfacial adhesion endows sufficient stress transfer to suppress crack generation in the blend film, which is consistent with that of the published works of literature on various types of compatibilizers.[17–19] The enhancement in the mechanical toughness of PHBH/PMMA polymer blends proves that the PMMA-*g*-PHBH worked as a compatibilizer, leading to the enhancement in interfacial adhesion of the blends.[18] Thus, the compatibilized PHBH/PMMA blends can be applied for the development of flexible materials, for example, food packaging, laminations, and coating materials. [41–43]

**Table 1.2.** Mechanical properties of neat PHBH and PMMA.

| Polymer | Young's Modulus (MPa) | Maximum strength (MPa) | Elongation at break (%) | Toughness ($MJ/m^3$) |
|---|---|---|---|---|
| PHBH | 510 ± 10 | 24.0 ± 0.8 | 460.0 ± 8.0 | 55.0 ± 2.0 |
| PMMA | 1970 ± 40 | 37.0 ± 1.0 | 5.9 ± 0.4 | 1.5 ± 0.1 |

**Table 1.3.** Mechanical properties of PHBH/PMMA/PMMA-*g*-PHBH films.

| PHBH/PMMA (wt%) | PMMA-*g*-PHBH (wt%) | Young's Modulus (MPa) | Maximum strength (MPa) |
|---|---|---|---|
| 90/10 | 0 | 530 ± 20 | 17.0 ± 1.0 |
| | 1 | 350 ± 20 | 18.0 ± 0.8 |
| | 5 | 430 ± 20 | 20.0 ± 0.7 |
| | 10 | 370 ± 30 | 19.0 ± 0.7 |
| 70/30 | 0 | 630 ± 10 | 15.0 ± 0.6 |
| | 1 | 450 ± 10 | 12.0 ± 0.8 |
| | 5 | 480 ± 3 | 16.0 ± 0.7 |
| | 10 | 460 ± 20 | 13.0 ± 0.8 |
| 50/50 | 0 | 720 ± 30 | 15.0 ± 0.6 |
| | 1 | 720 ± 30 | 14.0 ± 0.8 |
| | 5 | 700 ± 20 | 14.0 ± 0.3 |
| | 10 | 590 ± 4 | 13.0 ± 0.3 |
| 30/70 | 0 | 920 ± 50 | 16.0 ± 1.0 |
| | 1 | 750 ± 30 | 15.0 ± 0.2 |
| | 5 | 820 ± 30 | 17.0 ± 0.3 |
| | 10 | 650 ± 50 | 14.0 ± 0.8 |

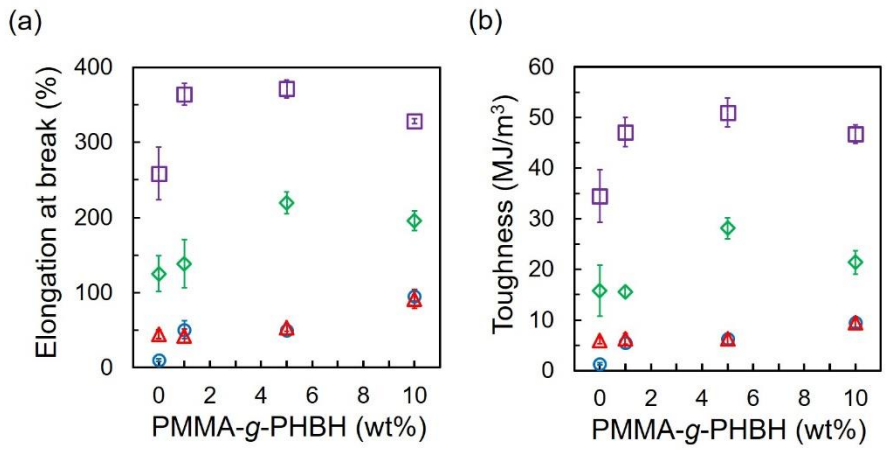


**Figure 1.8.** Mechanical properties of PHBH/PMMA blends: (a) Elongation at break and (b) toughness of PHBH/PMMA blends with a mixed ratio of 90/10 (purple square), 70/30 (green diamond), 50/50 (red triangle), and 30/70 (blue circle) wt%/wt% with PMMA-*g*-PHBH (0–10 wt%).

## 1.4. Conclusions

In this chapter, the synthesis of a compatibilizer for immiscible polymer blends of microbial PHBH, and PMMA is proposed, which was synthesized from Propargyl-PHBH as a starting material. PMMA-*g*-PHBH was successfully synthesized through radical copolymerization of MMA and Vinyl-PHBH derived from Propargyl-PHBH with AMS *via* CuAAC reaction. The obtained graft copolymer restricted the phase separation of the PHBH/PMMA blends, and the homogeneous surface morphology of the blends with the various mixed ratio was confirmed by the SEM observation. The DSC thermal analysis exhibited that the crystallization rate of PHBH in the blends decreased and its $T_g$ increased with increasing PMMA-*g*-PHBH loading ratio up to 10 wt%. Furthermore, the tensile test results show that the flexibility and toughness of the PHBH/PMMA/PMMA-*g*-PHBH mixed films were higher than those of PHBH/PMMA blends without the graft copolymers. The SEM, DSC, and tensile test data proves that the graft copolymer enhances the compatibility of the PHBH/PMMA blend. As a result, the mechanical properties of PHBH such as flexibility and toughness can be easily controlled by blending PMMA and PMMA-*g*-PHBH.

These experimental findings promisingly contribute towards the development of bio-based plastics as an alternative to oil-based resins which will potentially accelerate the applications of PHAs with tuned properties.

## 1.5. References


[1] H. Alata, T. Aoyama, Y. Inoue, *Macromolecules* **2007**, *40*, 4546.

[2] W. P. Xie, G. Q. Chen, *Biochem. Eng. J.* **2008**, *38*, 384.

[3] Y. Gao, L. Kong, L. Zhang, Y. Gong, G. Chen, N. Zhao, X. Zhang, *Eur. Polym. J.* **2006**, *42*, 764.

[4] Y. Xin, H. Uyama, *Chem. Lett.* **2012**, *41*, 1509.

[5] J. Lim, M. S. K. Chong, E. Y. Teo, G. Q. Chen, J. K. Y. Chan, S. H. Teoh, *J. Biomed. Mater. Res. - Part B Appl. Biomater.* **2013**, *101 B*, 752.

[6] R. A. Rebia, S. Rozet, Y. Tamada, T. Tanaka, *Polym. Degrad. Stab.* **2018**, *154*, 124.

[7] C. Samuel, J. M. Raquez, P. Dubois, *Polymer* **2013**, *54*, 3931.

[8] X. Liu, Y. Xiong, J. Shen, S. Guo, *Opt. Express* **2015**, *23*, 17793.

[9] K. Fujimoto, Z. Tang, W. Shinoda, S. Okazaki, *Polymer* **2019**, *178*, 121570.

[10] C. Koning, M. Van Duin, C. Pagnoulle, R. Jerome, *Prog. Polym. Sci.* **1998**, *23*, 707.

[11] C. E. Estridge, A. Jayaraman, *ACS Macro Lett.* **2015**, *4*, 155.

[12] S. Anjali, S. Aishwaryalakshmi, V. Ashwin, S. Neeraja, N. Rasana, K. Jayanarayanan, *Mater. Today Proc.* **2018**, *5*, 25524.

[13] Z. Fu, H. Wang, X. Zhao, X. Li, X. Gu, Y. Li, *J. Mater. Chem. A* **2019**, *7*, 4903.

[14] J. Feng, G. Zhang, K. MacInnis, Z. Li, A. Olah, E. Baer, *J. Polym. Sci. Part B Polym. Phys.* **2019**, *57*, 281.

[15] C. Yu, D. Shi, J. Wang, H. Shi, T. Jiang, Y. Yang, G. H. Hu, R. K. Y. Li, *Mater. Des.* **2016**, *107*, 171.

[16] Y. Zhang, F. Li, Q. Yu, C. Ni, X. Gu, Y. Li, J. You, *Macromol. Mater. Eng.* **2019**, *304*, 1900316.

[17] A. Bharati, R. Cardinaels, T. Van der Donck, J. W. Seo, M. Wübbenhorst, P. Moldenaers, *Polymer* **2017**, *108*, 483.

[18] T. Oyama, S. Kobayashi, T. Okura, S. Sato, K. Tajima, T. Isono, T. Satoh, *ACS Sustain. Chem. Eng.* **2019**, *7*, 7969.

[19] H. Wang, Z. Fu, W. Dong, Y. Li, J. Li, *J. Phys. Chem. B* **2016**, *120*, 9240.

[20] S. Bärwinkel, R. Bahrami, T. I. Löbling, H. Schmalz, A. H. E. Müller, V. Altstädt, *Adv. Eng. Mater.* **2016**, *18*, 814.

[21] T. Gegenhuber, M. Krekhova, J. Schöbel, A. H. Gröschel, H. Schmalz, *ACS Macro Lett.* **2016**, *5*, 306.

[22] X. Zhao, H. Wang, Z. Fu, Y. Li, *ACS Appl. Mater. Interfaces* **2018**, *10*, 8411.

[23] L. T. Strover, J. Malmström, J. Travas-Sejdic, *Chem. Rec.* **2016**, *16*, 393.

[24] D. Kai, X. J. Loh, *ACS Sustain. Chem. Eng.* **2014**, *2*, 106.

[25] M. Hyakutake, S. Tomizawa, I. Sugahara, E. Murata, K. Mizuno, H. Abe, T. Tsuge, *Polym. Degrad. Stab.* **2015**, *117*, 90.

[26] Z. Li, J. Yang, X. J. Loh, *NPG Asia Mater.* **2016**, *8*, e265.

[27] V. V. Rostovtsev, L. G. Green, V. V. Fokin, K. B. Sharpless, *Angew. Chem. Int. Ed.* **2002**, *114*, 2708.

[28] B. T. Worrell, J. a. Malik, V. V. Fokin, *Science* **2013**, *340*, 457.

[29] L. Liang, D. Astruc, *Coord. Chem. Rev.* **2011**, *255*, 2933.

[30] P. Lemechko, E. Renard, G. Volet, C. S. Colin, J. Guezennec, V. Langlois, *React. Funct. Polym.* **2012**, *72*, 160.

[31] P. Lemechko, E. Renard, J. Guezennec, C. Simon-Colin, V. Langlois, *React. Funct. Polym.* **2012**, *72*, 487.

[32] K. Shingo, T. Fujiki, **2018**, US 2018/0346943 A1.

[33] K. Hackethal, D. Döhler, S. Tanner, W. H. Binder, *Macromolecules* **2010**, *43*, 1761.

[34] Z. Jin, K. P. Pramoda, G. Xu, S. H. Goh, *Chem. Phys. Lett.* **2001**, *337*, 43.

[35] Y. Yoshimura, M. Nojiri, M. Arimoto, K. Ishimoto, Y. Aso, H. Ohara, H. Yamane, S. Kobayashi, *Polymer* **2016**, *90*, 342.

[36] N. Lotti, M. Pizzoli, G. Ceccorulli, M. Scandola, *Polymer* **1993**, *34*, 4935.

[37] S. Wang, W. Chen, H. Xiang, J. Yang, Z. Zhou, M. Zhu, *Polymers* **2016**, *8*, DOI 10.3390/polym8080273.

[38] J. González-Ausejo, E. Sánchez-Safont, J. M. Lagarón, R. Balart, L. Cabedo, J. Gámez-Pérez, *J. Appl. Polym. Sci.* **2017**, *134*, 1.

[39] D. C. Lee, L. W. Jang, *J. Appl. Polym. Sci.* **1996**, *61*, 1117.

[40] H. Essawy, D. El-Nashar, *Polym. Test.* **2004**, *23*, 803.

[41] S. J. Modi, K. Cornish, K. Koelling, Y. Vodovotz, *J. Appl. Polym. Sci.* **2016**, *133*, 1.

[42] S. Sun, P. Liu, N. Ji, H. Hou, H. Dong, *Food Hydrocoll.* **2017**, *72*, 81.

[43] M. Razavi, D. Huang, S. Liu, H. Guo, S. Q. Wang, *Macromolecules* **2020**, *53*, 323.

# Chapter 2

## Reinforcement of microbial thermoplastics by grafting to polystyrene with propargyl-terminated poly(3-hydroxybutyrate-*co*-3-hydroxyhexanoate)

## 2.1 Introduction

Bio-based materials including PLA, polysaccharides, and plant oils provide an alternative to petroleum-based resins to settle the recent environmental problems and achieve a sustainable society.[1] PHBH has also attracted great interest as one of biomass plastics to various applications, for example, commodity, engineering, and medical materials.[2,3] The mechanical flexibility and toughness of PHBH are superior to other series of PHAs with maintaining elastic modulus and tensile strength; additionally, its mechanical properties can be adjusted by 3HB/3HHx ratio.[4] However, currently, Young's modulus and tensile strength of PHBH is not enough to use further applications. Therefore, to employ PHBH as an industrial material, it is important to improve the mechanical strength with the unique ductility of PHBH maintained.

To reinforce the mechanical properties of PHBH, the preparation of the polymer blend consisting of PHBH/Polystyrene (PSt) is one of the strategies. PSt is well-known as a commodity plastic with good elastic modulus, high transparency, and low-cost product.[5–7] Recently, several studies revealed that PSt has potential as a recyclable and eco-friendly resin because recent studies show the biodegradability of PSt. For example, Patrick *et al.* developed the system of the chemo-biotechnological conversion of PSt to PHAs.[8] Also, it was reported that PSt can be degraded by mealworms (*T. molitor*), resulting in the conversion to carbon dioxide and water.[9–11] Indeed, some researchers have reported the polymer blends consisting of bio-based polymer and PSt to improve the physical properties of biomass plastics.[12–14] In terms of PHBH/PSt blend, the blending PHBH with PSt can overcome not

only the low elastic modulus and tensile strength of PHBH but also the low toughness and ductility of PSt because PSt is known as a brittle polymer due to its low fracture energy.[15] Additionally, the cost of biomass products is expected to be reduced by the preparation of PHBH and PSt blends. However, it is hard to mix PHBH homogeneously with PSt and generate a phase separation morphology because of their low compatibility. This also deteriorates the mechanical properties of the PHBH/PSt blend.

In the prior chapter, the graft copolymer consisting of PMMA and PHBH worked as a compatibilizer for PHBH/PMMA blend, which was synthesized with propargyl-terminated PHBH (Propargyl-PHBH) as a starting material. Moreover, Oyama *et al.* reported that PHBH can be compatibilized with PCL by adding PHBH-*b*-PCL prepared from Propargyl-PHBH and azide-terminated PCL.[16] Furthermore, the preparation of copolymer not only improves the mechanical properties of PHAs but also endows new physical properties for PHAs, including hydrophilicity,[3,17] electroconductivity,[18,19] thermoresponsibility,[20] and fluorescence property[21]. Thus, the synthesis of a graft copolymer can be supposed to improve the compatibility between PHBH and PSt, obtaining PHBH to comparable tensile properties and high transmittance.

In this chapter, the author attempted to synthesize the graft copolymer from Propargyl-PHBH with azide-modified PSt to improve their compatibility and mechanical properties. The films of the resultant graft copolymer were fabricated with a solvent casting method. The mechanical properties of PSt-*g*-PHBH were evaluated by a tensile test in comparison with PHBH/PSt blends. Interfacial adhesion and phase separation morphology of PSt-*g*-PHBH were evaluated with electron microscopic observation, thermal analysis, and theoretical analysis, Pukánszky model.[22]

## 2.2 Experimental section

### 2.2.1. Materials

PHBH ($M_n$ = 200,000, $M_w/M_n$ = 2.1, HH units = 11 mol%) and Propargyl-PHBH ($M_n$ = 20,000, $M_w/M_n$ = 2.1, HH units = 11 mol%) were kindly offered by KANEKA Co., (Osaka, Japan). The preparation method of Propargyl-PHBH was reported in the previous study.[23] PSt ($M_n$ ~ 170,000, $M_w$ ~ 350,000) was purchased from Sigma Aldrich Co. LLC (SIAL, St. Louis, USA). These polymers were purified by reprecipitation with chloroform as a good solvent and methanol as a poor solvent. *p*-Chloromethylstyrene (CMS) was purchased from Tokyo Chem. Ind., (TCI, Tokyo, Japan). CMS was passed through the alumina column (SIAL) to remove the inhibitor before use. 2,2'-Azobis(isobutyronitrile) (AIBN) was purchased from FUJIFILM Wako Pure Chemical Co. (WAKO, Osaka, Japan). AIBN was used after recrystallization in methanol. Styrene and *N, N*-dimethylformamide (DMF) was purchased from Nacalai Tesque Inc. (Nacalai, Kyoto, Japan). Styrene was purified by distillation under reduced pressure to remove the inhibitor. DMF was preserved with molecular sieves (4A) for drying. *N,N,N',N'',N''*-pentamethyldiethylenetriamine (PMDETA) was purchased from TCI. Methanol, copper(I) bromide, and chloroform were obtained from WAKO. Sodium azide and dichloromethane were purchased from Nacalai. These chemical reagents were used as received.

### 2.2.2. Synthesis of poly(*p*-azidemethylstyrene-*co*-styrene) [P(AMS-*co*-St)]

P(AMS-*co*-St) was synthesized by azidation of poly(*p*-chloromethylstyrene-*co*-styrene) (P(CMS-*co*-St)) with sodium azide, referred by the previous studies (**Scheme 2.1**).[24] In this experiment, two types of P(AMS-*co*-St) with different AMS unit ratio (5 mol% and 20 mol%) were prepared. First, CMS/styrene (0.76 mg/9.9 mg or 3.1 mg/8.4 mg, total vinyl monomer = 100 mmol) were dissolved in toluene (13 mL). Then, AIBN (41 mg, 25 μmol) was added to the mixture with stirring under a nitrogen atmosphere. Copolymerization of

CMS and styrene was carried out at 65 °C for 24 h under a nitrogen atmosphere. The products were reprecipitated twice in methanol (400 mL) and filtered. The obtained white powder was dried under vacuum overnight. Subsequently, the prepared P(CMS-*co*-St) powder (3 g) was dissolved in DMF (60 mL) under stirred at room temperature, and sodium azide (1.5 equiv. to *p*-chloromethylstyrene units) was then added into the polymer solution. The reaction was conducted at 35 °C for 48 h. The products were reprecipitated into water (800 mL) to remove unreacted sodium azide and washed with methanol several times. The resultant white powder was dried under vacuum overnight. To purify the synthesized P(AMS-*co*-St), the obtained white powder was dissolved in chloroform (30 mL), and then, reprecipitated in methanol (350 mL). The yield of P(AMS-*co*-St) was listed in **Table 2.1**. The copolymers were denoted as 'P(AMS-*co*-St)_*x*', where *x* represents the AMS unit mol% of the P(AMS-*co*-St), for example, P(AMS-*co*-St)_5 means that the molar ratio AMS unit in the copolymer was 5 mol%.

### 2.2.3. Preparation of PSt-*g*-PHBH by click chemistry

PSt-*g*-PHBH was prepared from Propargyl-PHBH and P(AMS-*co*-St) *via* CuAAC reaction (**Scheme 2.1**). First, Propargyl-PHBH (2 g, propargyl moiety = 0.1 mmol) and P(AMS-*co*-St) (2, 5, and 10 equiv. of AMS units to propargyl group of Propargyl-PHBH) were dissolved in dichloromethane (30 mL) under nitrogen atmosphere for 10 min. The amount and the type of P(AMS-*co*-St)s were summarized in **Table 2.1**. PMDETA (26 mg, 0.15 mmol) and copper(I) bromide (22 mg, 0.15 mmol) were added into the polymer solution. The reaction mixture was then degassed and stirred at 35 °C for 72 h under an argon atmosphere. The products were reprecipitated in methanol (400 mL). To purify the resultant polymers, PSt-*g*-PHBH was dissolved in chloroform again, and alumina was added into the polymer solution stirred with alumina to remove catalyst and ligand. After the filtration, the solution was reprecipitated with methanol to obtain the PSt-*g*-PHBH. The resultant graft copolymers were filtrated and dried under vacuum overnight. The yields of each PSt-*g*-

PHBH were summarized in **Table 2.1**. The resultant graft copolymers were denoted as 'PSt-*g*-PHBH_*x*', where *x* represents the weight ratio (wt%) of PSt, for example, PSt-*g*-PHBH_4.7 means that the weight ratio of PSt in the graft copolymer was 4.7 wt%.

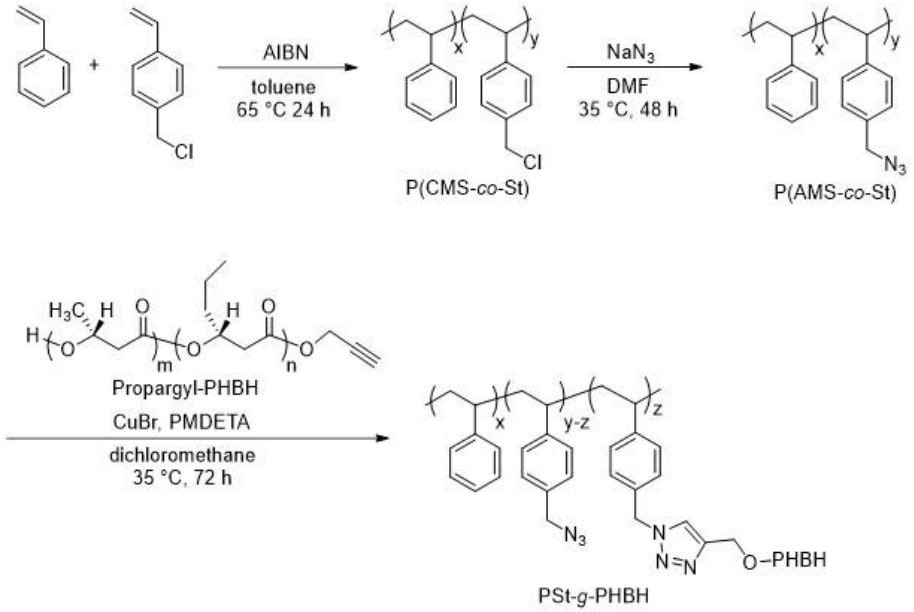


**Scheme 2.1.** Preparation of PSt-*g*-PHBH from Propargyl-PHBH and P(AMS-*co*-St) *via* CuAAC reaction.

### 2.2.3. Preparation of PSt-*g*-PHBH by click chemistry

PSt-*g*-PHBH was prepared from Propargyl-PHBH and P(AMS-*co*-St) *via* CuAAC reaction (**Scheme 1**). First, Propargyl-PHBH (2 g, propargyl moiety = 0.1 mmol) and P(AMS-*co*-St) (2, 5, and 10 equiv. of AMS units to propargyl group of Propargyl-PHBH) were dissolved in dichloromethane (30 mL) under nitrogen atmosphere for 10 min. The amount and the type of P(AMS-*co*-St)s were summarized in **Table 1**. PMDETA (26 mg, 0.15 mmol) and copper(I) bromide (22 mg, 0.15 mmol) were added into the polymer solution. The reaction mixture was then degassed and stirred at 35 °C for 72 h under an argon atmosphere. The products were reprecipitated in methanol (400 mL). To purify the resultant polymers, PSt-*g*-PHBH was dissolved in chloroform again, and alumina was added into the polymer solution stirred with alumina to remove catalyst and ligand. After the filtration, the solution

was reprecipitated with methanol to obtain the PSt-*g*-PHBH. The resultant graft copolymers were filtrated and dried under vacuum overnight. The yields of each PSt-*g*-PHBH were summarized in **Table 1**. The resultant graft copolymers were denoted as 'PSt-*g*-PHBH_*x*', where *x* represents the weight ratio (wt%) of PSt, for example, PSt-*g*-PHBH_4.7 means that the weight ratio of PSt in the graft copolymer was 4.7 wt%.

### 2.2.4. Fabrication of PSt-*g*-PHBH film

The PSt-*g*-PHBH films were fabricated by the solvent casting method with chloroform. The obtained PSt-*g*-PHBH (1 g) was dissolved in chloroform (13 mL, concentration= 5 wt%) with stirring. Then, the polymer solution was degassed under the reduced pressure for 1 min and poured into a Teflon petri dish ($\phi$ = 7.5 cm). After drying overnight at 30 °C under ordinary pressure, the PSt-*g*-PHBH film was obtained. To remove the residual solvent, the prepared film was dried under a vacuum at 80 °C for 24 h. PHBH/PSt blend films were also prepared by the same procedure mentioned above.

### 2.2.5. Characterization

The molecular weight of the products was determined by SEC, which condition and equipment were the same as Chapter 1. The chemical structures of the synthesized polymers were identified by $^{1}$H NMR spectroscopy. The NMR device and its measurement method are stated in the experimental section of Chapter 1. Fourier transferred infrared (FT-IR) spectroscopy measurement was carried out to confirm the chemical structure with a Nicolet iS5 FT-IR spectrometer with iD5 ATR accessory (Thermo Fisher Scientific Inc., Waltham, MA, USA) in resolution = 4 $cm^{-1}$ from 400 to 4000 $cm^{-1}$. Transparency of the films was

evaluated by a UV-vis spectroscopy with a Hitachi U2810 UV−visible spectrophotometer (Hitachi High-Technologies Co., Tokyo, Japan) in the range of 200–800 nm wavelength. Haze measurements of the obtained films were conducted with a Haze Meter NDH4000 (Nippon Denshoku Industries Co., Ltd, Tokyo, Japan). The surface morphology of PSt-*g*-PHBH films was observed by optical microscopy with an SE-2000WR (SELMIC Co., Shiga, Japan). Mechanical properties of the prepared films were measured in the same way as in Chapter 1. For tensile tests, these films were cut into a dumbbell-shaped sheet (0.6 cm × 3.5 cm) with a thickness of *ca.* 100 μm. The elastic modulus of the prepared specimen was defined as a slope of a stress-strain curve from 0 to 0.01 of strain. Morphology of the cryo-fracture surface of the films was observed by SEM, which detail of the condition and device are explained in Chapter 1. To investigate the viscoelasticity of the polymers as a function of temperature, dynamic mechanical analysis (DMA) was carried out using a DMS6100 (Hitachi High-Tech Science Co., Tokyo, Japan) in tensile mode with the frequency of 1 Hz at a heating rate of 3°C/min from −70 °C to 200 °C. When measuring DMA, the obtained films were cut into rectangular films (0.5 cm × 4.0 cm). The thermal properties of the present polymers were measured by DSC. The measurement condition of DSC was concretely written in the experimental section of Chapter 1.

## 2.3 Results and discussion

### 2.3.1. Synthesis of PSt-*g*-PHBH

The yield and physical properties of P(AMS-*co*-St) were summarized in **Table 2.1** and **Figure 2.1**. These results revealed that P(AMS-*co*-St) was successfully prepared through the reaction described in **Scheme 2.1**. **Figure 2.2a** shows the FT-IR spectra of Propargyl-PHBH and PSt-*g*-PHBH. In terms of PSt-*g*-PHBH, the remarkable peak appeared at 1720 $cm^{-1}$ in its FT-IR spectra, which was corresponded to C=O stretching of the PHBH main chain. Additionally, the FT-IR spectra of PSt-*g*-PHBH also displayed three characteristic peaks at around 700 $cm^{-1}$ and 3000 $cm^{-1}$ attributed to C−H stretching of the aromatic ring of PSt backbone, and 1490 $cm^{-1}$ corresponding to the out-of-plane bending mode of PSt aromatic ring. The peak at 2090 $cm^{-1}$ attributed to non-reacted azide groups grafted on the PSt backbone. $^{1}H$ NMR spectra of PSt-*g*-PHBH, shown in **Figure 2.2b**, demonstrated that the signal (a) corresponding to the end-propargyl group of PHBH was clearly erased after the reaction. Moreover, two characteristic signals (C) and (D) appeared, which were related to the aromatic group of PSt and triazole ring moiety, respectively. The signal at 4.2 ppm was attributed to the residual azide group of P(AMS-*co*-St). Molecular weight was estimated by the SEC measurement of PSt-*g*-PHBH. $M_n$ and $M_w/M_n$ of PSt-*g*-PHBH are summarized in **Table 2.2**. SEC measurements also showed the increment in the molecular weight of PSt-*g*-PHBH compared to that of the starting materials of P(AMS-*co*-St) and Propargyl-PHBH. Moreover, the chloroform solution of the PHBH/PSt mixture generated the liquid-liquid phase separation (**Figure 2.3a**). This phenomenon indicates that the compatibility between PHBH and PSt was low in chloroform. Conversely, the PSt-*g*-PHBH chloroform solution exhibited a uniform and clear appearance (**Figure 2.3b**). This observation result demonstrated that the compatibility of PHBH and PSt in chloroform was remarkably

improved by the '*grafting to*' method. Thus, these characterizations prove that PSt-*g*-PHBH was successfully prepared through the reactions, described in **Scheme 2.1**.

**Table 2.1.** Characterization of P(AMS-*co*-St) 5 and 20. [a]

| Polymer | Yield (%) | AMS unit (mol%) [b] | $M_n \times 10^{-4}$ (g/mol) [c] | $M_w/M_n$ [c] | $T_g$ (°C) [d] |
|---|---|---|---|---|---|
| P(AMS-*co*-St) 5 | 75 | 5 | 4.0 | 1.9 | 98 |
| P(AMS-*co*-St) 20 | 74 | 20 | 4.7 | 1.9 | 87 |

(a) Polymerization at 65 °C for 24 h under an argon atmosphere, (b) Calculated by $^1$H NMR results, (c) determined with SEC with polystyrene standard in chloroform as an eluent, and (d) Measured by DSC 2$^{nd}$ heating.

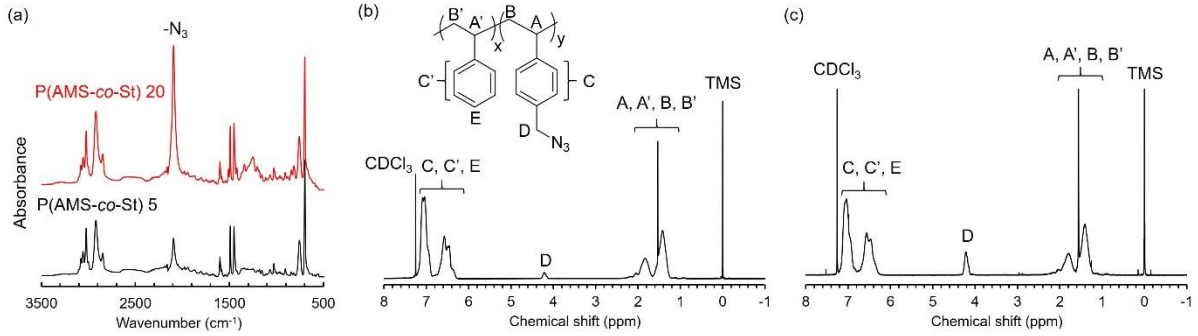


**Figure 2.1.**Characterization of P(AMS-*co*-St): (a) FT-IR spectra, $^1$H NMR spectra of (b) P(AMS-*co*-St) 5 and (c) P(AMS-*co*-St) 20.

**Table 2.2.** PHBH/PSt weight fraction and molecular weight of PSt-*g*-PHBH

| Sample | P(AMS-*co*-St) | azide/propargyl (mol/mol) | $M_n$ (kg/mol) [a] | $M_w/M_n$ [a] | Yield (%) |
|---|---|---|---|---|---|
| PSt-*g*-PHBH_4.7 | 20 | 2/1 | - [b] | - [b] | 56 |
| PSt-*g*-PHBH_11 | 20 | 5/1 | - [b] | - [b] | 60 |
| PSt-*g*-PHBH_14 | 5 | 2/1 | 160 | 3.5 | 58 |
| PSt-*g*-PHBH_19 | 20 | 10/1 | 230 | 3.1 | 48 |
| PSt-*g*-PHBH_31 | 5 | 5/1 | 100 | 3.2 | 65 |
| PSt-*g*-PHBH_47 | 5 | 10/1 | 84 | 2.4 | 69 |

(a) Measured with SEC, (b) Hyphen (-) means that $M_n$ and PDI were not measured by GPC because the molecular weight of PSt-*g*-PHBH_4.7 and 11 may be so high that the column in this experiment was clogged.

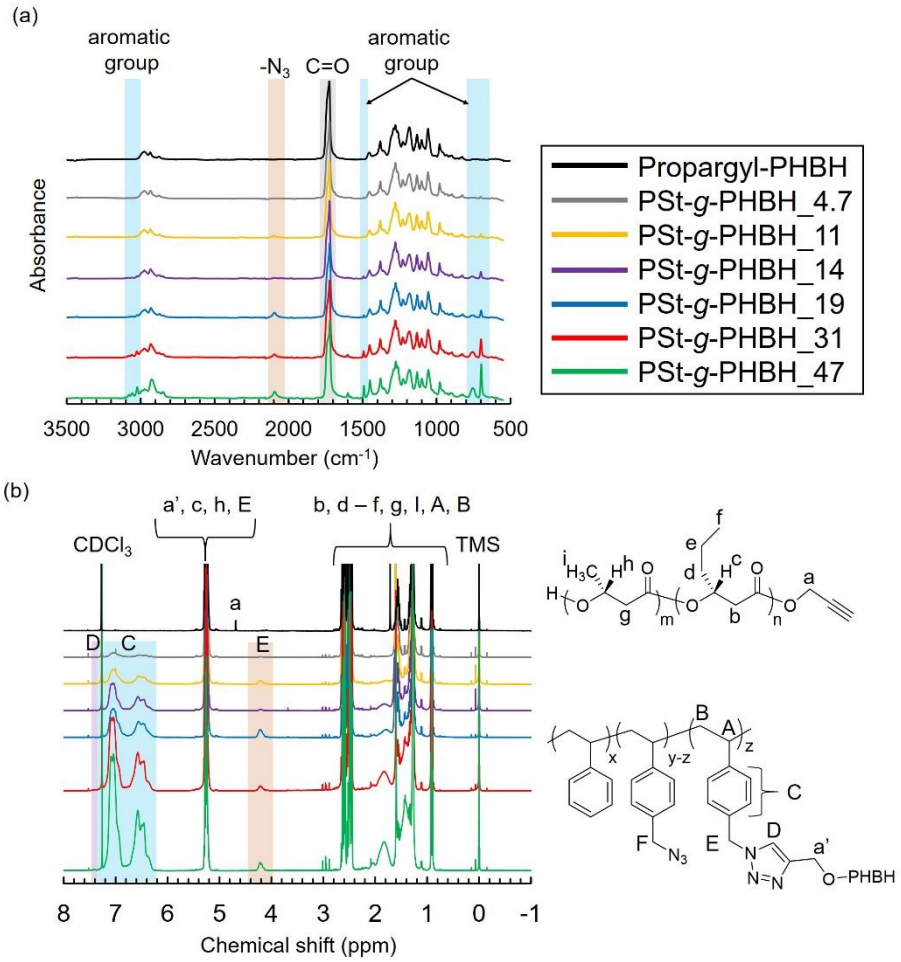


**Figure 2.2.** Identification of PSt-*g*-PHBH chemical structure: (a) FT-IR spectra, (b) $^{1}$H NMR spectra.

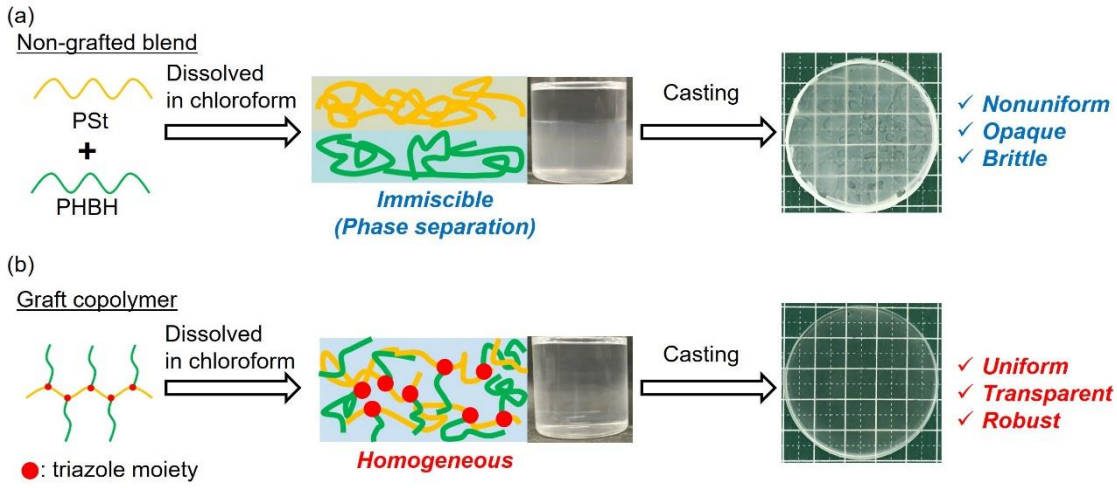


**Figure 2.3.** Illustration images and photographs of the chloroform solution and the film (a) PHBH/PSt = 50/50 (wt%/wt%) blend, and (b) PSt-*g*-PHBH_47.

### 2.3.2. Homogeneity and transparency of PSt-*g*-PHBH film

Homogeneity and compatibility of the polymer films consisting of PHBH and PSt are evaluated by direct observation and transparency with UV-vis spectra and haze measurement. Photo images exhibited that PHBH/PSt blends were heterogeneous and turbid (**Figure 2.4a**); in contrast, the PSt-*g*-PHBH films had good homogeneity and transparency with the PSt weight ratio increased (**Figure 2.4b**). UV-vis spectra of PHBH/PSt blend films displayed that their transmittance with the range of 400 – 800 nm quantitatively showed low value (around 0 – 10%) with independent of the PSt content, compared to that of neat PHBH and neat PSt film (**Figure 2.4a, c)**. On the other hand, the UV-vis spectra of PSt-*g*-PHBH films revealed that its transparency was apparently increased with the increment in the PSt weight ratio (**Figures 2.4b, c**). Remarkably, UV-vis spectra of PSt-*g*-PHBH_47 showed that the comparable transmittance (about 75 %) which was higher than that of pristine PHBH film. **Figure 2.4c** shows the change in the haze degree (%) of PHBH/PSt film and PSt-*g*-PHBH film as a function of the PSt weight ratio. The haze of PHBH/PSt film was also high, which the value was closed to 100%; conversely, that of PSt-*g*-PHBH film was apparently decreased with the PSt weight ratio increased. These results demonstrate that the grafting of PHBH onto PSt side chains has a significant influence on the homogeneity and transparency of PHBH.

The result of UV-vis spectra and haze measurements confirmed that the PHBH/PSt blend showed low optical properties due to the low compatibility between PHBH and PSt. However, the evaluation of the optical properties of PSt-*g*-PHBH films confirmed that its transparency can be controlled by changing Propargyl-PHBH and P(AMS-*co*-St) feed ratio. At a relatively high PHBH weight ratio (PSt-*g*-PHBH_4.7 to 19), the transparency of PSt-*g*-PHBH was drastically decreased because of the rough surface of its films, which was observed by optical microscopy (**Figure 2.5**). The surface structures on the PSt-*g*-PHBH

films can be generated by the large-size phase separation of polymer and solvent during the drying process.[25,26] Conversely, at a relatively high PSt weight ratio (PSt-*g*-PHBH_31 and 47), the transmittance of the PSt-*g*-PHBH films became higher than that of PSt-*g*-PHBH films with a high PHBH weight ratio. The transparency improvement of PSt-*g*-PHBH can be related to the decrease in the surface roughness area. Additionally, as shown in **Table 2.3** and **Figure 2.6b**, the melting enthalpy ($\Delta H_m$) of PHBH determined by DSC 1$^{st}$ heating charts (**Figure 2.6a**) was almost the same regardless of the amount of PSt. This result indicated that the crystallinity of PHBH was not changed by grafting to PSt. Thereby, the improvement in transparency of PSt-*g*-PHBH film was owing to the increment in the amount of amorphous PSt. These results revealed that grafting to PSt is useful to improve the transparency and homogeneity of PHBH/PSt blend at a relatively high PSt weight ratio (~ 50 wt%). Thus, although PHBH is a crystalline polymer, the fabricated PSt-*g*-PHBH films show a good optical performance corresponded to the high transparency of PSt.

In order to confirm the compatibility of the polymer blend films consisting of PHBH and PSt, the cryo-fracture surface morphology was observed with SEM. **Figure 2.7** shows the SEM images of the fracture surface of PHBH/PSt blend films and PSt-*g*-PHBH films at around 10 wt%, 30 wt%, and 50 wt% of PSt. The cross section of PHBH/PSt blend films showed the apparent phase separation morphology, indicating that PHBH is immiscible to PSt. In contrast, the fracture surface of PSt-*g*-PHBH was smooth and uniform without phase separation. The difference of SEM observation between PHBH/PSt blend films and PSt-*g*-PHBH films demonstrated that the compatibilities on the PHBH/PSt interface were enhanced by the formation of graft copolymer consisted of PHBH and PSt. The homogeneity of PHBH/PSt blend films can also influence their transparency mentioned above. Hence, the increase in the compatibility of PHBH and PSt can be achieved using Propargyl-PHBH, endowing PHBH with a good optical property.

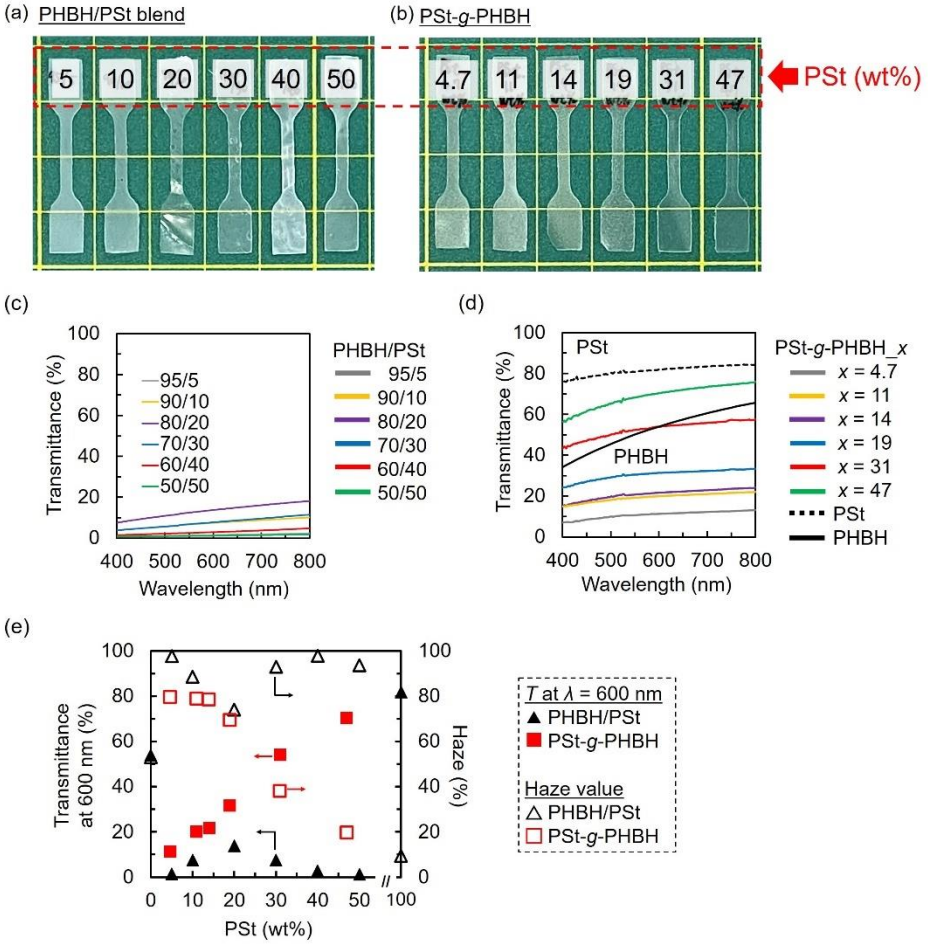


**Figure 2.4.** Optical properties of PHBH/PSt blend and PSt-*g*-PHBH films: (a, b) Photographs of their films, (c, d) UV-vis spectra of neat PSt, neat PHBH, and PSt-*g*-PHBH films [(a, c) PHBH/PSt blend, (b, d) PSt-g-PHBH film], (c) Transmittance at $\lambda$ = 600 nm and haze of PHBH/PSt blend films and PSt-*g*-PHBH films as a function of PSt weight ratio.

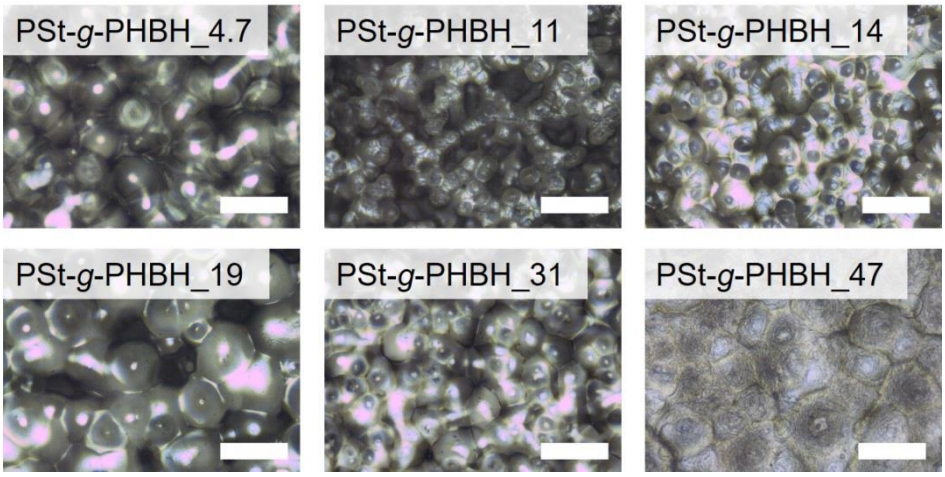


**Figure 2.5.** Photographs of surface morphology on the PSt-*g*-PHBH [scale bar: 50 μm].

**Table 2.3.** Melting enthalpy ($\Delta H_m$) of PSt-*g*-PHBH.

| Polymer | PHBH weight ratio (wt%) | $\Delta H_{m\_measured}$ (J/g) [a] | $\Delta H_{m\_PHBH}$ (J/g) [b] |
|---|---|---|---|
| PSt-g-PHBH_4.7 | 95.3 | 44.5 | 46.7 |
| PSt-g-PHBH_11 | 89.0 | 42.0 | 47.2 |
| PSt-g-PHBH_14 | 86.0 | 40.4 | 47.0 |
| PSt-g-PHBH_19 | 81.0 | 35.6 | 44.0 |
| PSt-g-PHBH_31 | 69.0 | 30.1 | 43.6 |
| PSt-g-PHBH_47 | 53.0 | 23.8 | 45.0 |

(a) $\Delta H_{m\_measured}$ is measured by DSC 1st heating. (b) $\Delta H_{m\_PHBH}$ is calculated by the following equation: $\Delta H_{m\_PHBH} = \Delta H_{m\_measured} / w_{PHBH}$, where $w_{PHBH}$ is the weight ratio of PHBH.

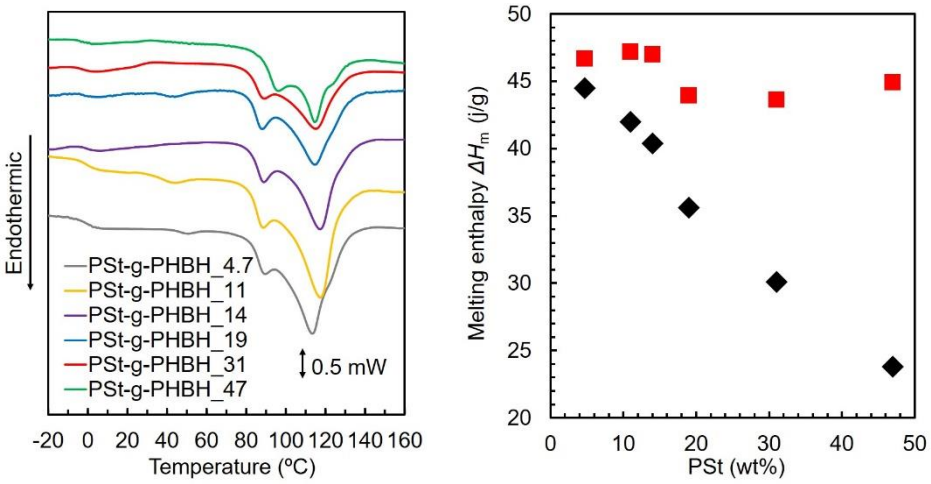


**Figure 2.6.** Crystallinity of PSt-g-PHBH with the change in PSt weight ratio: (a) DSC 1st heating of PSt-g-PHBH, (b) $\Delta H_m$ of PSt-*g*-PHBH (black diamond) and $\Delta H_m$ of PHBH in the PSt-*g*-PHBH (red square) as a function of PSt amount (wt%).

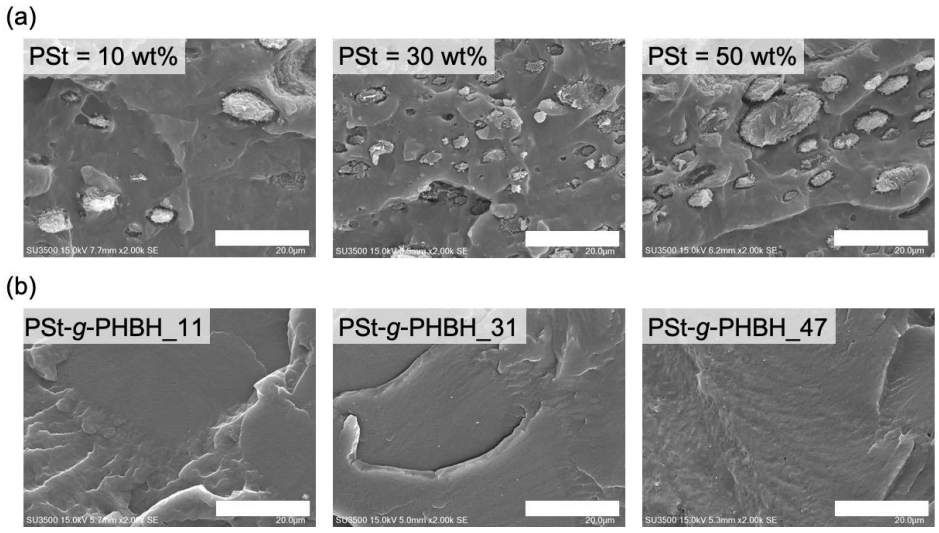


**Figure 2.7.** SEM image of the cryo-fracture surface of (a) PHBH/PSt with weight ratio of 10, 30, 50 and (b) PSt-*g*-PHBH _11, 31, and 47 [scale bar: 20 μm].

### 2.3.3. Glass transition behavior of PSt-*g*-PHBH

To investigate the influence of the '*grafting to*' method on the compatibility of PHBH and PSt in their blends, $T_g$ was measured by DMA and DSC.[27–30] The results of DMA showed that the temperature dependence of loss modulus (*E"*) of neat PHBH showed a peak at −11.3 °C corresponding to $T_g$ of PHBH; on the other hand, *E"* peak of PSt-*g*-PHBH was shifted to a higher temperature between -7.8 °C and −5.0 °C (**Figure 2.8a**). Furthermore, with the PSt weight ratio increased, new *E"* peak charts emerged at around 90 °C, which was attributed to $T_g$ of PSt backbones. The peak top of loss tangent (tan$\delta$) also corresponds to $T_g$ of polymers. The tan$\delta$ peak of neat PHBH appeared at −4.1 °C; in contrast, the tan$\delta$ peak of PSt-*g*-PHBH showed a higher temperature between −2.4 °C and 5.0 °C (**Figure 2.8b**). In detail, when increasing the PSt weight ratio to 11 wt%, the peak of tan$\delta$ clearly increased to 5.0 °C. However, in the range of 14 – 47 wt% of PSt content, this peak slightly decreased to −2.4 °C. DSC measurements also showed a similar tendency to the change in $T_g$ measured by DMA (**Table 2.4**). The height of the tan$\delta$ peak was clearly decreased from 0.2 to 0.1 with the increase in the weight ratio of PSt. Hence, the thermal analysis demonstrated that grafting PHBH to PSt induced the change of the glass transition behavior of the PHBH and PSt.

Thermal analysis results with DMA and DSC showed the rise in $T_g$ of PHBH by grafting to PSt. This result is related that the mobility of the PHBH backbone was declined by grafting to PSt with high $T_g$ (~ 100 °C). Additionally, the decrease in the PHBH chain mobility led to inhibiting the molecular mobility of PHBH chains at around $T_g$ of PHBH.[31] However, at more than 14 wt% of PSt, $T_g$ corresponding to PHBH grafted chains lowered and approached that of neat PHBH; conversely, $T_g$ corresponding to PSt main chains was detected at around 100 °C. The change in bimodal $T_g$ of PSt-*g*-PHBH is assumed that the microphase separation of PSt and PHBH was generated in the films, as shown in **Figure 2.8c**.[32] Furthermore, the height of the tan$\delta$ peak top corresponding to $T_g$ of PHBH became lower than that of PHBH, shown in **Figure 2.8b**. This tendency implies that the PSt-*g*-PHBH film

obtained elasticity instead of its viscosity.[6] Thus, DMA and DSC revealed that the compatibility between PHBH and PSt was enhanced and the microphase separation of PHBH and PSt was formed in PSt-*g*-PHBH films.

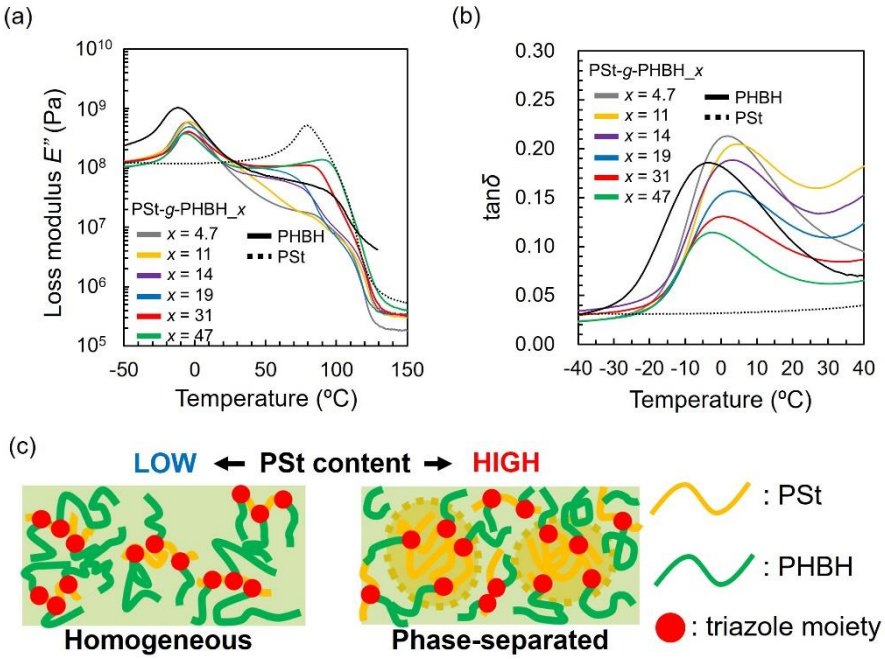


**Figure 2.8.** Temperature dependence of (a) loss modulus (*E''*) and (b) loss tangent (tan$\delta$) of PSt-*g*-PHBH films, and (c) illustration of the proposal morphological change of PSt-*g*-PHBH films with the change in PSt weight ratio.

**Table 2.4.** $T_g$ of PSt-*g*-PHBH determined by DSC.

| Sample name | $T_g$ of PHBH (°C) | $T_g$ of PSt (°C) |
|---|---|---|
| PSt-*g*-PHBH_4.7 | −3.3 | - |
| PSt-*g*-PHBH_11 | −2.5 | - |
| PSt-*g*-PHBH_14 | −2.0 | - |
| PSt-*g*-PHBH_19 | −2.6 | - |
| PSt-*g*-PHBH_31 | −2.9 | 73 |
| PSt-*g*-PHBH_47 | −3.8 | 88 |
| neat PHBH | −4.4 | - |
| neat PSt | - | 100 |

### 2.3.4. Mechanical properties of PSt-*g*-PHBH

Mechanical properties of PSt-*g*-PHBH including Young's modulus and maximum strength were determined by tensile tests and summarized in **Table 2.5**. Then, the obtained stress-strain curves were shown in **Figure 2.9**. **Figure 2.10** exhibits the change in Young's modulus and tensile strength of PSt-*g*-PHBH and PHBH/PSt films as a function of the PSt content (wt%). Young's modulus of PHBH/PSt was identical value between 0.6 GPa and 0.8 GPa with independent of the PSt weight ratio. The tensile strength of PHBH/PSt was apparently decreased by adding PSt. As a result, it is impossible to improve the mechanical strength of PHBH by blending PSt with PHBH. On the contrary, Young's modulus and tensile strength of PSt-*g*-PHBH were dramatically improved with the increment of the PSt weight ratio from 0.63 GPa and 15.0 MPa to 1.24 GPa and 30.0 MPa, respectively. In comparison with the mechanical properties of PHAs, Young's modulus and tensile strength of PSt-*g*-PHBH_47 were comparable to those of PHB (Young's modulus ~ 1.40 GPa and tensile strength ~ 27.0 MPa, respectively).[33] These values are also preferring to those of PHBH with a low 3HHx unit ratio.[34] In general, to obtain high elastic modulus for short-chain length PHAs copolymers including PHBH and poly(3-hydroxybutyrate-*co*-3-hydroxyvalerate), long-term crystallization time is needed, which indicates the low processability of PHAs.[35] Thereby, the transparency of the PHAs film also decreased because of its crystallization.[36] However, the obtained results claim that PSt-*g*-PHBH films have high mechanical properties with maintaining their good transparency without the aging process to crystalize PHBH chains. Elongation at break and fracture energy of PSt-*g*-PHBH were from 7.1 to 24.5 % and from 0.86 to 2.56 MJ/m$^3$, respectively, which were higher than those of neat PSt (**Table 2.5**). Therefore, the '*grafting to*' method with Propargyl-PHBH and

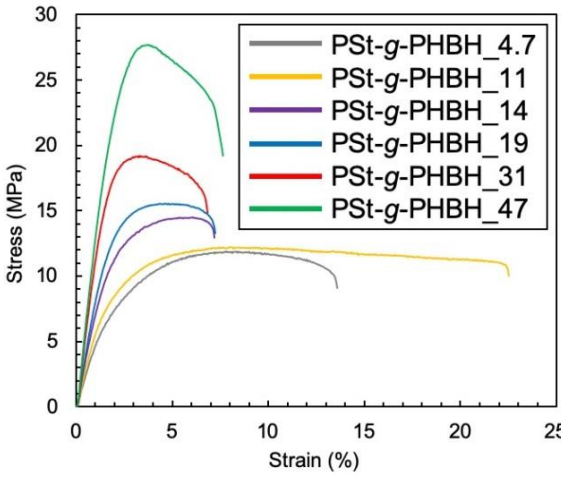


**Figure 2.9.** Typical stress-strain curves of PSt-*g*-PHBH measured by tensile test.

azide-modified PSt is one of the effective strategies to improve the mechanical properties of PHBH biomass plastics.

**Table 2.5.** Mechanical properties of PSt-*g*-PHBH.

| Sample name | Young's modulus (GPa) | Tensile strength (MPa) | Elongation at break (%) | Fracture energy ($MJ/m^3$) |
|---|---|---|---|---|
| PSt-*g*-PHBH_4.7 | 0.49±0.02 | 12.1±0.8 | 13.3±1.2 | 1.35±0.21 |
| PSt-*g*-PHBH_11 | 0.55±0.02 | 11.7±0.8 | 24.5±3.0 | 2.56±0.35 |
| PSt-*g*-PHBH_14 | 0.73±0.06 | 14.7±1.0 | 7.1±0.8 | 0.86±0.20 |
| PSt-*g*-PHBH_19 | 0.76±0.08 | 14.9±1.5 | 7.5±1.1 | 0.91±0.14 |
| PSt-*g*-PHBH_31 | 0.86±0.03 | 21.8±2.6 | 7.5±3.7 | 1.35±0.81 |
| PSt-*g*-PHBH_47 | 1.24±0.08 | 27.4±3.4 | 8.4±2.6 | 1.75±0.80 |
| Neat PHBH | 0.64±0.02 | 14.7±0.4 | 412.0±14.0 | 65.77±4.49 |
| Neat PSt | 2.25±0.18 | 29.4±7.2 | 1.5±0.4 | 0.16±0.12 |

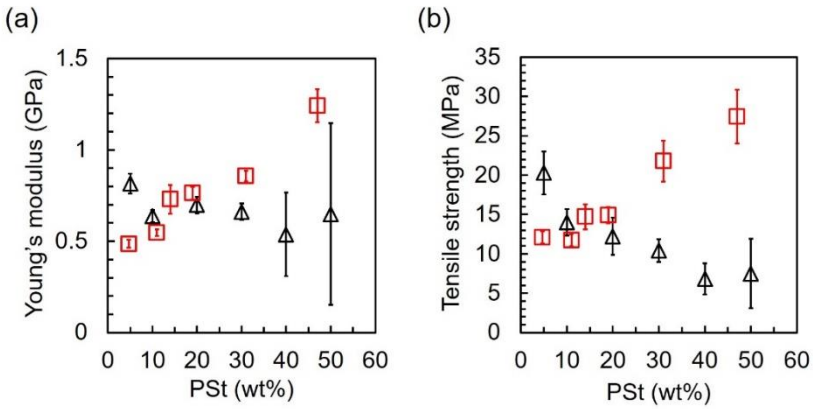


**Figure 2.10.** (a) Young's modulus and (b) Tensile strength of PHBH/PSt blend film (black triangle) and PSt-*g*-PHBH film (red square) as a function of the amount of PSt content (wt%).

To discuss the influence of the 'grafting to' method with Propargyl-PHBH on the interfacial adhesion between PHBH and PSt, the Pukánszky model was applied to the tensile test results of PHBH/PSt and PSt-*g*-PHBH. This model is described as the following **eq (2-1)**, which can quantitively evaluate the stress transfer efficiency of composite materials,

$$\ln(\sigma_{red}) = \ln[\sigma_c \bullet (1 + 2.5\varphi_d) / (1 - \varphi_d)] = \ln\sigma_m + B\varphi_d \quad (2\text{-}1)$$

where $\sigma_m$ and $\sigma_c$ mean tensile strength of a matrix polymer and a composite material, and $\varphi_d$ is the volume fraction of a dispersed phase material, respectively.[27] The $\varphi_d$ value of filler is calculated by following **eq (2-2)**:

$$\varphi_d = (w_d / \rho_d) / \{w_d / \rho_d + (1 - w_d) / \rho_m\} \quad (2\text{-}2)$$

where, $w_d$ is a weight ratio of the dispersion phase, and $\rho_d$ (= 1.05 g/cm$^3$) and $\rho_m$ (= 1.2 g/cm$^3$) represent the density of the dispersion phase and the matrix, respectively. SEM observation (**Figure 2.7**) and DMA analysis (**Figure 2.8**) imply that in this experiment, PSt phases were dispersed in the PHBH matrix. Thereby, it can be hypothesized that PSt was dispersion phase in the PHBH matrix phase, and the resultant **eq (2-1)** curves of PHBH/PSt blend films and PSt-*g*-PHBH films were depicted in **Figure 2.11**. The *B* calculated from the slope and the coefficient of determination ($R^2$) of **eq (2-1)** were embedded in **Figure 2.11**. The absolute value of *B* of PSt-*g*-PHBH became 4.8, which was almost 5 times higher than that of PHBH/PSt (*B* = 1.0). Generally, the increase in the value of *B* indicates that the compatibility of dispersion and matrix on their interface is enhanced.[22,27] In short, PSt-*g*-PHBH has higher compatibility on the PHBH/PSt interface. As a result, the analysis with the Pukánszky model reveals that the interfacial compatibility of the PHBH/PSt mixture was marginally improved by the 'grafting to' method. Additionally, the monotonical decrease in the tensile strength of PHBH/PSt as a function of the PSt weight ratio implies their low interfacial adhesion; conversely, the monotonical increase in the tensile

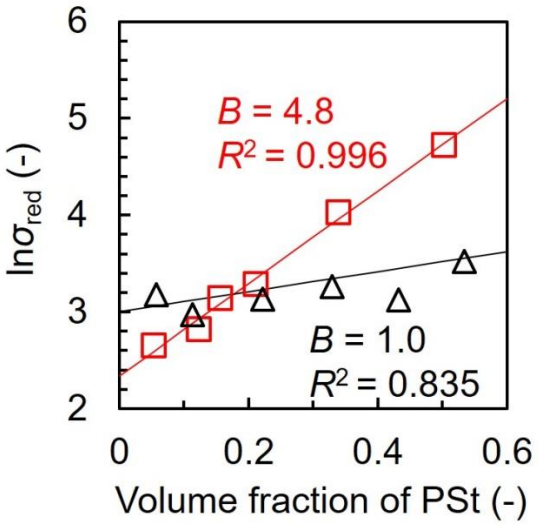


**Figure 2.11.** Pukánszky model of PHBH/PSt blend film (black triangle) and PSt-*g*-PHBH film (red square).

strength of PSt-*g*-PHBH as a function of PSt content indicates the strong interaction between PHBH and PSt.[37] SEM image shown in **Figure 2.7** also exhibited that PHBH/PSt blend had a heterogeneous cross section due to their phase separation, in contrast, PSt-*g*-PHBH was a homogeneous and smooth surface. The heterogeneity of the PHBH/PSt blend induced the ununiform stress propagation in the films, deteriorating their mechanical properties. On the contrary, the homogeneous PSt-*g*-PHBH films obtained the good mechanical strength of PHBH compared with that of PHBH/PSt because the tensile stress can be uniformly propagated on the bulk films. These results support the discussion of the improvement in the compatibility of the PHBH/PSt interface. Thus, the preparation of graft copolymers from PHBH and PSt is an effective strategy to reinforce the mechanical properties of biomass plastics.

## 2.4 Conclusions

This chapter reported that grafting PHBH to PSt provided PHBH with sufficient optical and mechanical properties. PSt-*g*-PHBH was successfully synthesized from Propargyl-PHBH and P(AMS-*co*-St) through CuAAC reaction. **Figure 2.12** describes that grafting to PSt influence the physical properties of PHBH mentioned below. The PSt-*g*-PHBH films showed not only good homogeneity (transmittance ~ 80%) but also high Young's modulus and tensile strength (1.2 GPa and 27 MPa, respectively) when the PSt content was lower than 50 wt%. These results indicated that the optical and mechanical properties of PHAs-based materials were improved by grafting to PSt. Furthermore, elastic modulus and tensile strength of PSt-*g*-PHBH were comparable to those of commodity plastics. Pukánszky model analysis demonstrated that stress transfer efficiency between PHBH and PSt was dramatically increased by the preparation of the graft copolymer consisted of PHBH and PSt. The DMA and DSC measurements displayed the rise in $T_g$ of PHBH by grafting to PSt, which

demonstrated the improvement in the compatibility between PHBH and PSt. Besides, *E"* curves of the graft copolymers showed the change in $T_g$ of PHBH and PSt and the generation of microphase separation of PHBH and PSt in the films. As a result, theoretical and thermal analysis proved that the compatibility and interfacial adhesion of PHBH/PSt were enhanced by grafting to method with Propargyl-PHBH and azide-modified PSt, endowing PHBH with good physical properties such as good homogeneity and mechanical strength. This chapter reported that Propargyl-PHBH is one of the promising materials to improve the physical properties of biomass plastics by grafting to other functional polymers. The obtained consequence can also contribute to the expansion of the industrial applications of PHBH in various fields such as engineering, packaging, and medical materials.

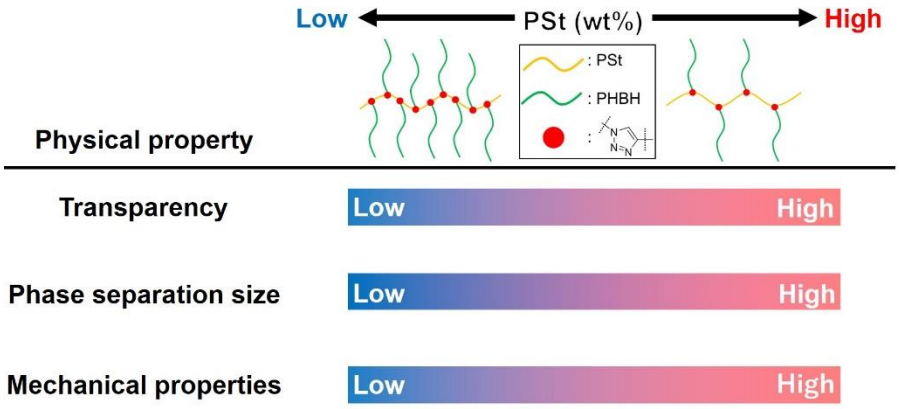


**Figure 2.12.** Summary of physical properties of PSt-*g*-PHBH with the change in PSt wt%.

## 2.5 References


[1] G. Q. Chen, M. K. Patel, *Chem. Rev.* **2012**, *112*, 2082.

[2] G. Q. Chen, *Chem. Soc. Rev.* **2009**, *38*, 2434.

[3] Z. Li, X. J. Loh, *Chem. Soc. Rev.* **2015**, *44*, 2865.

[4] H. Alata, T. Aoyama, Y. Inoue, *Macromolecules* **2007**, *40*, 4546.

[5] O. Parlak, M. M. Demir, *ACS Appl. Mater. Interfaces* **2011**, *3*, 4306.

[6] J. Zhao, Y. Liu, J. Cheng, S. Wu, Z. Wang, H. Hu, C. Zhou, *Polym. Int.* **2017**, *66*, 1827.

[7] H. Gu, C. Ma, C. Liang, X. Meng, J. Gu, Z. Guo, *J. Mater. Chem. C* **2017**, *5*, 4275.

[8] P. G. Ward, M. Goff, M. Donner, W. Kaminsky, K. E. O'Connor, *Environ. Sci. Technol.* **2006**, *40*, 2433.

[9] S.-S. Yang, W.-M. Wu, A. M. Brandon, H.-Q. Fan, J. P. Receveur, Y. Li, Z.-Y. Wang, R. Fan, R. L. McClellan, S.-H. Gao, D. Ning, D. H. Phillips, B.-Y. Peng, H. Wang, S.-Y. Cai, P. Li, W.-W. Cai, L.-Y. Ding, J. Yang, M. Zheng, J. Ren, Y.-L. Zhang, J. Gao, D. Xing, N.-Q. Ren, R. M. Waymouth, J. Zhou, H.-C. Tao, C. J. Picard, M. E. Benbow, C. S. Criddle, *Chemosphere* **2018**, *212*, 262.

[10] A. M. Brandon, S. H. Gao, R. Tian, D. Ning, S. S. Yang, J. Zhou, W. M. Wu, C. S. Criddle, *Environ. Sci. Technol.* **2018**, *52*, 6526.

[11] A. M. Brandon, S. H. El Abbadi, U. A. Ibekwe, Y.-M. Cho, W.-M. Wu, C. S. Criddle, *Environ. Sci. Technol.* **2019**, *54*, 364.

[12] L. Gu, E. E. Nessim, C. W. Macosko, *Polymer* **2018**, *134*, 104.

[13] V. Nikolic, S. Velickovic, A. Popovic, *Environ. Sci. Pollut. Res.* **2014**, *21*, 9877.

[14] Y. Ma, J. Dai, L. Wu, G. Fang, Z. Guo, *Polymer* **2017**, *114*, 113.

[15] R. J. M. Smit, W. A. M. Brekelmans, H. E. H. Meijer, *J. Mater. Sci.* **2000**, *35*, 2855.

[16] T. Oyama, S. Kobayashi, T. Okura, S. Sato, K. Tajima, T. Isono, T. Satoh, *ACS Sustain. Chem. Eng.* **2019**, *7*, 7969.

[17] C. Jain-Beuguel, X. Li, L. Houel-Renault, T. Modjinou, C. Simon-Colin, R. Gref, E. Renard, V. Langlois, *Biomacromolecules* **2019**, *20*, 3324.

[18] J. S. F. Barrett, A. A. Abdala, F. Srienc, *Macromolecules* **2014**, *47*, 3926.

[19] H. Yao, L. P. Wu, G. Q. Chen, *Biomacromolecules* **2019**, *20*, 645.

[20] H. Yao, D. Wei, X. Che, L. Cai, L. Tao, L. Liu, L. Wu, G. Q. Chen, *Polym. Chem.* **2016**, *7*, 5957.

[21] L. P. Yu, X. Zhang, D. X. Wei, Q. Wu, X. R. Jiang, G. Q. Chen, *Biomacromolecules* **2019**, *20*, 3233.

[22] B. Pukánszky, *Composites* **1990**, *21*, 255.

[23] K. Shingo, T. Fujiki, **2018**, US 2018/0346943 A1.

[24] N. Alkayal, H. Durmaz, U. Tunca, N. Hadjichristidis, *Polym. Chem.* **2016**, *7*, 2986.

[25] J. S. Kim, P. K. H. Ho, C. E. Murphy, R. H. Friend, *Macromolecules* **2004**, *37*, 2861.

[26] S. Y. Heriot, R. A. L. Jones, *Nat. Mater.* **2005**, *4*, 782.

[27] K. Hamad, M. Kaseem, F. Deri, Y. G. Ko, *Mater. Lett.* **2016**, *164*, 409.

[28] V. Romhányi, D. Kun, B. Pukánszky, *ACS Sustain. Chem. Eng.* **2018**, *6*, 14323.

[29] D. Kai, K. Zhang, S. S. Liow, X. J. Loh, *ACS Appl. Bio Mater.* **2018**, *2*, 127.

[30] N. Uthaman, A. Majeed, Pandurangan, *Polym. Eng. Sci.* **2012**, *52*, 233.

[31] D. J. Lohse, S. Datta, E. N. Kresge, *Macromolecules* **1991**, *24*, 561.

[32] J. Zhang, T. Li, A. M. Mannion, D. K. Schneiderman, M. A. Hillmyer, F. S. Bates, *ACS Macro Lett.* **2016**, *5*, 407.

[33] C. Mangeon, L. Michely, A. Rios De Anda, F. Thevenieau, E. Renard, V. Langlois, *ACS Sustain. Chem. Eng.* **2018**, *6*, 16160.

[34] P. Xu, Q. Zeng, Y. Cao, P. Ma, W. Dong, M. Chen, *Carbohydr. Polym.* **2017**, *174*, 716.

[35] M. J. Jenkins, K. E. Robbins, C. A. Kelly, *Polym. J.* **2018**, *50*, 365.

[36] T. Aoyama, H. Sato, Y. Ozaki, *Polym. Cryst.* **2019**, *2*, e10076.

[37] Y. Zare, A. Rahmani, *J. Colloid Interface Sci.* **2016**, *470*, 245.

# Chapter 3

## Improvement in interfacial adhesion of poly(3-hydroxybutyrate-*co*-3-hydroxyhexanoate)/$SiO_2$ composite

## 3.1. Introduction

As mentioned in the general introduction, recently, microbial PHBH has attracted sustainable interest as biomass plastics because the use of oil-based resins has been regulated to achieve a sustainable society: however, its mechanical properties are low to apply to industrial materials. To improve Young's modulus and tensile strength of PHBH, some researchers prepared and evaluated PHBH with inorganic fillers as already explained in the general introduction.[1–9] Although these fillers reinforced PHBH bulk film, Young's modulus of PHBH/filler composite materials remains small because of the low interfacial adhesion between hydrophilic filler surface and the hydrophobic PHBH matrix.[1,7] Furthermore, the low interfacial adhesion between filler and matrix causes the agglomeration of fillers and generates crack and void on the PHA/filler interface; these phenomena induce the decrease in the yield stress and toughness of PHAs.[1,3] Therefore, the interfacial compatibility between PHAs and the inorganic filler must be improved, leading to expanded usage of PHAs.

To enhance the interfacial adhesion between the filler and the matrix, surface-modified silica-based materials have been studied.[10] In previous works, surface modified $SiO_2$ have been developed by using varied silane coupling reagents[11–14] and grafting polymers on the $SiO_2$ surface.[15–24] In silane coupling methods, amine groups,[11,12] epoxy groups,[13] and vinyl groups[14] were introduced onto $SiO_2$. Besides that, grafting various polymers to $SiO_2$ was achieved by free radical polymerization,[15] living radical polymerization,[16–18] condensation reaction,[19–22] and click chemistry[23,24]. In order to modify the $SiO_2$ surface with PHAs,

PHAs must be polymerized using a specific catalyst by a complicated chemical process.[25] Therefore, a 'grafting to' method through click reaction will be suitable. Recently, end-reactive PHAs have attracted great interest, such as those having hydroxy, methoxy, vinyl, and propargyl as end groups.[26]

In this chapter, PHBH-grafted $SiO_2$ ($SiO_2$-PHBH) was prepared by Propargyl-PHBH and azide-modified $SiO_2$ ($SiO_2$-azide) *via* a CuAAC reaction to reinforce the compatibility on the interface between the filler and the matrix. The unmodified $SiO_2$ and $SiO_2$-PHBH were added to PHBH as a filler. The mechanical properties of the PHBH/$SiO_2$-PHBH composite films were measured by a tensile test and compared to PHBH/$SiO_2$ films. The dispersity of $SiO_2$-PHBH or $SiO_2$ in the PHBH matrix was evaluated by electron microscopic observation and theoretical analysis by using the Halpin-Tsai model.[1,27–29] Finally, the difference of interfacial adhesion between the filler and the matrix was discussed with theoretical analysis including the Pukánszky model,[30] the Nicolais – Narkis model,[31–33] thermal analysis with dynamic mechanical analysis (DMA) and differential scanning calorimetry (DSC). In this chapter, the author presents a new application of end-reactive PHAs for surface modification of fillers for the first time. Additionally, the obtained results can contribute to the expansion of the industrial application of PHBH.

## 3.2 Experimental section

### 3.2.1. Materials

Neat PHBH ($M_w$ = 660,000, HHx units = 11 mol%) and Propargyl-PHBH ($M_n$ = 25,000, $M_w/M_n$ = 2.1, HHx units = 11 mol%) were kindly provided by KANEKA Co., (Osaka, Japan). The synthesis of Propargyl-PHBH has been reported in a previous study.[34] Propargyl-PHBH was purified by precipitation with chloroform as a good solvent and methanol as a poor solvent. Monodisperse silica colloidal particles ($SiO_2$; type MP-3040, particle diameter = 450

nm, $SiO_2$ concentration in water = 40 vol%, silica density = 2.2 g/mL) were donated by Nissan Chemical Company (Tokyo, Japan). 4-(Chloromethyl)phenyltrimethoxysiliane (CTS) as a silane-coupling reagent was purchased from Fluorochem Ltd. (Derbyshire, UK). Sodium azide, dichloromethane, and chloroform were purchased from Nacalai Tesque Inc. (Kyoto, Japan). Methanol and copper(I) bromide were purchased from FUJIFILM Wako Pure Chemical Co. (Osaka, Japan). *N, N, N', N'', N''*-Pentamethyldiethylenetriamine (PMDETA) was purchased by Tokyo Chem. Ind., (Tokyo, Japan). Except for the Propargyl-PHBH, the reagents were used as received.

### 3.2.2. Preparation of $SiO_2$-PHBH

$SiO_2$-azide used for $SiO_2$-PHBH preparation was synthesized using chloride-modified $SiO_2$ ($SiO_2$-chloride) and sodium azide, based on previous studies (**Scheme 3.1**).[17,35,36] First, the dispersion medium of the $SiO_2$/water dispersion was exchanged to methanol by centrifugation which was repeated several times. Subsequently, CTS (5 mL) was added to the prepared $SiO_2$/methanol dispersion (20 mL), stirring at 50 °C for 24 h for the silane coupling reaction. Then, the $SiO_2$/methanol dispersion was washed by methanol several times to remove the unreacted CTS. The dispersion medium of the obtained $SiO_2$-chloride/methanol dispersion was exchanged in Milli-Q water (total volume = 30 mL). Then, sodium azide (2.0 g) was added into the dispersion and reacted at 80 °C for 24 h with stirring to prepare $SiO_2$-azide. $SiO_2$-azide/water dispersion was washed by Milli-Q water several times to remove unreacted sodium azide, then, $SiO_2$-azide particles were re-dispersed in methanol. Finally, the dispersion medium of $SiO_2$-azide was exchanged from methanol to dichloromethane by centrifugation.

$SiO_2$-PHBH was prepared using Propargyl-PHBH and $SiO_2$-azide following the CuAAC reaction (**Scheme 3.1**). Propargyl-PHBH (7.0 g, propargyl group = 0.28 mmol) was

initially dissolved in dichloromethane (55 mL) under stirring, then, $SiO_2$-azide/dichloromethane dispersion (30 mL, conc. = 80 mg/mL) was added into the polymer solution. PMDETA (20 mg, 0.14 mmol) as a ligand and copper(I) bromide (24 mg, 0.14 mmol) as a catalyst were then added to the mixture under a nitrogen atmosphere under stirring. The reaction was conducted at 35 °C for 72 h in an argon atmosphere. The obtained $SiO_2$-PHBH/dichloromethane dispersion was washed several times by chloroform to remove the ligand, catalyst, and unreacted Propargyl-PHBH. Subsequently, the solvent of $SiO_2$-PHBH/dichloromethane dispersion was exchanged in chloroform. The final concentration of the obtained $SiO_2$-PHBH/chloroform dispersion was ~81 mg/mL.

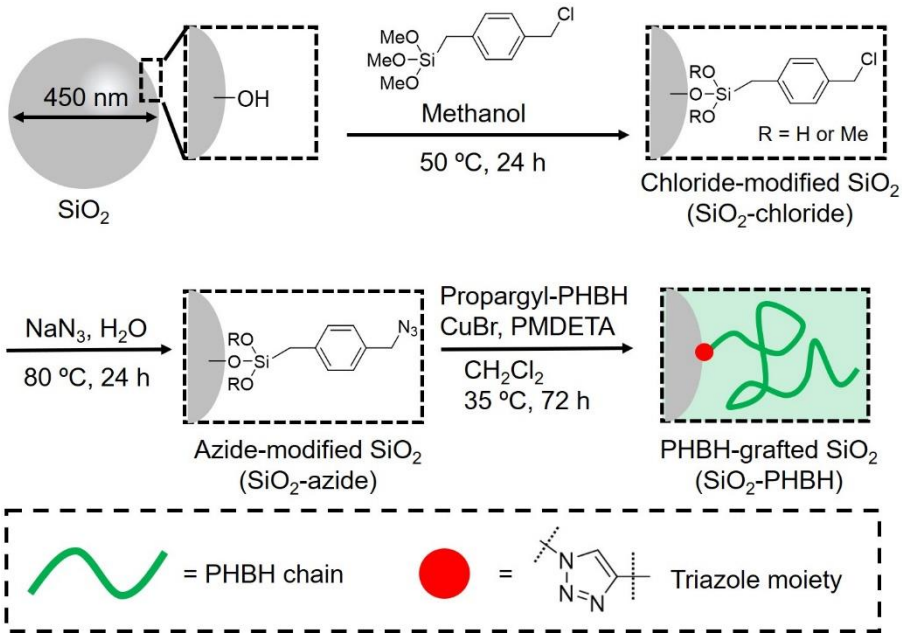


**Scheme 3.1.** Preparation of $SiO_2$-PHBH: (1st step) introduction of chloride groups to the $SiO_2$ surface with CTS, (2nd step) conversion to azide groups from chloride groups with $NaN_3$, (3rd step) coupling $SiO_2$-azide and Propargyl-PHBH through CuAAC reaction.

### 3.2.3. Fabrication of PHBH/$SiO_2$-PHBH composite films

PHBH/$SiO_2$ and PHBH/$SiO_2$-PHBH composite films were prepared by solvent casting with chloroform. PHBH (1 g) was dissolved in chloroform (13 mL) under stirring. $SiO_2$-

PHBH (or $SiO_2$)/chloroform was then added to the PHBH solution, and the mixture solution was added into a perfluoroalkoxy alkane petri dish. The concentration of $SiO_2$-PHBH (or $SiO_2$) in the matrix was adjusted by changing the content of the $SiO_2$-PHBH/chloroform dispersion. After drying at 30 °C overnight, the samples were dried under a vacuum at 80 °C for 24 h to remove chloroform. The thickness of the obtained composite films was approximately 100 μm. The obtained films were cut into appropriate shapes as followed: dumbbell shape (2 mm × 20 mm) for tensile tests, and rectangular shape (5 mm × 40 mm) for DMA.

### 3.2.4. Measurement

The chemical structure was confirmed by attenuated total reflectance-Fourier transform infrared (ATR-IR) spectroscopy with the same equipment as in Chapter 2. To measure the weight ratio of PHBH on the $SiO_2$-PHBH, the samples (approximately 5 mg) were placed into a Pt pan and TGA was carried out using the same device as in Chapter 1 under $N_2$ atmosphere over a temperature range from 40 °C to 800 °C with a scanning rate of 10 °C/min. The transparency of the films was measured by UV-vis spectroscopy with the same device as in Chapter 2. The mechanical properties of the neat PHBH film and the prepared composite films were determined by the tensile test, which condition is stated in the experimental section of Chapter 1. The morphology of the cryo-fracture surface of the resultant films was observed by SEM using the same devices as in Chapter 1. DMA was used to confirm the interfacial adhesion between filler and matrix. DMA measurement was the same as the previous chapter. $T_g$ of the sample was measured by DSC, and see chapter 1 for this measurement condition.

## 3.3 Results and Discussion

### 3.3.1. Characterization of $SiO_2$-PHBH

The ATR-IR spectra of the obtained $SiO_2$-PHBH showed a peak at 1740 $cm^{-1}$, corresponding to the symmetric stretching of the C=O group of the PHBH main chain (**Figure 3.1a**). The amount of PHBH was ~1.2 wt%, calculated from the TGA curves as the difference of the weight loss of the $SiO_2$-azide and $SiO_2$-PHBH at 650 °C (**Figure 3.1b**) because PHBH is completely decomposed at 550 °C. The images of $SiO_2$, $SiO_2$-azide, and $SiO_2$-PHBH dispersion in chloroform (80 mg/mL) are shown in **Figure 3.1c**. Both the $SiO_2$ and $SiO_2$-azide were immediately precipitated in chloroform, while the $SiO_2$-PHBH particles were uniformly dispersed in chloroform after 6 h. The difference in dispersion stability revealed that the enhancement in the compatibility between the $SiO_2$ surface and the chloroform is due to the introduction of the PHBH chains to the surface of $SiO_2$. After changing the solvent from chloroform to methanol with centrifugation, the $SiO_2$-PHBH particles were aggregated rapidly and precipitated in methanol, surrounded by a red broken line circle, as described in **Figure 3.1d**. Subsequently, the solvent was repeatedly exchanged from methanol to chloroform and the $SiO_2$-PHBH was re-dispersed in chloroform. This phenomenon takes place because chloroform is a good solvent while methanol is a

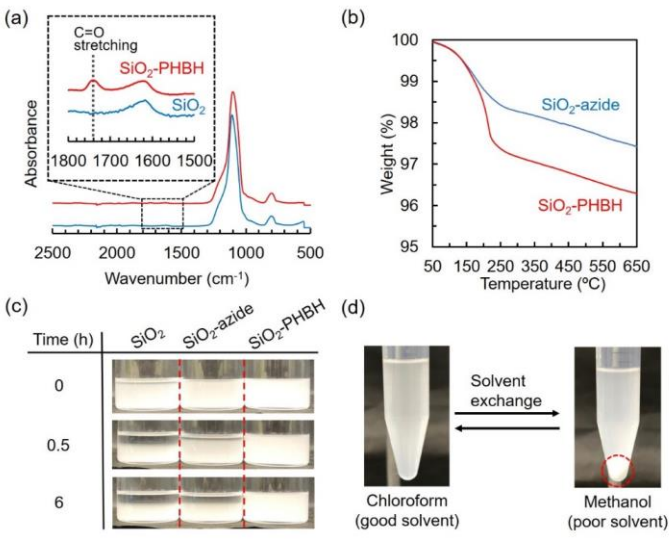


**Figure 3.1.** Characterization of $SiO_2$-PHBH: (a) ATR-IR spectra, (b) TGA charts, (c) dispersion stability of $SiO_2$, $SiO_2$-azide, and $SiO_2$-PHBH in chloroform, and (d) dispersity of $SiO_2$-PHBH in chloroform and methanol.

poor solvent for PHBH. These results indicated that the $SiO_2$-PHBH was successfully prepared from Propargyl-PHBH and $SiO_2$-azide through click chemistry.

The disparities of $SiO_2$ and $SiO_2$-PHBH in the PHBH matrix were evaluated by UV-vis spectroscopy and SEM observation. **Figure 3.2a** shows images of the dispersion consisting of PHBH and $SiO_2$ or $SiO_2$-PHBH in chloroform at 10 wt% of filler content to the PHBH amount. The PHBH/$SiO_2$ chloroform solution became cloudy; in contrast, the dispersion of PHBH/$SiO_2$-PHBH became more transparent. Furthermore, after 24 h, the $SiO_2$ was precipitated in a PHBH/chloroform solution, which is shown in the red rectangular frame in **Figure 3.2a**. On the other hand, the $SiO_2$-PHBH maintained good dispersity in PHBH/chloroform after 24 h. These results are related to the enhancement of the interfacial adhesion of $SiO_2$ and PHBH/chloroform solution by surface modification with Propargyl-PHBH. **Figures 3.2b and c** show the transparency of PHBH/$SiO_2$ and PHBH/$SiO_2$-PHBH films with different $SiO_2$ or $SiO_2$-PHBH contents. After adding non-modified $SiO_2$ as a filler, the PHBH/$SiO_2$ film became opaque. Moreover, the PHBH/$SiO_2$ composite films with 5 wt% and 10 wt% of $SiO_2$ showed that the white parts appeared due to the agglomeration of $SiO_2$. The transmittance at 500 nm of PHBH/$SiO_2$ films was also dramatically decreased from 35% to 12% with increasing $SiO_2$ content. Conversely, PHBH/$SiO_2$-PHBH composite films relatively maintained their transparency, and the transmittance of PHBH/$SiO_2$-PHBH films at 500 nm was higher than those of PHBH/$SiO_2$ films. The SEM images of the cryo-fracture surface of PHBH/$SiO_2$ and PHBH/$SiO_2$-PHBH films are shown in **Figure 3.2d**. The obtained SEM images show that $SiO_2$ fillers were aggregated in the PHBH film, in contrast to the $SiO_2$-PHBH fillers, which were uniformly dispersed in the PHBH matrix. These results confirm that the surface modification of $SiO_2$ with Propargyl-PHBH improves the dispersion efficiency of the filler in the PHBH casting film, inhibiting $SiO_2$ agglomeration. Thereby, this phenomenon confirmed that the dispersity of $SiO_2$ filler in chloroform is also important for

fabricating uniform PHBH/$SiO_2$ composite films by the solvent casting method. Thus, the obtained results indicate that the $SiO_2$-PHBH was well-dispersed in the PHBH film more uniformly without the agglomeration of the pristine $SiO_2$ fillers.

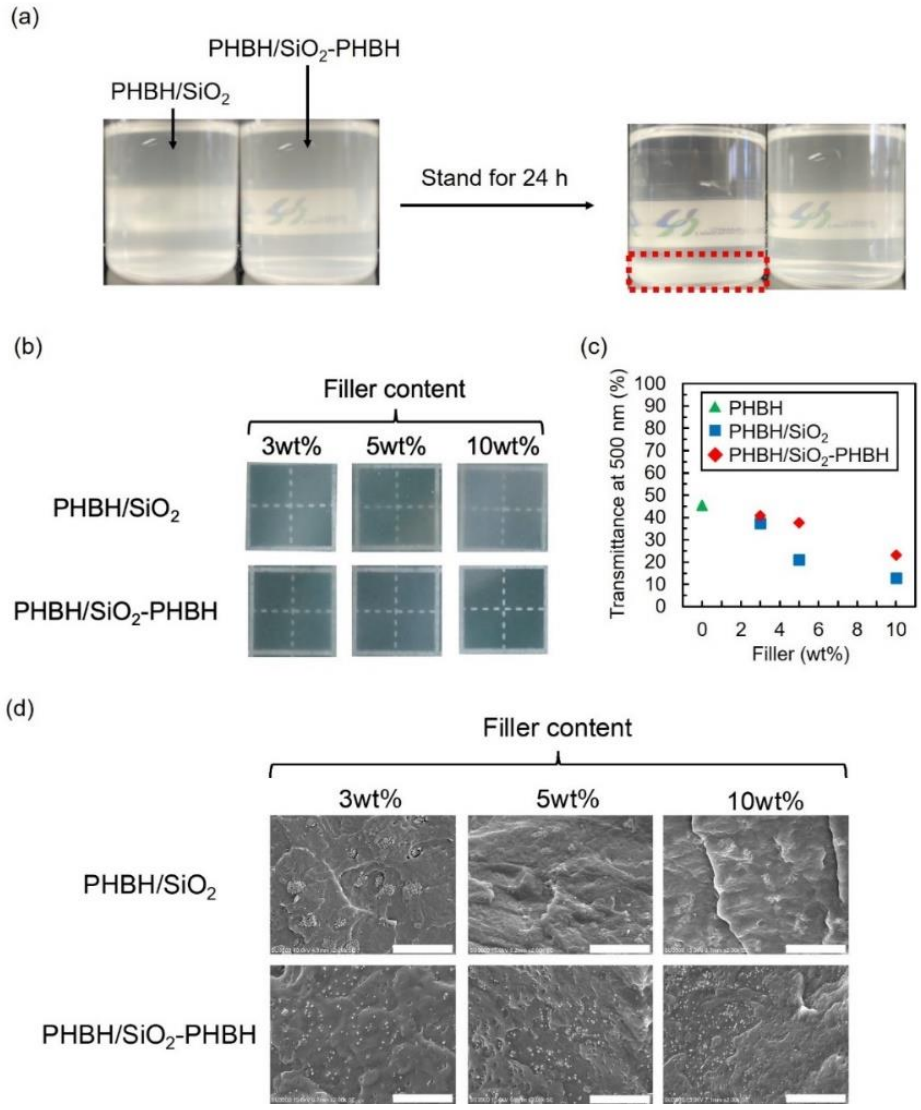


**Figure 3.2.** Preparation of PHBH/$SiO_2$ and PHBH/$SiO_2$-PHBH films by solvent casting method: (a) dispersion stability after 24 h of $SiO_2$ and $SiO_2$-PHBH in PHBH/chloroform solution at 10 wt% of filler content, (b) photographs of PHBH/$SiO_2$ and PHBH/$SiO_2$-PHBH films, (c) transmittance of the prepared films at 500 nm as a function of filler content (wt%) determined by UV-vis spectra, and (d) SEM images of the cryo-fracture surface of PHBH/$SiO_2$ (3 – 10 wt%) and PHBH/$SiO_2$-PHBH (3 – 10 wt%) [Scale bar: 20 μm].

### 3.3.2. Thermal analysis of PHBH/$SiO_2$ and PHBH/$SiO_2$-PHBH composite films

To discuss the interface interaction between the $SiO_2$ filler and the PHBH matrix, $T_g$ of the composite films is evaluated by thermal analysis, such as DMA and DSC, as shown in **Figures 3.3 and 3.4**, respectively. **Figure 3.3** shows the loss tangent (tan$\delta$) of PHBH/$SiO_2$ and PHBH/$SO_2$-PHBH films. Generally, the peak top of the tan$\delta$ is equivalent to $T_g$ of polymers. $T_g$ of PHBH/$SiO_2$ (from −2.9 to −1.1 °C) composite films was slightly higher than that of neat PHBH (−3.6 °C), whereas $T_g$ of PHBH/$SiO_2$-PHBH composite films was shifted to much higher temperatures (0.1–3.0 °C) than that of PHBH/$SiO_2$. $T_g$ was determined by DSC and DMA and they are summarized in **Table 3.1.** The DSC results confirmed that by adding $SiO_2$ as a filler $T_g$ of PHBH at around −4.4 °C does not change, whereas, adding $SiO_2$-PHBH as a filler led to an increase in $T_g$ of PHBH from −4.4 °C to −3.4 °C with increasing content of $SiO_2$-PHBH.

Generally, the rise in $T_g$ of the matrix polymer indicates the increase in interfacial adhesion of the filler/matrix composite materials.[1,37,38] The obtained thermal analysis demonstrates that the interaction of the PHBH/$SiO_2$-PHBH films was higher than that of PHBH/$SiO_2$ films. The interface of the PHBH/$SiO_2$ composite material has weak interactions corresponding to hydrogen bonding between the OH bond on the $SiO_2$ surface and the C=O bond of the PHBH backbone.[1] However, it has been reported that $T_g$ of PHBH in the PHBH/$SiO_2$ film does not change regardless of the filler dispersion and aggregation.[1] On the contrary, the change in $T_g$ of PHBH in PHBH/$SiO_2$-PHBH films can be attributed to the inhibition of the mobility of PHBH chains due to the good interaction between filler and matrix.[38] Additionally, the $SiO_2$-PHBH was uniformly distributed in the PHBH matrix and efficiently behaved as a filler with strong interaction on the composite interface. Thus, $SiO_2$-

PHBH can improve not only the dispersity in the PHBH but also the interfacial adhesion between the filler and matrix, compared to pristine $SiO_2$.

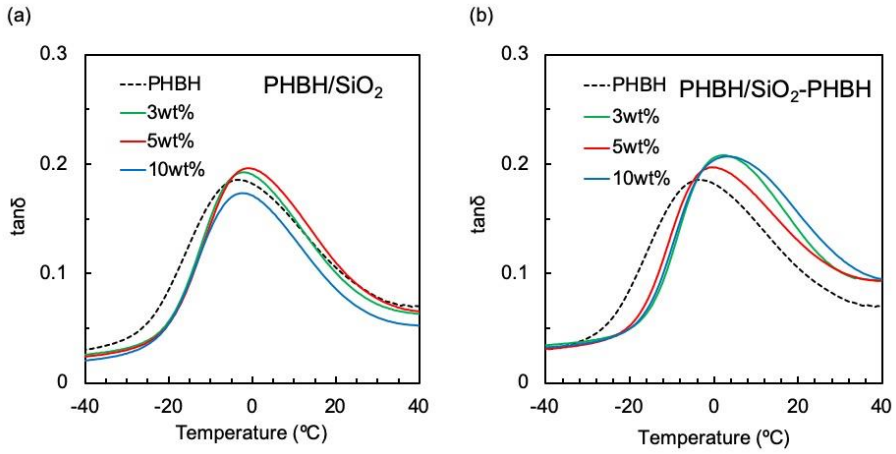


**Figure 3.3.** Loss tangent (tanδ) of (a) PHBH/$SiO_2$ and (b) PHBH/$SiO_2$-PHBH composite films measured by DMA (freq. = 1 Hz).

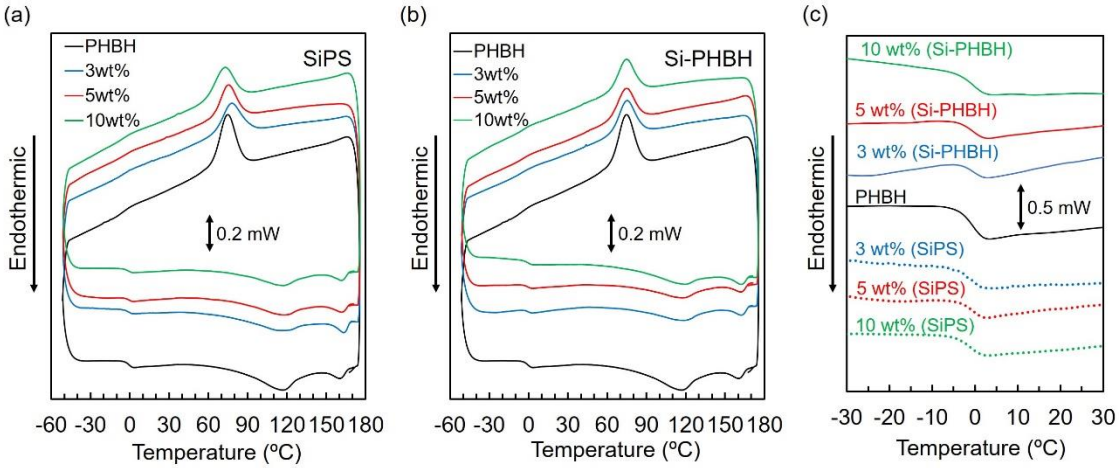


**Figure 3.4.** DSC charts of (a) PHBH/SiPS and (b) PHBH/$SiO_2$-PHBH and (c) enlarged view from -30 °C to 30 °C.

**Table 3.1.** $T_g$ of PHBH, PHBH/$SiO_2$, and PHBH/$SiO_2$-PHBH determined by DSC.

| Sample | Filler (wt%) | $T_g$ (°C) |
|---|---|---|
| Neat PHBH | 0 | –4.44 |
| PHBH/$SiO_2$ | 3 | –4.57 |
| | 5 | –4.40 |
| | 10 | –4.94 |
| PHBH/$SiO_2$-PHBH | 3 | –3.55 |
| | 5 | –3.44 |
| | 10 | –3.40 |

### 3.3.3. Mechanical properties of PHBH/$SiO_2$ and PHBH/$SiO_2$-PHBH

The mechanical properties of PHBH/$SiO_2$ and PHBH/$SiO_2$-PHBH composite films were evaluated by tensile tests. The values of tensile properties and the example of stress-strain curves are summarized in **Table 3.2** and **Figure 3.5, and 3.6**, respectively. After adding $SiO_2$ as a filler, Young's modulus (670 MPa) of PHBH/$SiO_2$ films was slightly higher than that of neat PHBH (640 MPa). However, the yield stress of PHBH/$SiO_2$ slightly decreased from 15 MPa to 13 MPa as the $SiO_2$ content increased. In contrast, adding $SiO_2$-PHBH as a filler into PHBH enhanced Young's modulus of PHBH from 640 MPa to 740 MPa, and also increased the yield stress of PHBH from 15 MPa to 17 MPa. Moreover, the elongation at a break of PHBH decreased with the addition of $SiO_2$ or $SiO_2$-PHBH; in contrast, the toughness of PHBH/$SiO_2$-PHBH exceeded that of PHBH/$SiO_2$. This result was related that the stress at plastic deformation of PHBH/$SiO_2$-PHBH became higher than that of PHBH/$SiO_2$. These results indicate that compared with neat PHBH and PHBH/$SiO_2$ composite films, the usage of $SiO_2$-PHBH as a filler can efficiently reinforce the mechanical properties of PHBH. These results imply that the dispersity and surface-modification of silica particles is an influential point for strengthening PHBH.

**Table 3.2.** Mechanical properties of PHBH, PHBH/$SiO_2$, and PHBH/$SiO_2$-PHBH.

| Sample | Filler (wt%) | Elongation at break (%) | Toughness ($MJ/m^3$) |
|---|---|---|---|
| Neat PHBH | 0 | 412 ± 14 | 65 ± 1 |
| PHBH/$SiO_2$ | 3 | 384 ± 31 | 55 ± 7 |
| | 5 | 279 ± 70 | 37 ± 10 |
| | 10 | 284 ± 38 | 34 ± 5 |
| PHBH/$SiO_2$-PHBH | 3 | 364 ± 25 | 63 ± 4 |
| | 5 | 331 ± 40 | 49 ± 4 |
| | 10 | 289 ± 57 | 44 ± 9 |

To investigate the efficiency of the $SiO_2$-PHBH as a filler, the change in mechanical strength was analyzed theoretically. When fillers are uniformly dispersed in the matrix, Young's modulus of composite materials follows the Halpin-Tsai model prediction **eq (3-1)**:

$$E_c = E_m \{(1 + \xi\eta\phi_f) / (1 - \eta\phi_f)\} \quad (3\text{-}1)$$

$$\eta = (E_f / E_m - 1) / (E_f / E_m + \xi) \quad (3\text{-}2)$$

where, $E_c$, $E_m$, and $E_f$ are Young's modulus of composites (c), matrix (m), and filler (f), respectively.[27,28] $E_f$ = 70,000 MPa is referred to in a previous report[39] and $E_m$ = 640 MPa is calculated by tensile tests. The value $\eta$ can be calculated by **eq (3-2)**. The shape factor (ξ) is defined as the following equation: $\xi = 2(L/D)$, where $L/D$ is the aspect ratio of the filler. In the case of the sphere-shaped filler, the value of $L$ is equal to that of $D$, thus $\xi$ is identically determined as 2.[1,39] The volume fraction of filler ($\phi_f$) is calculated by the following **eq (3-3)**:

$$\phi_f = (w_f / \rho_f) / \{w_f / \rho_f + (1 - w_f) / \rho_m\} \quad (3\text{-}3)$$

where, $w_f$ is a weight ratio of filler, and $\rho_f$ (= 2.2 g/cm$^3$) and $\rho_m$ (= 1.2 g/cm$^3$)[40] represent the density of the filler and the matrix, respectively. The theoretical value of **eq 3-1** is depicted in **Figure 3.5**; Young's modulus of PHBH/$SiO_2$ composite film is lower than the theoretical curve and does not follow the curve described in **eq 3-1**, indicating that the $SiO_2$ were aggregated and not dispersed homogeneously in the PHBH film.[40] In contrast, Young's modulus of PHBH/$SiO_2$-PHBH follows Halpin-Tsai model, demonstrating that the $SiO_2$-PHBH was uniformly dispersed in the PHBH.[1,40] The

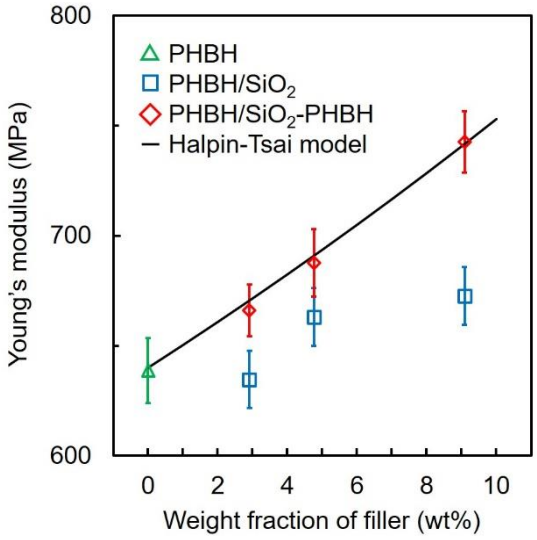


**Figure 3.5.** Young's modulus of PHBH, PHBH/$SiO_2$, and PHBH/$SiO_2$-PHBH composite materials as a function of filler content (wt%) with the line of the Halpin-Tsai model.

results of the SEM images correspond to the analysis of the tensile properties by the Halpin-Tsai model (**Figure 3.2d**). Thus, by surface modification of $SiO_2$ with Propargyl-PHBH, uniform dispersion of silica spherical fillers was achieved in composite materials, leading to sufficient improvement in Young's modulus of the PHBH.

To investigate the relationship of the yield stress of composite films to the spherical filler, the Nicolais-Narkis model was used:

$$\sigma_c = \sigma_m (1 - a\ \phi_f^{\ 2/3}) \quad (4)$$

where $\sigma_c$ and $\sigma_m$ (15 MPa) are yield stress of the composite (c) and the matrix (m), respectively. The constant *a* represents the parameter of interfacial adhesion between filler and matrix; especially, in the case of no interaction between filler and matrix, the value of *a* is equal to 1.21.[32,33] On the contrary, when fillers have some interactions with matrix polymer on their interface, the value of *a* can be estimated by **eq (3-5)**, as advocated by Zara and Rahmani:

$$a = 3.28 - B \quad (3\text{-}5)$$

where the constant *B* is calculated by the Pukánszky model for the composite materials consisted of polymer and particles as a filler.[33] The equation of the Pukánszky model is described in **eq (3-6)**:

$$\ln(\sigma_{red}) = \ln[\sigma_R(1+2.5\phi_f^{2/3}) / (1-\phi_f^{2/3})] = B\phi_f^{2/3}+b \quad (3\text{-}6)$$

where $\sigma_R$ is the relative yield strength as $\sigma_R = \sigma_c / \sigma_m$, and *b* is the intercept at $\phi_f^{2/3} = 0$. *B* is an interfacial parameter related to the efficiency of stress transfer between filler and matrix and is determined by plotting the $\ln(\sigma_{red})$ against $\phi_f^{2/3}$ as the slope of **eq (3-6)**. In the present study, the interfacial adhesion of PHBH/$SiO_2$ and PHBH/$SiO_2$-PHBH films was assumed by the critical parameters of *a* and *B* using **eqs (3-5) and (3-6)**. The lines of the Pukánszky model for PHBH/$SiO_2$ and PHBH/$SiO_2$-PHBH are depicted in **Figure 3.6a**. Regarding the PHBH/$SiO_2$-PHBH films, the value of *B* (= 4.19) is higher than that of PHBH/$SiO_2$ (*B* = 2.40).

The increase in the slope of *B* indicates that the interfacial compatibility between filler and matrix was improved. As predicted by the Nicolais-Narkis model, the parameter '*a*' of PHBH/$SiO_2$ and PHBH/$SiO_2$-PHBH was calculated by **eq (3-5)** and is 0.88 and -0.91, respectively. The curves of the Nicolais-Narkis model described in **eq (3-4)** for the prepared composite materials are described in **Figure 3.6b**. In general, $a < 1.21$ means good interfacial adhesion between filler and matrix.[32,33] The PHBH/$SiO_2$ shows a slightly smaller value '*a*' than 1.21, which is that of a composite material with no interaction between a filler and a matrix. This can be related to the low interaction corresponding to hydrogen bonding between the surface hydroxyl group on the $SiO_2$ surface and the carbonyl group of the PHBH backbone.[41] The decrease in the yield stress of PHBH/$SiO_2$ with decreasing $SiO_2$ content was roughly followed by the theoretical curve (blue broken line, **Figure 3.6b**). Conversely, the *a* of PHBH/$SiO_2$-PHBH was dramatically lower than that of PHBH/$SiO_2$. The PHBH/$SiO_2$-PHBH showed an increase in its yield stress as the $SiO_2$-PHBH content increased, which also followed the Nicolais-Narkis equation (red broken line, **Figure 3.6b**). These results clearly indicate that the interfacial adhesion between the $SiO_2$ filler and the PHBH matrix was improved by grafting PHBH chains onto the $SiO_2$ surface. The trend of improving the interfacial interaction was similar to the results of the change in $T_g$ determined by DMA and DSC, shown in **Figures 3.3 and 3.4** and listed in **Table 3.1**. These results demonstrated that the fracture energy of PHBH/$SiO_2$-PHBH is higher than that of PHBH/$SiO_2$ (**Table 3.2**). Hence, the theoretical analysis performed with the Nicolais-Narkis model proved that the enhancement of the interaction between PHBH and $SiO_2$ can increase mechanical properties such as tensile strength and toughness.

**Figure 3.7** describes the proposed mechanism of the improvement in the mechanical properties of PHBH by using $SiO_2$-PHBH as a filler, supported by results obtained by SEM observations, thermal and mechanical analysis, and theoretical discussion. $SiO_2$ fillers were

easily aggregated in the PHBH film because of the low dispersity of $SiO_2$ in the PHBH/chloroform solution. The generated agglomeration of $SiO_2$ can also lead to less stress transfer in the PHBH film. In contrast, $SiO_2$-PHBH fillers were uniformly dispersed in PHBH and exhibited good interfacial adhesion between filler and matrix. These changes promote the stress transfer on the filler and matrix interface during tensile deformation.[40] Consequently, surface modification of $SiO_2$ with Propargyl-PHBH can endow PHBH/$SiO_2$-PHBH composite materials with sufficient mechanical properties. Therefore, to reinforce Young's modulus and tensile strength of a PHBH with silica filler, the enhancement of interfacial adhesion between filler and matrix is one of the crucial factors. Additionally, these results reveal that Propargyl-PHBH can be useful for improving not only the dispersion stability of $SiO_2$ in PHBH but also the interfacial compatibility between PHBH and $SiO_2$.

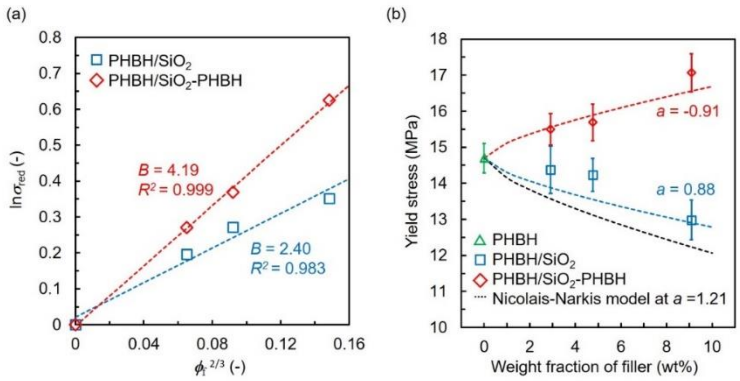


**Figure 3.6.** (a) Plots of the Pukánszky model and (b) yield stress of PHBH/$SiO_2$ and PHBH/$SiO_2$-PHBH with the change in the filler loading ratio compared to a theoretical equation.

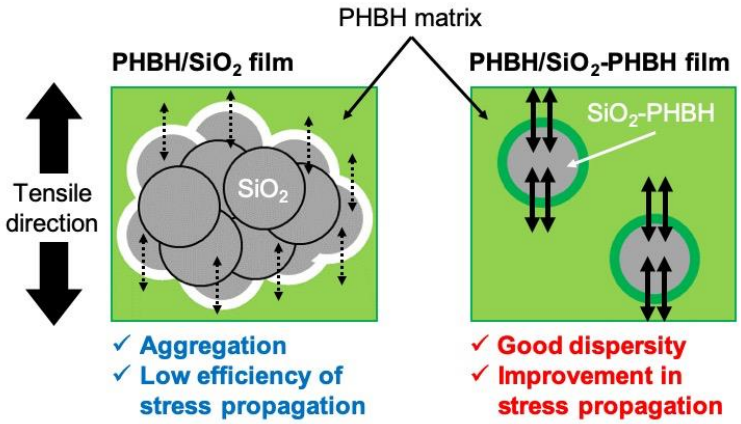


**Figure 3.7.** Illustration of the influence of the dispersity and interfacial adhesion between the $SiO_2$ filler and PHBH matrix on tensile properties of PHBH/$SiO_2$ (left) and PHBH/$SiO_2$-PHBH (right).

## 3.4 Conclusion

In this chapter, the author summarized that the surface modification of $SiO_2$ with Propargyl-PHBH can improve the interfacial adhesion between the PHBH matrix and $SiO_2$ filler. $SiO_2$-PHBH was successfully prepared using $SiO_2$-azide and Propargyl-PHBH through a CuAAC reaction. The structure of $SiO_2$-PHBH and the PHBH-to-$SiO_2$ loading ratio were confirmed by ATR-IR spectra and TGA, respectively. Compared with $SiO_2$, the $SiO_2$-PHBH showed higher dispersion stability in chloroform, revealed with UV-vis spectra and SEM images. DMA and DSC also showed that $T_g$ of PHBH slightly rose when $SiO_2$-PHBH was added as a filler. The Young's modulus of PHBH/$SiO_2$-PHBH was efficiently improved with increasing content of $SiO_2$-PHBH comparing to that of PHBH/$SiO_2$. The change in Young's modulus of PHBH/$SiO_2$-PHBH is verified by the Halpin-Tsai model equation, indicating that $SiO_2$-PHBH particles are uniformly dispersed in PHBH without agglomeration. The yield stress of PHBH/$SiO_2$ was monotonically decreased as a function of the weight ratio of $SiO_2$. Conversely, the yield stress of PHBH/$SiO_2$-PHBH was increased with increasing filler amount. These trends can be explained by the Nicolais-Narkis and Pukánszky models. Furthermore, calculation of parameter *a* of the Nicolais-Narkis model and *B* of the Pukánszky model, it was suggested that the interfacial adhesion of PHBH/$SiO_2$-PHBH was higher than that of PHBH/$SiO_2$. These results proved that the improvements in the dispersity of $SiO_2$ filler in the PHBH matrix and the interfacial adhesion between PHBH and $SiO_2$ can reinforce their mechanical properties, including Young's modulus, tensile strength, and toughness. Thus, this consequence demonstrates that the homogeneous dispersion and high compatibility between the $SiO_2$-PHBH filler and the PHBH matrix were successfully achieved by using propargyl-PHBH, leading to the increased mechanical strength of PHBH. Therefore, the surface modification of $SiO_2$ with end-reactive PHBH is an effective strategy to improve the mechanical properties of PHBH/silica filler composite materials.

## 3.5 References


[1] Y. Xie, D. Kohls, I. Noda, D. W. Schaefer, Y. A. Akpalu, *Polymer* **2009**, *50*, 4656.

[2] D. Li, J. Fu, X. Ma, *Polym. Compos.* **2019**, *41*, 381.

[3] Q. Zhang, Q. Liu, J. E. Mark, I. Noda, *Appl. Clay Sci.* **2009**, *46*, 51.

[4] J. Yang, Y. Li, G. Qin, *J. Macromol. Sci. Part B Phys.* **2017**, *56*, 373.

[5] A. W. Ajmal, F. Masood, T. Yasin, *Appl. Clay Sci.* **2018**, *156*, 11.

[6] S. Ke, Y. Yang, L. Ren, Y. Wang, Y. Li, H. Huang, *Compos. Sci. Technol.* **2012**, *72*, 370.

[7] M. Seggiani, P. Cinelli, N. Mallegni, E. Balestri, M. Puccini, S. Vitolo, C. Lardicci, A. Lazzeri, *Materials (Basel).* **2017**, *10*, 326.

[8] A. Willson, K. Takashi, *Polym. Compos.* **2018**, *39*, 491.

[9] A. Willson, K. Takashi, *Polym. Compos.* **2018**, *39*, 1331.

[10] H. Zou, S. Wu, J. Shen, *Chem. Rev.* **2008**, *108*, 3893.

[11] W. Yuan, F. Wang, Z. Chen, C. Gao, P. Liu, Y. Ding, S. Zhang, M. Yang, *Polymer (Guildf).* **2018**, *151*, 242.

[12] K. J. Hodder, J. A. Nychka, R. J. Chalaturnyk, *Int. J. Adhes. Adhes.* **2018**, *85*, 274.

[13] M. Joubert, C. Delaite, E. B. Lami, P. Dumas, *New J. Chem.* **2005**, *29*, 1601.

[14] W. Qiu, K. Mai, H. Zeng, *J. Appl. Polym. Sci.* **2000**, *77*, 2974.

[15] H. Ihara, S. Kubota, A. Uchimura, Y. Sakai, T. Wakiya, M. M. Rahman, S. Nagaoka, M. Takafuji, *Mater. Chem. Phys.* **2009**, *114*, 1.

[16] K. Ohno, T. Morinaga, K. Koh, Y. Tsujii, T. Fukuda, *Macromolecules* **2005**, *38*, 2137.

[17] T. Koriyama, Y. Takayama, C. Hisatsune, T. A. Asoh, A. Kikuchi, *J. Biomater. Sci. Polym. Ed.* **2017**, *28*, 900.

[18] T. Krentz, M. M. Khani, M. Bell, B. C. Benicewicz, J. K. Nelson, S. Zhao, H. Hillborg, L. S. Schadler, *J. Appl. Polym. Sci.* **2017**, *134*, 44347.

[19] F. Wu, B. Zhang, W. Yang, Z. Liu, M. Yang, *Polymer* **2014**, *55*, 5760.

[20] M. Sandomierski, B. Strzemiecka, M. M. Chehimi, A. Voelkel, *Langmuir* **2016**, *32*, 11646.

[21] J. I. Lee, H. Kang, K. H. Park, M. Shin, D. Hong, H. J. Cho, N. R. Kang, J. Lee, S. M. Lee, J. Y. Kim, C. K. Kim, H. Park, N. S. Choi, S. Park, C. Yang, *Small* **2016**, *12*, 3119.

[22] Z. Li, J. K. Muiruri, W. Thitsartarn, X. Zhang, B. H. Tan, C. He, *Compos. Sci. Technol.* **2018**, *159*, 11.

[23] M. Arslan, M. A. Tasdelen, *Polymers* **2017**, *9*, 499.

[24] G. Bissadi, R. Weberskirch, *Polym. Chem.* **2016**, *7*, 1271.

[25] X. Tang, E. Y. X. Chen, *Nat. Commun.* **2018**, *9*, 1.

[26] D. Kai, X. J. Loh, *ACS Sustain. Chem. Eng.* **2014**, *2*, 106.

[27] A. Tessema, D. Zhao, J. Moll, S. Xu, R. Yang, C. Li, S. K. Kumar, A. Kidane, *Polym. Test.* **2017**, *57*, 101.

[28] M. Eriksson, T. Peijs, H. Goossens, *Nanocomposites* **2018**, *4*, 112.

[29] M. S. Reid, T. C. Stimpson, E. Niinivaara, M. Villalobos, E. D. Cranston, *Ind. Eng. Chem. Res.* **2018**, *57*, 220.

[30] B. Pukánszky, *Composites* **1990**, *21*, 255.

[31] L. Nicolais, M. Narkis, *Polym. Eng. Sci.* **1971**, DOI 10.1002/pen.760110305.

[32] Y. Zare, *Int. J. Adhes. Adhes.* **2016**, *70*, 191.

[33] Y. Zare, A. Rahmani, *J. Colloid Interface Sci.* **2016**, *470*, 245.

[34] K. Shingo, T. Fujiki, **2018**, US 2018/0346943 A1.

[35] S. L. Jain, B. S. Rana, B. Singh, A. K. Sinha, A. Bhaumik, M. Nandi, B. Sain, *Green Chem.* **2010**, *12*, 374.

[36] H. Awada, C. Daneault, *Appl. Sci.* **2015**, *5*, 840.

[37] C. Mahoney, C. M. Hui, S. Majumdar, Z. Wang, J. A. Malen, M. N. Tchoul, K. Matyjaszewski, M. R. Bockstaller, *Polymer* **2016**, *93*, 72.

[38] H. Yao, G. Weng, Y. Liu, K. Fu, A. Chang, Z. R. Chen, *J. Appl. Polym. Sci.* **2015**, *132*, 41980.

[39] A. Jumahat, C. Soutis, F. R. Jones, A. Hodzic, *J. Mater. Sci.* **2010**, *45*, 5973.

[40] P. Xu, Y. Cao, B. Wu, P. Ma, W. Dong, H. Bai, H. Zhang, H. Zhu, M. Chen, *New J. Chem.* **2018**, *42*, 11972.

[41] H. Lijing, H. Changyu, C. Wenling, W. Xuemei, B. Junjia, D. Lisong, *Polym. Eng. Sci.* **2012**, *52*, 250.

# Concluding Remarks

In this doctoral thesis, the author summarized the results of the research on the improvement and emergence of functionalities of PHBH-based polymer blends and composite materials by focusing on the interfacial affinity between PHBH and different materials. Particularly, this thesis highlights that the miscibility and interfacial adhesion of PHBH binary blend and PHBH/filler composites were enhanced by Propargyl-PHBH. This strategy can make PHBH/different materials good compatibilization under a mild environment without deterioration of PHBH. So, the method the author proposed in this study is better than the conventional method. A summary of the contents is given below.

In Chapter 1, it was discovered that PMMA-*g*-PHBH synthesized from terminally reactive PHBH as a starting material behaved as a compatibilizer for PHBH/PMMA blend. The synthesis process of PMMA-g-PHBH is mentioned below; at first, Vinyl-PHBH was derived from Propargyl-PHBH with AMS through CuAAC reaction; next, Vinyl-PHBH and MMA were polymerized by radical polymerization. By adding PMMA-*g*-PHBH to various PHBH/PMMA blends, the phase separation structure was clearly erased. Moreover, DSC results showed a decrease in PHBH crystallinity and a rise in $T_g$ of PHBH with increment in additive amounts. The mechanical properties of the PHBH/PMMA/PMMA-g-PHBH films could be controlled by varying the blend ratio. These results indicate that PMMA-*g*-PHBH works as a compatibilizer.

In Chapter 2, the author revealed that grafting PHBH to PSt can not only reinforce the PHBH bulk film but also improve the optical properties of crystalline PHBH. The graft copolymer PSt-*g*-PHBH was synthesized by coupling Propargyl-PHBH with azide-functionalized PSt *via* CuAAC reaction. PSt-g-PHBH films looked uniform and transparent though PHBH/PSt blend film was heterogeneous and opaque. UV-vis spectra and haze measurement revealed that optical transmittance and a haze value of PSt-g-PHBH were

improved with the increase in PSt weight ratio in the obtained graft copolymers. As for mechanical properties, Young's modulus and tensile strength of PSt-*g*-PHBH were dramatically improved with increment in PSt wt%. Especially, at PSt = 47 wt%, its mechanical stiffness was higher than other types of PHAs and comparable to that of commodity plastics. Until now, it has been difficult to achieve high transparency, high strength, and high modulus of elasticity of PHAs due to their high crystallinity. However, the newly developed material in this work was able to achieve both by grafting PHBH onto PSt. In summary, PSt-*g*-PHBH films showed excellent optical and mechanical properties.

In Chapter 3, the author discussed the improvement of filler dispersion and filler/matrix interface affinity in PHBH/$SiO_2$ composites by grafting PHBH onto the $SiO_2$ surface. The surface modification of $SiO_2$ was succeeded by using Propargyl-PHBH. The obtained $SiO_2$-PHBH was well-dispersed in the PHBH matrix; conversely, non-modified $SiO_2$ was easily aggregated. The author proved that with Halpin-Tsain model, this dispersity improvement enhanced the elastic modulus of PHBH. Furthermore, using the Nicolais-Narkis model, the filler/matrix interfacial adhesion of PHBH/SiO2-PHBH was found to be higher than that of PHBH/$SiO_2$. Thanks for improving the interfacial adhesion, the tensile strength of the PHBH/$SiO_2$ composite was increasing. Thus, this chapter suggested that the dispersity and the interfacial compatibility of PHBH/$SiO_2$ composites were effectively enhanced by Propargyl-PHBH.

In conclusion, this study presented that the physical properties of PHBH can be improved by controlling the interface in polymer blends and composites with Propargyl-PHBH. Especially, the author emphasizes in this doctoral thesis that the technology obtained in this work can be applied to other biobased plastics, which will contribute to the expansion of applications of biomass plastics and lead to the solution of various environmental problems.

# List of Publications

1. Enhancement of interfacial adhesion in immiscible polymer blend

by using a graft copolymer synthesized from propargyl-terminated

poly(3-hydroxybutyrate-*co*-3-hydroxyhexanoate)

**Toshiki Tamiya**, Xinnan Cui, Yu-I Hsu, Tomonari Kanno, Taka-Aki Asoh, and Hiroshi Uyama*

European Polymer Journal, **2020**, *130*, 109662.

DOI: 10.1016/j.eurpolymj.2020.109662.

2. Reinforcement of Microbial Thermoplastics by Grafting to Polystyrene

with Propargyl-Terminated Poly(3-hydroxybutyrate-*co*-3-hydroxyhexanoate)

**Toshiki Tamiya**, Yu-I Hsu, Taka-Aki Asoh, and Hiroshi Uyama*

ACS Applied Polymer Materials, **2020**, *2 (9)*, 3948-3956.

DOI: 10.1021/acsapm.0c00624.

3. Improvement of Interfacial Adhesion between

Poly(3-hydroxybutyrate-*co*-3-hydroxyhexanoate) and Silica Particles

**Toshiki Tamiya**, Yu-I Hsu, Taka-Aki Asoh, and Hiroshi Uyama*

Industrial & Engineering Chemistry Research, **2020**, *59 (30)*, 13595-13602.

DOI: 10.1021/acs.iecr.0c02284.

# Acknowledgments

This study was carried out from 2018 to 2021 at the Department of Applied Chemistry, Graduate School of Engineering, Osaka University. During this fantastic experience in the doctoral 3 years, I have received a lot of invaluable assistance from all people around me. Their support and advice contribute to the accomplishment of the thesis.

First and foremost, I would like to express my deepest gratitude to my supervisor, Prof. Hiroshi Uyama, for his continuous guidance and discussion on my studies, and his kind-hearted encouragement as well. During my life in this laboratory for five years, he has been kindly enthusiastic about teaching me how to proceed with a study. I also sincerely thank him for providing many opportunities to attend the academic conferences, by which my views were broadened, my knowledge was expanded and my ability was improved. Definitely, his keen and vigorous advice, which I have obtained since I was a master course student, must benefit me in my future career.

I am profoundly grateful to Assoc. Prof. Taka-Aki Asoh, for his suggestions and inspirations, to improve the quality of my research. His amazing advice and knowledge sharing helped my thesis' accomplishment. I also thank him for his suggestions and revision about my published articles to make them easier to understand and improve their quality. In addition to my research, he helped me a lot with my private life and life advice, which enriched my life in the laboratory. I am incredibly grateful for all the advice he gave me, which will be extremely useful in my life in the future.

I appreciate Assist. Prof. Yu-I Hsu for her discussions and advice about my subject at any time and the knowledge sharing. I also deeply thank her for the manuscript revising, inspirations, and experience sharing. Without her support, my doctoral thesis cannot be finished smoothly.

I am grateful to Assoc. Prof. Takashi Tsujimoto belonging to Teikyo University of Science for his careful and enthusiastic education. When he was belonging to Uyama Lab. as an assistant professor at Osaka University, I had received many blessings, scientific knowledge, techniques, and so on. Absolutely, his advice helps me improving this doctoral thesis.

I also deeply appreciate the care and valuable reviewing my doctoral thesis from Prof. Takashi Hayashi and Takahiro Kozawa. Thanks to their advice, this thesis is dramatically improved.

I would like to express my gratitude to KANEKA Corporation and Nissan Chemical Corporation for providing PHBH samples and $SiO_2$, respectively.

I wish to appreciate the kind help and warm-hearted support from Ms. Yoko Uenishi and Mrs. Tomoko Shimizu.

I am very thankful to the past and present fellow lab mates in Uyama Lab: Dr. Yasushi Takeuchi, Dr. Nao Hosoda, Dr. Xinnann Cui, Dr. Yu Shu, Dr. Tomonari Kanno, Dr. Qidong Wang, Dr. Masatoshi Kato, Dr. Chen Qian, Dr. Zhengtian Xie, Dr. Jia Yankun, Mr. Shunsuke Mizuno, Mr. Akihide Sugawara, Mr. Naharullah Bin Jamaluddin Mr. Raghav Soni, Ms. Hanyu Wen, Ms. Yanting Lyu, Mr. Mark Adam Malaluan Ferry, Mrs. Wang Yan, Mr. Zhang Lu Wei, Ms. Wei Meng, Mr. Yuxiang Jia, Ms. Qian Jin, Ms. Yiying Wang, Mr. Haoyan Zhou, Mr. Weiting Wu, Ms. Lulu Huang, Ms. Jiaxin Chen, Ms. Zeying Cao, Ms. Xuran Guo, Ms. Linxiuan Li, Mr. Ryota Kumei, Mr. Tsukasa Kitatani, Mr. Shun Takawa, Mr. Kenta Chashiro, Mr, Yusuke Hinamoto, Mr. Hayato Hirono, Mr. Yuki Hayashi, Mr. Tasyuya Higashigaki, Mr. Yuya Higuchi, Ms. Moe Sugahara, Ms. Megumi Nakamura, Ms. Anna Shigaki, Mr. Ginga Hoshi, Mr. Toshiki Honda, Mr. Tatsuya Yamamoto, Ms. Airi Ozaki, Ms. Shiho Takai, Mr. Yuya Fujiwara, Mr. Yuka Kashihara, Mr. Kohei Kikkawa, Mr. Yuji Kiba, Mr. Atsusi Koizumi, Mr. Yuki Shioji, Mr. Takeshi Hiraoka, Mr. Motoi Oda, Mr. Kaita Kikuchi, Mr.

Koki Tsujita, Mr. Hajime Fujimori, Ms. Suzune Miki, Ms. An Thuy Le huynh, etc. for their kind-hearted help both in my research and daily life.

I am very grateful to the Japanese idol groups "Niji no Conquistador (Nijicon)" and "Dempa-gumi. inc (Dempa)" for giving me energy when I was having a hard time. Especially, Ms. Ayame Okada, a member of Nijicon, and Ms. Ayane Fujisaki, a member of Dempa make me happy and my research was greatly facilitated by their cheering.

Last but not least, I would like to express appreciation to my parents Yoshikatsu Tamiya and Atsuko Tamiya for their endless support throughout my life. Then, I also thank my young brother, Hiroyuki Tamiya for encouraging me to study much harder and doing the scientific discussion. The warm encouragement from my family motivates me to persist in my research and study.

January 2021

Toshiki Tamiya